UNIVERSITY OF TURIN

Department of Oncology

School of Life and Health Sciences

Doctorate in Molecular Medicine

Cycle XXXVI

Academic years 2020-2024

Cisplatin and temozolomide combinatorial treatment triggers hypermutability and immune surveillance in colorectal cancer

Tutor

Prof. Alberto Bardelli

PhD candidate

Pietro Paolo Vitiello

Coordinator

Prof. Paola Cappello

Table of Contents

1. ABSTRACT

Hypermutation induced by inactivation of mismatch repair (MMR) leads to increased neoantigen formation and immune surveillance in colorectal cancer (CRC) and in several other malignancies. Interestingly, commonly used cytotoxic agents present a known mutagenic potential, and exposure to chemotherapy has been associated to an increased tolerance to DNA damage. We investigated the impact of rationally designed combinations of chemotherapeutics on the generation of hypermutation and immunogenicity in otherwise immune refractory MMR-proficient CRC. We found that combinatorial treatment with cisplatin (CDDP) and temozolomide (TMZ) induces clonal and subclonal hypermutability resulting in an increase in predicted neoantigens. This combination specifically alters the immune fitness of the tumors and ultimately leads to immunoediting of chemotherapy-induced neoantigens and CD8+ T cell-mediated tumor rejections. Treatment-induced hypermutation and immune surveillance were also confirmed in a model of immune-refractory breast cancer.

By following the fate of treatment-induced mutations in the CRC model, we discovered that the neoantigens undergoing active immune deletion derive from mutations that are etiologically linked to chemotherapy treatment. Importantly, mice that had successfully rejected cells treated with CDDP-TMZ are vaccinated against their untreated counterpart. The same effect is not observed when priming is performed using the clinically approved combination of 5-flourouracil, oxaliplatin and irinotecan (FOLFOXIRI). Treatment with CDDP, TMZ, and anti-PD1 induces long lasting responses and complete rejections. Altogether, these results indicate that rational combinations of chemotherapeutic agents can promote immune surveillance through the induction of immunologically-relevant mutations.

2. INTRODUCTION

2.1 Immune surveillance in cancer

The interaction between cancer cells and immune system is a constant event during carcinogenesis, and the capability of the immune system to recognize and destroy clones of transformed cells before they grow into tumors or to kill tumors after they are formed is defined *immune surveillance*[1,2].

The interplay with the immune system impacts in various ways with the growth of the tumors and sculpts the antigenic features of cancers through the process of *immunoediting*[2]. During this process, the recognition of tumor cells by the immune system leads to the elimination of the more immunogenic cancer subclones, that can either result in complete cancer eradication or in adaptive evolution of cancer cells to neutralize and counteract immune-mediated killing and eventually escape from immune surveillance[3]. Indeed, the evasion from the immune surveillance constitutes a well-recognized hallmark of cancer[4,5].

The pivotal breakthrough in immunotherapy came from recognizing that cancer cells are able to hijack physiological mechanisms to suppress excessive immune responses[6–8]. Some of these mechanisms, known as *immune checkpoints*, constitute a group of inhibitory pathways hardwired into the immune system that are crucial for maintaining self-tolerance and modulating the duration and amplitude of physiological immune responses in peripheral tissues in order to minimize collateral tissue damage[9] (**Figure 1)**.

The understanding of these key mechanisms paved the way to the development of a new class of drugs, defined as *immune checkpoint inhibitors* (ICIs), able to unleash the activity of the immune cells against the tumor[9]. Among the checkpoints that are most commonly targeted, the two most relevant are Cytotoxic T-lymphocyte antigen 4 (CTLA-4), Programmed Death 1 (PD-1) and its ligand (PD-L1) [9].

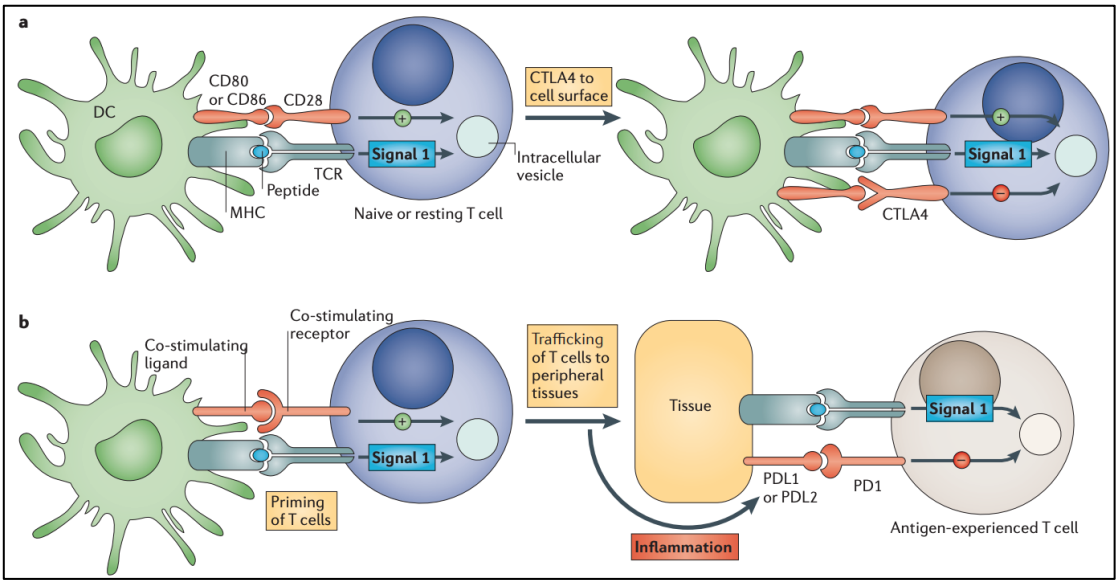

Figure 1: Immune checkpoints regulate different components in the evolution of an immune response. a*: The cytotoxic T-lymphocyte-associated antigen 4 (CTLA4)-mediated immune checkpoint is induced in T cells at the time of their initial response to antigen. The level of CTLA4 induction depends on the amplitude of the initial T cell receptor (TCR)-mediated signalling. High-affinity ligands induce higher levels of CTLA4, which dampens the amplitude of the initial response. The key to the regulation of T cell activation levels by the CD28–CTLA4 system is the timing of surface expression. Naive and memory T cells express high levels of cell surface CD28 but do not express CTLA4 on their surface. Instead, CTLA4 is sequestered in intracellular vesicles. After the TCR is triggered by antigen encounter, CTLA4 is transported to the cell surface. The stronger the stimulation through the TCR (and CD28), the greater the amount of CTLA4 that is deposited on the T cell surface. Therefore, CTLA4 functions as a signal dampener to maintain a consistent level of T cell activation in the face of widely varying concentrations and affinities of ligand for the TCR.* ***b****: By contrast, the major role of the programmed cell death protein 1 (PD1) pathway is not at the initial T cell activation stage but rather to regulate inflammatory responses in tissues by effector T cells recognizing antigen in peripheral tissues. Activated T cells upregulate PD1 and continue to express it in tissues. Inflammatory signals in the tissues induce the expression of PD1 ligands, which downregulate the activity of T cells and thus limit collateral tissue damage in response to a microorganism infection in that tissue. The best characterized signal for PD1 ligand 1 (PDL1; also known as B7-H1) induction is interferon-γ (IFNγ), which is predominantly produced by T helper 1 (TH1) cells, although many of the signals have not yet been defined completely. Excessive induction of PD1 on T cells in the setting of chronic antigen exposure can induce an exhausted or anergic state in T cells. MHC, major histocompatibility complex. Adapted from: Pardoll D.M., Nature Reviews Cancer, 2012.*

In the last 15 years, immunotherapy with ICIs has revolutionized oncology, largely extending the hopes of long-term survival -and perhaps cure- in several advanced cancer types including melanoma, renal cell carcinoma (RCC) and non-small cell lung cancer (NSCLC)[10]. Despite the clinical success of immunotherapy across different cancers and in up to 15% of all cancer patients, we still lack universal biomarkers that are predictive of response, despite both the tumor mutation load and the presence of tumor infiltrating lymphocytes have been largely correlated with responses [11,12].

Finding new strategies to increase the number of cancers that are susceptible to immunotherapy constitutes an active area of investigation. Such endeavor requires a deeper understanding of the mechanisms regulating the interaction between tumor and immune system.

2.1.1 Determinants of cancer immune recognition

In order for the immune system to activate against tumors, some specific requirements must be fulfilled[13,14]. These requirements include both tumor-specific and host features[15]. Among the tumor-specific determinants we have *antigenicity* and *adjuvanticity.* The former refers to the presence of antigens that can be recognized by a circulating naïve T cell clone on cancer cells. The most relevant sources of antigenicity include active or latent viral infections[16], somatic mutations generating cancer specific neoantigens[17], re-expression of genes product that are normally silenced at the end of the embryological development (so-called "oncofetal antigens") [18], and the aberrant expression of peptides cryptically encoded by non-coding RNAs[19].

Adjuvanticity refers to the delivery of danger signals from malignant cells to antigen-presenting cells. These signals are physiologically involved in the recognition of exogenous microbes (microbe-associated molecular patterns, MAMPs) or endogenous damage (damage-associated molecular patterns, DAMPs)[20]. DAMPs encompass changes in the surface and microenvironment of cells responding to stress that reflect either the secretion of danger signals, typically type I interferon (IFN), or the release of increased intracellular components in the microenvironment upon cell death, such as ATP[21]. Both MAMPs and DAMPs signal through the so-called pattern recognition receptors (PRRs), thus favoring the activation of antigen-presenting cells and, ultimately, their aibility to prime adaptive immune responses against tumor-specific antigens[22].

With regards to the host determinants of immune activation, the overall proficiency of the immune system to react to potentially dangerous stimuli (*reactogenicity*) must be considered. This feature does not correspond to a single mechanism and results from the balance of various tissue and secreted factors, regulating the relative abundance of reactive effector cells over immune suppressor cells[23,24]. Notably, host determinants of immune activation are not independent from tumor-specific ones, and need to be considered in a continuum[24].

2.1.2 The effect of cytotoxic treatment on cancer immunogenicity

A vast number of conventional chemotherapeutics have been shown to boost tumor immunogenicity through their impact on tumor-specific or host determinants of immune activation.

The most investigated immunogenic mechanisms elicited by chemotherapy on cancer cells involve an increase of adjuvanticity[25]. In particular, the exposure to cytotoxic agents can activate adaptive responses in malignant cells as part of the integrated stress response (ISR)[26]. For instance, the aberrant accumulation of nucleic acids in the cytosol as a consequence of chemotherapy-induced DNA damage can stimulate innate immune signalling via cyclic GMP-AMP synthase (cGAS), Toll-like receptor 9 (TLR9) or TLR3, ultimately resulting in the production of type I IFN [27,28]. Additionally, endoplasmic reticulum stress promotes the translocation of molecular chaperones like calreticulin and heat shock proteins to the cell surface, which serve as "eat-me" signals for antigen-presenting cells, thus facilitating tumor cell phagocytosis and cross-priming of T cells[29]. Eventually, cellular stress can precipitate in *immunogenic cell death* (ICD), that characterizes a form of regulated cell death that enables the initiation of adaptive immunity[30]. During ICD, dying cancer cells secrete ATP and release an abundance of cytoplasmic or nuclear proteins into the microenvironment, including annexin A1 (ANXA1) and high mobility group box 1 (HMGB1), that are considered markers of this process[21,30]. Altoghether, ATP, ANXA1 and HMGB1 constitute DAMPs and promote cross-presentation of tumour antigens to CD8+ cytotoxic T lymphocytes (CTLs) by dendritic cells (DC) in the context of an immunostimulatory milieu[31].

Several commonly used chemotherapeutics, such as oxaliplatin or doxorubicin, display a strong induction of ICD and their anticancer activity is hampered when used in immunodeficient mice[15]. However, the ICD inducing potency of other commonly used cytotoxics such as 5-fluorouracil or cisplatin is more debated, though several reports have correlated their activity with immune modulation[15].

While the stimulation of adjuvanticity by chemotherapeutics has been investigated experimentally and clinically[32], much less information is available on the ability of conventional chemotherapies to increase the antigenicity of cancer cells. However, it has been observed that chemotherapy can increase MHC class I molecules and antigen presentation, as well as induce quantitative and qualitative changes in the immunopeptidome of cancer cells[33]. Additionally, it is plausible that the mutagenic effect of cytotoxic agents induces changes in DNA sequence, potentially leading to the generation of potent neoantigens[34,35], even if the clonal fraction of cells carrying the resulting neoantigens may be too low to provide an immunogenic impact[36,37]. Interestingly, another mechanism through which cytotoxic agents may increase antigenicity is the adaptive dysregulation of DNA repair mechanisms. In particular, we

and others have shown that cancer cells acquire resistance to the alkylating agent temozolomide by inactivating mismatch repair (MMR) genes, potentially fostering hypermutation and neoantigen load [38,39]. This concept has been already tested in the clinical setting, providing preliminary evidence of efficacy (see following sections)[40,41]. Notably, other drugs, such as cisplatin, could induce a similar adaptation in malignant cells and impair MMR function, thus increasing antigenicity[42–44]. Another way that cytotoxic therapy could increase antigenicity is by the so-called *antigen spreading*, the process whereby antigenic epitopes distinct from the immunity-initiating epitope become major targets of an ongoing immune response[45].

On the other hand, multiple reports indicate a direct effect of chemotherapeutics on the immune compartment of the host. Importantly, while immunosuppressive effects tend to predominate when chemotherapy is delivered at doses close to the maximum tolerated dose (MTD) owing to cytotoxic effects on immune cells and bone marrow, the doses mostly used in clinical practice are not likely to be immunosuppressive[46,47]. Multiple mechanisms of stimulation of the immune cell subsets against cancer cells have been associated to chemotherapy: the depletion of immunosuppressive cells such as FOXP3+ regulatory T (Treg), myeloid-derived suppressor cells (MDSCs) and tumor-associated macrophages[48,49]; the activation of immune effector cells, including DCs and CD8+ cytotoxic T lymphocytes (CTLs)[50]. Multiple chemotherapeutic agents, including 5-fluorouracil[51], docetaxel[52] and cisplatin[53] have been shown to promote anticancer immune cell polarization independently from their effects on malignant cells, even if a definitive involvement of such mechanisms in their clinical efficacy remains to be clarified.

The array of immunostimulatory activities of chemotherapeutics is outlined in **Figure 2**.

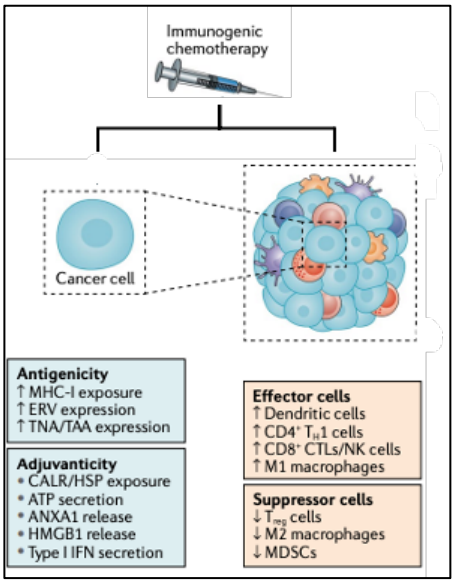

Figure 2. Immune modulation by conventional chemotherapeutics. *Conventional chemotherapeutics can promote the initiation of anticancer immune responses by enhancing the antigenicity or adjuvanticity of cancer cells (tumor-specific determinants) or by promoting the activation of immune effector cells and/or hampering the functions of immunosuppressive cells (host determinants). ANXA1, annexin A1; CALR, calreticulin; CTL, cytotoxic T lymphocyte; ERV, endogenous retrovirus; HMGB1, high mobility group box 1; HSP, heat shock protein; IFN, interferon; MDSC, myeloid-derived suppressor cell; MHC-I, major histocompatibility complex class I; NK, natural killer; TAA, tumourassociated antigen; TH1, T helper 1; TNA, tumour neoantigen; Treg, regulatory T. Adapted from: Galluzzi L et al, Nat Rev Clin Oncol 2020.*

2.2 The immunogenomic landscape of colorectal cancer

Colorectal cancer (CRC) is the third most common cancer in both women and men and the third leading cause of cancer-related death in Western countries [54]. Despite the advent of targeted therapy, 5-fluorouracil-based cytotoxic chemotherapy combined with oxaliplatin and/or irinotecan still represents the backbone for treating most metastatic CRC (mCRC) cases [55]. Notably, chemotherapy ± targeted therapy is hardly ever curative in this setting, and the 5-year survival rate is a dim 11-14% in stage IV CRC (mCRC)[54]. More recently, immune checkpoint inhibitors such as PD-1/PD-L1 and CTLA-4 blocking antibodies have demonstrated striking efficacy in the molecular subgroups of CRC characterized by either deficient mismatch repair (dMMR) or inactivating mutations in the proofreading domain of polymerase Epsilon (POLE), and are now included in clinical practice guidelines for the treatment of advanced dMMR CRC [56–60]. Unfortunately, dMMR CRCs are few and collectively represent only 4-5% of mCRC [55]. Conversely, the majority of mCRCs (>95%) are characterized by MMR proficiency (pMMR) and do not benefit from immunotherapy. This clinically relevant distinction reflects the profound genomic and immunological differences between colorectal cancer with a proficient or a deficient activity of the mismatch DNA repair system.

2.2.1 Microsatellite stable and instable colorectal cancer as distinct genomic entities

Mismatch repair is a multicomplex protein system that is required for the detection and replacement of single-nucleotide mismatches, in addition to large and small deletions that escape proofreading during replication[61]. Genetic and epigenetic alterations in MMR genes characterize early events in colorectal carcinogenesis, and influence massively the subsequent genomic evolution of cancer[62]. For this reason, CRCs can be classified into two distinct molecular subgroups: a) the ones with a proficient MMR system (pMMR), in which chromosomal instability is the main driver of genomic instability, and b) the ones with a deficient MMR system (dMMR), in which karyotypic aberrations are not common and the impairment of the MMR machinery fuels genomic instability [61]. At the genomic level, dMMR tumors are characterized by microsatellite instability (MSI), a condition in which the length of the microsatellite regions changes frequently during cell division. Moreover, dMMR tumors tend to accumulate many frameshifts (FSs) and single-nucleotide variants (SNVs) and are thus characterized by a high mutational burden [61,63]. On the other hand, pMMR tumors maintain a constant length of microsatellites and are thus defined as microsatellite stable tumurs (MSS). MSS tumors represent the vast majority of CRCs, whereas MSI account for approximately 15-20% of cases in early stages (I-III) and only 5% in stage IV[60,64]. This differential distribution across stages suggests a more difficult progression of dMMR CRCs to the advanced stage, establishing dMMR/MSI status as a positive prognostic factor in local disease [65–67]. Beside this prognostic role, MSI tumors display peculiar clinical and pathological features with respect to MSS tumors. Indeed, MSI CRCs are more common in elderly patients, more frequently located in the right colon, are more often poorly differentiated, and often present mucinous features and an abundant immune infiltrate[68]. The majority of dMMR/MSI CRCs are the result of somatic mutations in MMR genes or the epigenetic downregulation of MutL Homolog1 (*MLH1)* expression [69]. However, as many as 3% of all CRCs (about 28% of dMMR/MSI CRCs) occur within the context of Lynch syndrome (LS), also known as hereditary nonpolyposis colorectal cancer (HNPCC) [68,70]. LS is a hereditary cancer syndrome characterized by heterozygous germline mutations in *MLH1*, MutS protein homologue 2 (*MSH2)*, MutS protein homologue 6 (*MSH6)* or PMS1 Homologue 2 (*PMS2)* [70].

On the genomic level, MSI cancers are characterized by hypermutation and by peculiar mutational scars[63]. Indeed, the enrichment of specific nucleotide changes (C > T and T

> C), double base substitution and small insertion deletion were clearly associated with dMMR tumors, allowing the identification of specific single base substitution (SBS) signatures, namely SBS6, SBS15, SBS21, SBS26[63]. Importantly, dMMR-dependent hypermutation is genomically distinguished from other causes of hypermutation (e.g., *POLE* or *POLD1* mutant tumors), as the mutational contexts affected are distinct [63,71–73]. With regards to the mutational spectrum, MSI CRCs are significantly enriched in *BRAF* mutations with respect to MSS CRCs (34% vs. 6% of cases), while the incidence of APC and p53 alterations is higher in MSS than in MSI tumors[74,75].

2.2.2 Immunological features of colorectal cancer

The contribution of the immune compartment in the evolution of CRC is well known, and the localization and phenotype of T-Cytotoxic, type 1 T-helper (Th1), and T-memory infiltrating cells strongly affect survival of patients[76]. In particular, both the presence of a Th1 immune response and the enrichment of cytotoxic T cells in the tumor microenvironment correlate with a significant reduction of tumor recurrence and an improved overall survival[76]. The independent prognostic role of the immune repertoire in CRC was first presented by Galon and colleagues, who elaborated the "immunoscore" as a classification system based on the number and localization of CD3+ and CD8+ T cell subpopulations in the tumor microenvironment, independently from MMR status[76,77]. Of note, in stage I-III colorectal cancer, a high immunoscore is associated with a lower risk of relapse independently from MMR status[78,79] . Nevertheless, the most striking difference between MSS and MSI cancers relies of their immunological features, and a conspicuous lymphocyte infiltrate is frequently associated with MSI status in CRC[80], suggesting that the better prognosis of these tumors is related to their high immune infiltration [79]. Since the 1990s, numerous reports highlighted the presence of a robust T cell infiltration in MSI CRC tumors[60,81–83]. Gene expression profiles of MSS and MSI tumors revealed an inflamed environment in MSI CRC tumors characterized by a prominent infiltration of M1 macrophages, CD8+ T cells, CD4+ cells, and natural killer (NK) cells, and an augmented expression of INF-ɣ in MSI specimens, supporting an active Th1 anti-tumoral response associated with MMR deficiency[83,84]. Similar biological findings derive from the transcriptomic classification of colorectal tumors in consensus molecular sub-subtypes (CMSs), in which the CMS1 is enriched for MSI tumors and markers of immune activation[85]. In particular, CMS1 includes tumors harbouring high tumor mutational burden and

increased neoantigen load, immune cell infiltration (T cell, CD68+ macrophages), high levels of chemokines, but also high expression of immune checkpoint inhibitors[86,87]. Among the mechanisms that could underlie the inflamed immune environment of MSI tumors, neoantigens' role is thought to be central, as MSI CRCs generate 10–50 times more tumor-specific antigens than MSS tumors [61,83,88]. The functional impairment of MMR machinery leads to hypermutation in the form of single nucleotide variants (SNVs) and insertions/deletions (indels) events that contribute to the mutational landscape of dMMR tumors[89]. SNVs are individual nucleotide alterations that include synonymous changes (that do not affect the aminoacidic sequence of the protein) and non-synonymous changes (that alter the protein sequence). Non-synonymous changes include non-sense and missense mutations that can lead to a different amino acidic sequence compared to the wild-type protein in case the mutations take place in a coding gene. These types of mutations are easy to identify using next-generation sequencing (NGS) technology. Conversely, small insertions and deletions generate frameshifts (FS), which are more challenging to detect[90]. These genetic alterations can generate new antigens (neoantigens) and may activate an immune response against cancer cells. Neoantigens are presented by both MHC class I and II, triggering the activation of cytotoxic CD8+ T cells (class I mediated) and the helper capacity of CD4+ T cells (class II mediated) [91]. Advanced bioinformatic tools can be used to identify and predict immune activating neoantigens derived from SNVs and indels by first detecting mutations or frameshifts in a specific genomic sequence followed by in silico HLA-binding predictions[92–94]. The relationship between MMR activity and the onset of immunogenic mutations has been investigated in the past by several research groups, including ours[39,95,96]. In particular, our group demonstrated that genetic inactivation of *MLH1* in pre-clinical models led to the dynamic accumulation of mutations able to trigger a robust CD8+ T-cell-dependent immune response[39]. Additional studies have underlined the importance of neoantigens in triggering T cell infiltration and in positively affecting the response to immunotherapy in several tumor types[97–99]. The correlation between the number of mutations and the response to ICIs reflects the concept of the "winning neoantigens", deriving from early clinical observations in melanoma patients[100,101]. As a matter of fact, tumor mutational burden (TMB) has been adopted in 2020 by FDA as an agnostic biomarker for access to anti-PD1 treatment, even if retrospective analyses show that not all sources of hypermutation induce the same sensitivity to ICIs as dMMR [102,103]. In addition to the number of mutations that

impact on the likelihood of having immunogenic neoantigens, another key aspect to consider is the quality of the mutations and the derived neoantigens[104]. Specifically, even if a single immunogenic antigen can trigger an immune response, it's been evidenced that the number of putative neoantigens per alterations is higher if they arise from frameshifts[105]. Moreover, the clonal distribution of neoantigens has been shown to play an important role in immune surveillance[106]. McGranahan and colleagues have correlated the clonality of neoantigens with the response to immunotherapy in both non-small cell lung cancer (NSCLC) and melanoma[107]. In particular, they have found that, even in presence of a high mutational burden, the absence of clonal neoantigens is associated to a poor response to ICI therapy. A similar pattern was identified in samples derived from dMMR CRCs that have been treated with anti-PD1, in which the presence of clonal immunogenic mutations and clonally expanded T cells positively correlate with the response to the treatment [108].

While neoantigens constitute crucial contributors to the effectiveness of immune surveillance in dMMR cancers, recent publications have also pinpointed the contribution of other players to the immune response in MSI tumors. For instance, interferon responses may stimulate immune surveillance in MSI tumors by increasing tumor adjuvanticity[109,110]. In particular, the cGAS-STING (cyclic GMP-AMP synthase–stimulator of interferon gene) pathway connects the recognition of cytosolic double strand DNA (dsDNA) to the activation of an inflammatory response[111]. Particularly, cGAS expression by tumor cells triggers c-GAMP, which is translocated and activates STING and interferon-β production in myeloid and B cells[112,113]. The activation of cGAS, STING, and interferon regulatory factor 3 (IRF3) is tumor-DNA-dependent and contributes to dendritic cell activation[114]. The cGAS-STING pathway has been suggested to directly participate in T-cell activation by MMR deficient tumors[110]. Specifically, in CRC and breast cancer models with defects in MMR, cytosolic DNA is accumulated and triggers a CD8+ T cell response[110].

On the other hand, the immunological background behind the unresponsiveness of pMMR CRCs to ICB is characterized by a paucity of immune cells [83]. Interestingly, seminal observations highlighted that MSS CRCs contain potentially relevant clonal neoantigens, but these are broadly expressed at lower levels than in MMR-deficient cancer, thus affecting productive cross-priming and ultimately driving T cell dysfunction[115].

Recently, it has been shown that some CRCs are characterized by a heterogeneity of the MMR status, which can be pharmacologically modulated in order to enrich for the more immunogenic dMMR component and boost immune surveillance[116].

Overall, the immunogenic features of CRC favor an effective immune control in the small minority of dMMR/MSI tumors, defined as immunologically "*hot*" and immune activated, as opposed to pMMR/MSS tumors that are immunologically "*cold*" and less infiltrated by immune cells [86] **(Figure 3).**

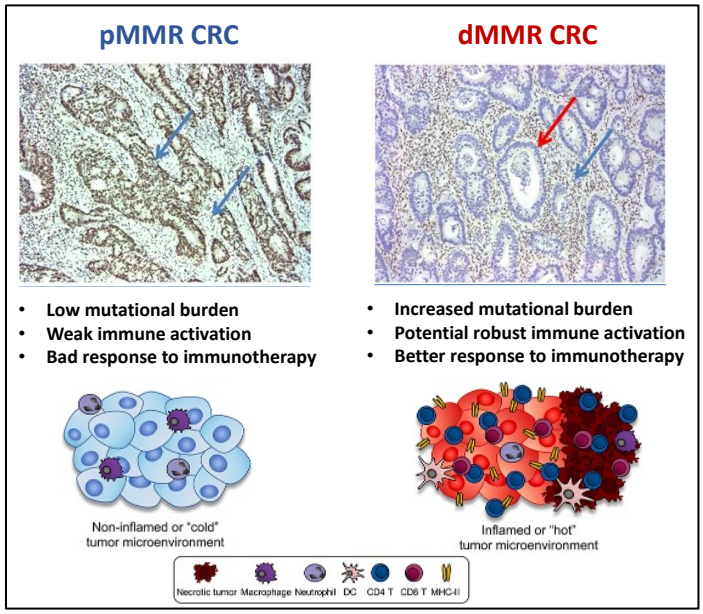

Figure 3. Immunological features of colorectal cancers with a proficient or a deficient MMR. *Upper part: representative immunohistochemistry for MLH1 in pMMR and dMMR. In pMMR CRC MLH1 is positive (blue arrow) both in the stroma and in cancer cells; whereas in dMMR CRC MLH1 is positive (blue arrow) in the stroma, but is negative (red arrow) in cancer cells. Lower part: the main immunogenomic features of pMMR and dMMR CRCs are listed, together with a schematic representation of the tumor microenvironment for both types of CRC. Adapted from: Kim ST et al, J Cancer 2017.*

2.2.3 Treatment with ICIs in CRC

As previously shown, MSI CRCs are greatly sensitive to immunotherapy, while MSS CRCs are largely resistant to immune checkpoint inhibitors (ICIs). Interestingly, the correlation between dMMR and immune activation was not systematically considered until a decade ago, despite the long-known abundance of lymphocyte infiltration in dMMR/MSI CRC[117–119]. The initial causative association between dMMR status and immunogenicity stems from a series of observations that were rightfully connected: the finding that somatic mutations are substantially increased by 10-100-fold in dMMR tumors compared with pMMR tumors[120,121] and the realization that somatic mutations found in tumors can be recognized by the patient's own immune system[97]. These observations were contextualized when examining the complete response in a single patient with metastatic CRC in a molecularly unselected population during an early phase clinical trial with an anti-PD-1 agent[122], paving the way for the first successful

clinical trial assessing anti-PD-1 treatment for dMMR tumors [123]. As matter of fact, the presence of dMMR status constitutes a positive predictive biomarker for immunotherapy efficacy across all histologies, making it the first tissue-agnostic biomarker appointed by FDA [103,124].

Several large clinical trials such as KEYNOTE-177, CheckMate 142 and CheckMate 8HW have established anti-PD1 +/- anti-CTLA-4 agents as the mainstay for the treatment of advanced dMMR/MSI CRC[56–58,125], and more trials are investigating these agents in the early setting[126,127]. The relationship between the genetic features and response to immunotherapy of CRC tumors has been confirmed in multiple prospective trials. In the metastatic setting, approximately 45% of MSI CRCs present a tumor objective response upon first-line treatment with anti-PD1 monotherapy, with a duration of response that exceeds 36 months in more than 75% of patients[56]. These results indicate that ICIs constitute a great therapeutic success in the small subgroup of dMMR metastatic CRCs, although primary and acquired resistance restrict the efficacy of the treatment[71,128,129].

However, the vast majority of metastatic CRCs (>95%), characterized by MMR proficiency (pMMR), still do not benefit from immunotherapy[123,130,131].

One notable exception is characterized by CRCs presenting pathogenic mutations in the exonuclease (proofreading) domain of the polymerase epsilon (*POLE*) or delta 1 (*POLD1*), associated to a MMR-independent hypermutator phenotype that confers strong sensitivity to ICIs through generation of novel neoantigens[59,132] .

Additionally, other exceptions are emerging regarding the sensitivity of pMMR CRCs in the non-metastatic setting or with novel new generation ICIs. In the NICHE trial (ClinicalTrials.gov: NCT03026140), Chalabi and colleagues reported that up to 27% of early (stage I-III) pMMR colon cancers exhibited a complete pathological response to the combination of nivolumab and ipilimumab given as neoadjuvant treatment [133]. With respect to metastatic pMMR CRC, recent evidence supports the efficacy of new ICI agents in treating this typically immune refractory disease at the metastatic stage. In particular, the combination of balstilimab (an anti-PD-1 antibody) with botensilimab (a novel Fc-enhanced anti-CTLA-4 antibody) has shown an overall response rate (ORR) of 22% in a population of pMMR CRC patients without liver metastases, who were preferentially enrolled in the expansion phase of the trial [134].

In conclusion, even if the emergence of novel ICIs has the potential to increase the number of CRCs amenable to immunotherapy, the identification of new strategies to

convert *cold* immune refractory CRCs into more immune sensitive tumors still represents an unmet need and an active area of investigation.

2.3 Using chemotherapy to increase the immunogenicity of CRC

Cytotoxic chemotherapy ± targeted agents (anti-EGFR or anti-VEGF) remains the mainstay of treatment for the vast majority (>95%) of metastatic CRCs characterized by MMR proficiency [135,136].

Several attempts to convert immunologically *cold* into *hot* tumors have been described, typically by combining ICIs with other therapies[137]. Limited data on the activity of DNA damage response inhibitors (DDRi) such as PARPi, ATRi, or ATM have been reported in CRC, and whether DDRi treatment can induce neoantigens, immune surveillance and improvement in the efficacy of immune checkpoint blockade remains unknown [138]. Interestingly, cytotoxic chemotherapy has been suggested as a strategy to increase immunogenicity, and concomitant and/or sequential chemo-immunotherapy combinations have already been investigated in several cancer types such as breast, gastro-esophageal, and non-small cell lung cancer (NSCLC), and are currently under assessment for CRC[15,139]. As previously discussed, chemotherapy may elicit immune stimulatory effects by interacting with crucial determinants of immune activation (Figure 2)[15]. For this reason, it is no wonder that chemo-immunotherapy combinations or sequences characterize the main strategy to maximize the efficacy of ICIs in otherwise immune-resistant MSS CRCs[15].

2.3.1 Chemotherapy given in combination with immunotherapy

The concurrent treatment with chemotherapy and ICIs constitutes a successful strategy in several tumor types[139]. Of note, chemo-immunotherapy clinical investigations are already ongoing in mCRC[86]. In this setting, chemotherapy is used as a mean to boost tumor immunogenicity mainly through the induction of adjuvant molecules and the reshaping of tumor microenvironment[15]. The AtezoTRIBE (NCT03721653) is a multicentric, open-label, controlled, phase 2 study in which patients were randomized to receive first-line FOLFOXIRI (5-fluorouracil/oxaliplatin/irinotecan) and the anti-angiogenic agent bevacizumab with or without atezolizumab (an anti-PD-L1 antibody). In this study, the median progression-free survival in the overall population was 13.1

months (80% CI 12.5–13.8) in the atezolizumab group and 11.5 months (80% CI 10.0–12.6) in the control group, with a significant hazard ratio (0.71, 80% CI 0.58–0.87, p=0.015); however, no significant difference in OS was found[140,141]. Interestingly, a post-hoc exploratory analysis identified high TMB and immunoscore as biomarkers associated with benefit for pMMR CRCs treated with atezolizumab[142]. Similarly, the results from the phase II CheckMate 9X8 trial (NCT03414983) investigating the addition of nivolumab (anti-PD-1) to FOLFOX and bevacizumab in first-line therapy failed to demonstrate a PFS benefit, although favourable trends in both the ORR and PFS rate at 18 months were observed in the nivolumab arm[143]. Additionally, studies with comparable designs, such as the NIVACOR trial (NCT4072198), are currently investigating similar hypotheses in the same patient population[144]. Overall, these studies did not show a clinically meaningful effect of combined chemo-immunotherapy in unselected mCRC patients. However, the post-hoc exploratory analyses suggest that there may be a significant effect of these combinations in selected patients, advocating for more clinical investigations in biomarker-selected populations.

2.3.2 Chemotherapy priming with temozolomide followed by immunotherapy

As previously discussed, preclinical studies have shown that the onset of resistance to some cytotoxic drugs, such as the alkylating agents temozolomide and dacarbazine, is accompanied by the inactivation of the MMR[38,39]. This knowledge paved the way to a different approach to turn *cold* immune refractory pMMR/MSS tumors into *hot* tumors, by hijacking mechanisms of resistance to cytotoxic agents to induce hypermutation and foster immune surveillance[145]. In this case, the immunogenicity is sustained by both an increase of cancer antigenicity and the release of adjuvant molecules by malignant cells as a consequence of the MMR inactivation[145]. However, this approach is only feasible in patients whose cancers display gene silencing of O6-methylguanine-DNA methyltransferase (*MGMT*), which encodes for a DNA repair enzyme with a key role in chemoresistance to O6-alkylating agents such as temozolomide[39]. The prevalence of MGMT inactivation in MSS mCRC is around 5-20%, with variability between the different tests used to measure its inactivation[146–148]. In case of MGMT silencing, temozolomide induces alkylation of guanine at O6-methylguanine, which mismatches with thymine during DNA replication. In the case of functional MMR, these mismatches are recognized, initiating a futile cycle of repair and leading to cytotoxicity

and cell death. Conversely, upon MMR inactivation these mismatches are fixed into the DNA, providing escape from cell death, but at the same time affecting the mutational landscape of cancer cells, and consequently their neoantigen repertoire [149].

This approach has been clinically investigated in two independent phase II trials, ARETHUSA and MAYA[40,41]. In the ARETHUSA trial, a cohort of 30 MGMT-silenced, pMMR and RAS-mutant metastatic CRC patients received TMZ treatment as priming therapy; at the time of disease progression, patients advanced to the ICB phase with pembrolizumab only in the case of a TMB increase above 20 mutations per megabase[40]. In ARETHUSA, the TMB and mutational signatures analysed in tissue biopsy samples and circulating tumor DNA revealed the induction of alterations in MMR genes and tumor hypermutation. In 94% of the cases where TMZ mutational signature emerged, a p.T1219I *MSH6* variant was detected. Results from the initial analysis revealed that among the first six patients treated with pembrolizumab, four experienced disease stabilization[40]. In the MAYA trial, patients who achieved disease control after two cycles (8 weeks) of TMZ treatment were enrolled to receive a combination of ipilimumab, nivolumab and TMZ, with no mandatory biomarker assessment. Notably, the ORR was 45% in 33 evaluable patients who accessed to the combined chemoimmunotherapy phase, with an 8-month PFS rate (the primary endpoint of the trial) of 36%[41]. The results of these two studies support further investigations of this strategy, though an optimization of the sequencing schedule would be desirable.

A summary of the studies (completed and ongoing) that use chemotherapy to turn a cold tumor into hot is present in **Table 1**.

Chemo-immunotherapy trials in first-line setting			
Study name and reference	**Phase**	**Description**	**Status/Results***
AtezoTRIBE NCT03721653	II	Randomized, open-label, treatment with Atezolizumab plus FOLFOXIRI/Bevacizumab vs FOLFOXIRI/Bevacizumab in the first-line treatment of patients with mCRC	Complete mPFS: 13.1 vs 11.5 months (p:0.015); ORR: 59 vs 64%: mOS: 33 vs 27.2 months (p:0.136)
CheckMate 9X8 NCT03414983	II/III	Randomized, open-label, treatment with Nivolumab plus FOLFOX/Bevacizumab versus FOLFOX/Bevacizumab in the first-line treatment of patients with mCRC	Complete mPFS by BICR: 11.9 months in both arms (p:0.3); 18-months-PFS rate: 28% vs 9%; ORR: 60% vs 46%; mDoR: 12.9 vs 9.3 months
HCRN GI14-186 NCT02375672	II	Single arm, treatament with Nivolumab plus FOLFOX in previously untreated mCRC patients	Complete mPFS: 8.8 months; ORR: 56.7%
MEDITREME NCT03202758	Ib/II	Single arm, treatment with FOLFOX plus Durvalumab and Tremelimumab in first-line treatment of RAS-mutated mCRC patients	Complete 3-month-PFS rate: 90.7%; ORR: 64.5%; mPFS: 8.2 months
NIVACOR NCT04072198	II	Single arm, Nivolumab plus FOLFOXIRI/Bevacizumab in first-line treatment of patients with RAS/BRAF mutated mCRC	Ongoing
POCHI NCT04262687	II	Single arm, Pembrolizumab plus Xelox/Bevacizumab as first-line treatment in MSS mCRC patients with resected primary tumors presenting a high immune infiltrate	ORR: 74% (17% complete responses). Immature survival data.
METIMMOX NCT03388190	II	NordicFLOX vs alternate treatment with 2 cycles of NordicFLOX followed by 2 cycles of Nivolumab in previously untreated patients with MMRp/MSS mCRC	Ongoing
METIMMOX-2 NCT05504252	II	Single arm, alterate treatment with 2 cycles of NordicFLOX and 2 cycles of Nivolumab in previously untreated patients with MMRp/MSS mCRC	Ongoing
CIFOXRC NCT05468177	II	Single arm, treatment with cetuximab plus anti-PD1 plus FOLFOX in previously untreated metastatic or locally advanced RAS/BRAF wt right-sided colon cancer	Ongoing
NCT05970302	II	Single arm, treatment with XELOX/Bevacizumab plus Tislelizumab in previously untreated MSS/MMRp RAS-mutated mCRC patients	Ongoing
FOBECAMS NCT06176885	II	Single arm, treatment with Camrelizumab plus FOLFIRI/Bevacizumab in previously untreated MSS mCRC patients	Ongoing
CLIMB NCT03698461	II	Single arm, neoadjuvant treatment with Atezolizumab + plus FOLFOX/Bevacizumab in patients with colorectal liver metastases (CRLM)	Complete No results available
Chemo-immunotherapy trials in chemo-refractory setting			
Study name	**Phase**	**Description**	**Status/Results***
NCT03396926	II	Single arm, treatment with Pembrolizumab plus Capecitabine/Bevacizumab in patients with non-resectable MSS mCRC who have not responded to previous fluoropyrimidine treatment	Complete ORR: 5%; mPFS: 4.3 months
NCT02860546	II	Single arm, treatment with Nivolumab plus TAS-102 in chemorefractory MSS mCRC patients	Complete ORR: 0%. ; irRC-mPFS: 2.2 months
MAYA NCT03832621	II	Single arm, treatment with Temozolomide in combination with Nivolumab and Ipilimumab in MGMT-silenced MSS chemorefractory mCRCs patients who achieved disease control with 2 cycles of Temozolomide	Complete 8-month PFS rate: 36%; ORR: 45%; mPFS: 7 months; mOS: 18.4 months
ARETHUSA NCT03519412	II	Single arm, priming treatment with Temozolomide in MGMT-silenced MSS chemorefractory mCRC patients; at progression, treatment with Pembrolizumab in case of tumor TMB elevation	Ongoing

BACCI NCT02873195	II	Randomized, Double-Blind, Placebo-Controlled Study of Capecitabine Bevacizumab Plus Atezolizumab or Placebo in patients with chemo-refractory mCRC	Ongoing
KEYNOTE-651 NCT03374254	Ib	Open-label, multi-cohort, treatment with Pembrolizumab plus Binimetinib (MEKi) or Pembrolizumab plus chemotherapy with or without Binimetinib in previously treated mCRC patients	Ongoing
NCT04457284	II	Single arm combination of Temozolomide, Cisplatin, and Nivolumab in chemorefractory MMRp mCRC patients	Ongoing
NCT03626922	Ib	Single arm, treatment with Pembrolizumab plus Pemetrexed and Oxaliplatin in MSS chemorefractory mCRC patients	Ongoing

Table 1: ***Summary of clinical trials investigating chemotherapy combination or sequence with ICIs in unselected or mismatch repair proficient (pMMR) metastatic colorectal cancer (mCRC) patients.*** *MSS: microsatellite instability; mPFS: median Progression-free survival; ORR: overall response rate; OS: overall survival; BICR: Blinded Independent Central Review; mDoR: median duration of response; irRC: immune-related Response Criteria. References to published results of the listed trials are present in the text. *In case a control arm is present, results are expressed as experimental arm (containing ICB) vs control arm. Adapted from: Amodio V-Vitiello PP et al, Br J Cancer 2024.*

3 AIM OF THE STUDY

The vast majority of CRCs are not eligible to immunotherapy and are thus lacking the long lasting anticancer effects of ICIs[150]. In a previous work we have demonstrated that priming treatment with temozolomide increases mutational load and boosts immunogenicity by adaptive inactivation of MMR in MGMT-deficient MSS CRCs[40]. This raises the possibility to exploit the mutagenic effect of chemotherapy with the aim to increase the neoantigen load and foster immune surveillance. However, the mutagenic potential of temozolomide is hampered by MGMT enzymatic activity, which is preserved in the majority of MSS CRCs[40,151]. Therefore, the identification of more widely applicable chemotherapeutic regimens capable of impacting on tumor immunogenicity is necessary. Among the cytotoxic agents, cisplatin stands out as a good candidate to combine with temozolomide. We hypothesized that the concurrent treatment with TMZ and CDDP may result in MMR impairment as a convergent adaptation to the repeated exposure to these two alkylating agents, potentially resulting in drug-related hypermutation while providing tolerance to the treatment, similarly to what we observe with TMZ treatment in MGMT-deficient tumors[145]. In particular, it has been shown that the activation of base excision repair (BER) by the cytosines flanking CDDP-induced DNA interstrand cross-links leads to futile cycles of mismatch repair[43,152], that in part mediate CDDP cytotoxic effects. As matter of fact, MMR deregulation has been directly associated to decreased sensitivity to CDDP[42,153–155]. Interestingly, MSH2 promoter hypermethylation has been correlated with the efficacy of platinum-based chemotherapy in ovarian cancer, supporting the concept that MMR downregulation modulates platinum sensitivity in clinical settings[156,158,160].

The main goal of this study was to test whether the combination of two different alkylating agents, temozolomide and cisplatin, is truly able to generate hypermutation and increase neoantigen burden in a translationally relevant model of pMMR CRC with intact MGMT function. Moreover, we aimed to dissect the causative role of the chemotherapy-induced mutations by following the immunoediting process *in vivo* and analyzing changes in the immune fitness of cancer cells expressing treatment-induced neoantigens. Of note, in order to detect the peculiar immunogenic features of the temozolomide and cisplatin combination, the experimental treatment was compared with the standard-of-care chemotherapeutic agents used in CRC treatment, 5-fluorouracil, oxaliplatin, and irinotecan. Finally, with the aim to also identify non-antigen dependent mechanisms of immune sensitization elicited by the combination,

we also performed simultaneous chemo-immunotherapy with cisplatin, temozolomide and an anti-PD1 agents in mice models bearing chemotherapy-naïve established tumors.

Overall, the final purpose of this proof-of-concept study was to investigate, from a preclinical point of view, whether a rationally designed combination of cytotoxic agents might increase immunogenicity and extend the fraction of CRC patients eligible for immunotherapy.

4 RESULTS

Workflow to validate the immunogenic potential of chemotherapy priming

To study how chemotherapy-induced mutations impact immunogenicity, we designed a workflow involving both *in vitro* and *in vivo* experiments of mouse pMMR CRC cells. In parallel, we also tested a breast cancer murine cell line, with the aim to exclude histology or model-specific effects. We tested cisplatin (CDDP) and temozolomide (TMZ) as single agents or in combination. In parallel, for the CRC model we also examined the impact of 5-fluorouracil (5FU), oxaliplatin (Oxa), or irinotecan (more specifically SN38, its most active metabolite), which represent the backbone of medical treatments for advanced CRC, individually or in combination (FOLFOXIRI triplet), the most intense treatment regimen used in CRC [136]. To mimic the intermittent exposure of cancer cells to chemotherapy agents in the clinical setting, cells were treated in a pulsatile fashion by alternating 2 days of treatment and 3-5 days of recovery without treatment for a total of 12 cycles, using clinically relevant concentrations of the cytotoxic agents (**Figure 4**) [157].

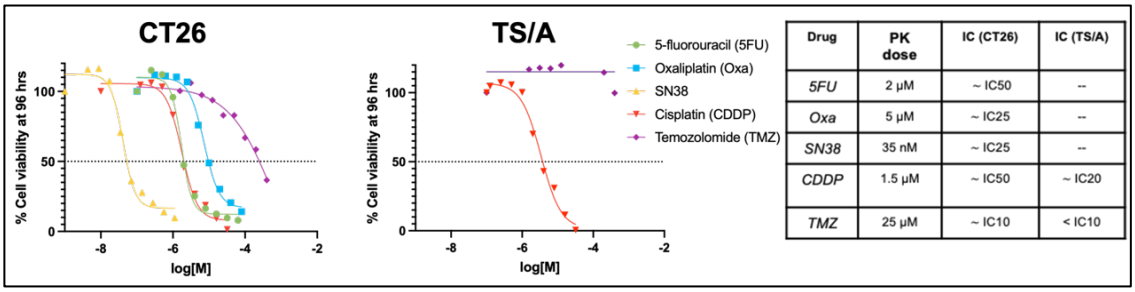

Drug	PK dose	IC (CT26)	IC (TS/A)
5FU	2 µM	~ IC50	--
Oxa	5 µM	~ IC25	--
SN38	35 nM	~ IC25	--
CDDP	1.5 µM	~ IC50	~ IC20
TMZ	25 µM	~ IC10	< IC10

Figure 4: In vitro sensitivity and selected concentrations of CRC and breast murine cell lines to the cytotoxic agents used in the study. *Sensitivity of CT26 and TS/A cell lines to the cytotoxic drugs used in this study was assayed after a short-term treatment (96 hrs). The clinically-relevant concentrations (PK dose) used for the long-term pulsatile treatment correspond to an inhibitory concentration (IC) between 20% and 50% for all the drugs, with the exception of TMZ to which CT26 and TS/A are resistant at the clinically relevant concentration used. See methods for details.*

Whole exome sequencing (WES) at different time points and concurrent subcutaneous injection in immunodeficient and immunocompetent mice were exploited to monitor mutations and test the immunogenicity of cancer cells after treatment with cytotoxic agents, respectively (**Figure 5**). In particular, we used the exome data to identify the mutations acquired upon treatment with cytotoxic agents or vehicle control (T1-T0). We later followed the fate of these treatment-induced mutations in tumors derived *in vivo* in either immune deficient or competent mice (T2-NODSCID and T2-BALB/c, respectively). Additionally, we evaluated the predicted the acquired neoantigens based on whole exome and RNA sequencing data, as previously reported[88].

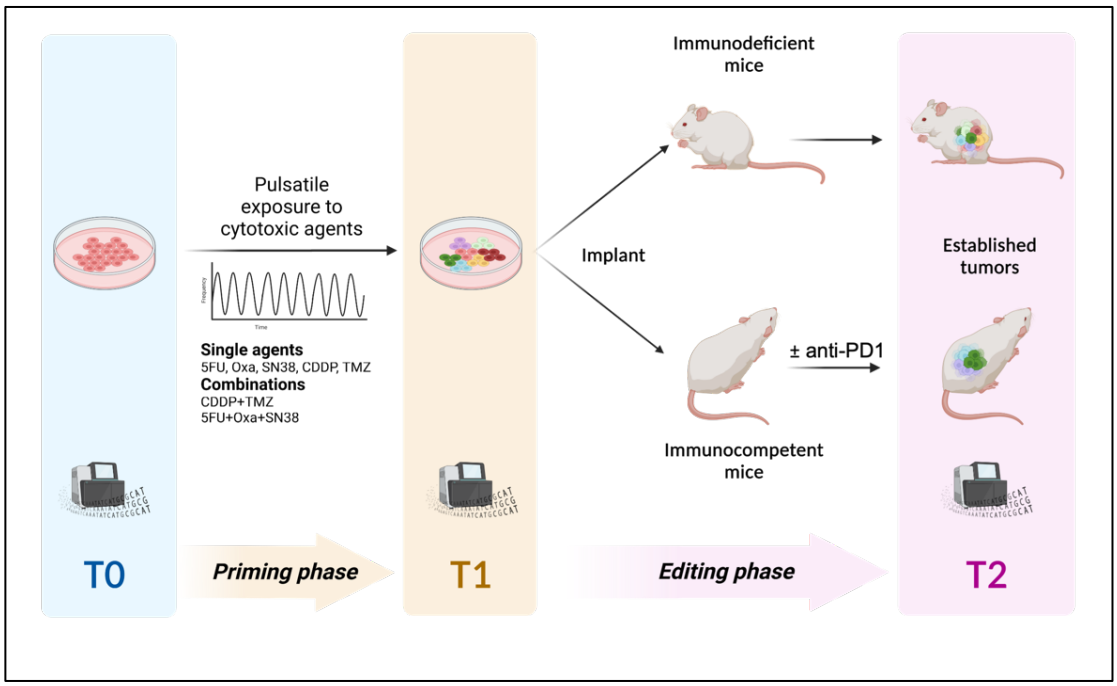

Figure 5: Schematic representation of the experimental workflow. *Syngeneic murine CRC and breast cancer cells were treated with TMZ and/or CDDP at clinically relevant concentrations in a pulsatile schedule (2 days treatment followed by drug washout and cell passaging) for a total of 12 in vitro treatment cycles (priming phase). Drug concentrations were: 25 μM for TMZ; 1.5 μM for CDDP. Additionally, CRC cells were also treated with the standard-of-care cytotoxic agents: 2 μM for 5FU; 5 μM for Oxa; 35 nM for SN38. Primed cells were kept in drug-free medium for two passages and then injected subcutaneously into immunodeficient and immunocompetent mice to study the extent of immunological control induced by treatment with chemotherapeutic agents (editing phase). Whole exome sequencing (WES) was performed at baseline (T0), at the end of the in vitro priming phase (T1) and on established tumors at the end of the in vivo challenge phase (T2).*

Combinatorial treatment with CDDP and TMZ increases clonal and subclonal mutational and neoantigen burden

WES analysis on samples collected at the end of the *in vitro* priming unveiled that treatments with chemotherapeutic agents at clinically relevant doses were generally associated with an increase in TMB with respect to baseline (**Figure 6A-B**). Interestingly, in both CRC (CT26) and breast cancer (TS/A) models, the CDDP-TMZ combination was the most effective treatment in inducing clonal and subclonal mutations (**Figure A-B**) (cut-off for clonality set at 10% allele frequency, see Methods). The increase in TMB was driven mainly by the acquisition of single nucleotide variants (SNVs) (**Figure 6C-D)**, while modulation of indels was negligible (**Figure 6E-F)**. Of note, the mutagenic potential of the FOLFOXIRI triplet in the CRC model was in line with that of each single drug administered alone (**Figure 6A**).

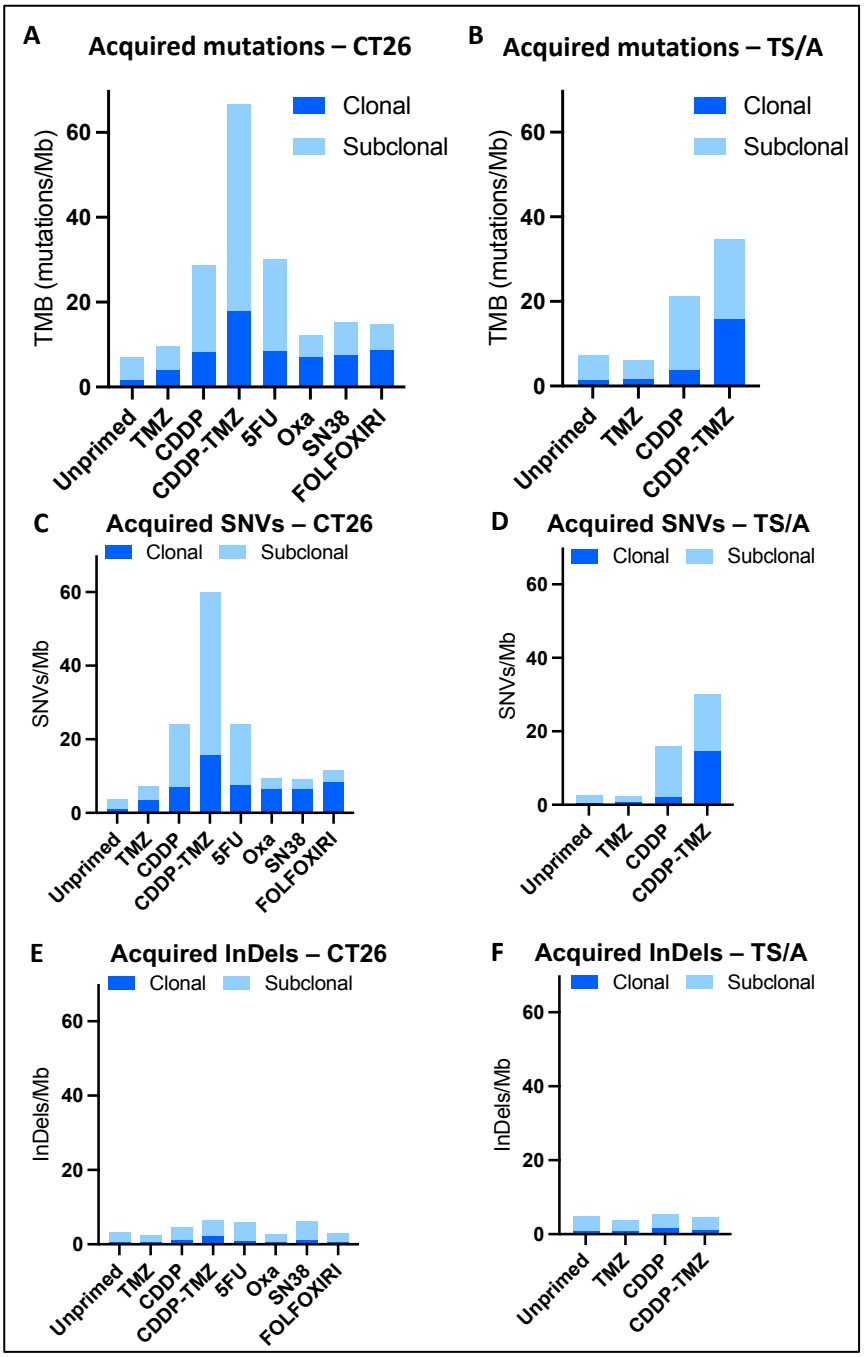

Figure 6: Combinatorial treatment with CDDP and TMZ causes clonal and subclonal hypermutability, with preferential accumulation of SNVs in both CT26 and TS/A. *(A) TMB increase (intended as the sum of SNVs and InDels) upon in vitro chemotherapy priming in CT26. (B-C) SNV (B) and InDels (C) levels of CT26 cells after 12 cycles of treatment with the indicated drugs used as single agents or combinations. (D) TMB increase (intended as the sum of SNVs and InDels) upon in vitro chemotherapy priming in TS/A. (E-F) Specific levels of SNVs (E) and InDels (F) according to the priming treatment in TS/A. Results represent only the acquired mutations compared to baseline (T0).*

Next, employing a computational workflow that we previously developed to predict neoantigens from sequencing data [88], we found that CDDP-TMZ was also the most effective combination in increasing predicted neoantigen levels, driven mainly by the

acquisition of SNVs (**Figure 7**).

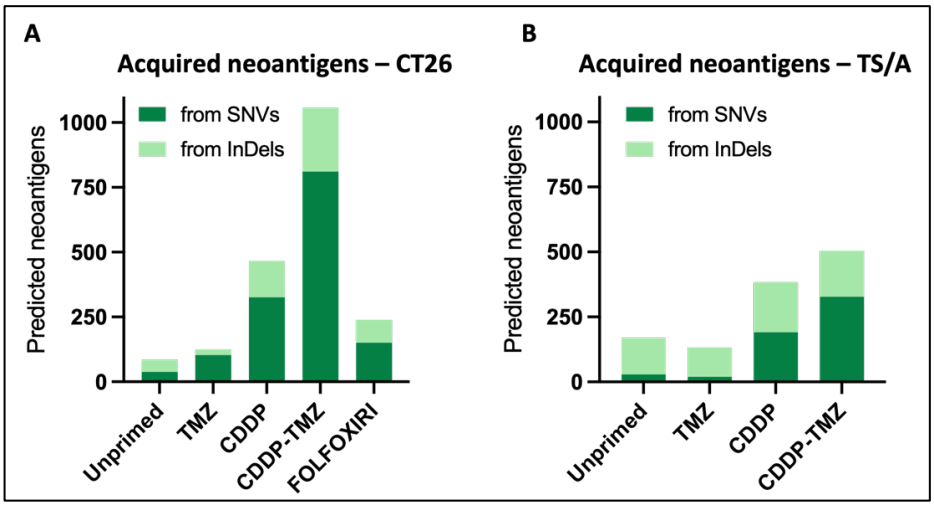

Figure 7: Prediction of acquired neoantigens derived from chemotherapy treatment. *(A) Neoantigens derived from SNVs and InDels in CT26; (B) Neoantigens derived from SNVs and InDels in TS/A (see methods for details).*

In addition, we assessed the impact of CDDP-TMZ treatment on mutational processes by mutational signature analyses (**Figure 8A**). This revealed the co-occurrence of the mutational signature SBS11 (associated to treatment with TMZ) and SBS31/35 (associated to treatment with platinum agents) [63] in both CT26 and TS/A cells primed with CDDP-TMZ, consistently with the treatment performed. Interestingly, SBS11 did not emerge in cells treated with TMZ as a single agent (**Figure 8B**), suggesting that only CDDP-TMZ treatment triggers the functional impairment of the MMR system that is needed to generate SBS11[35,40].

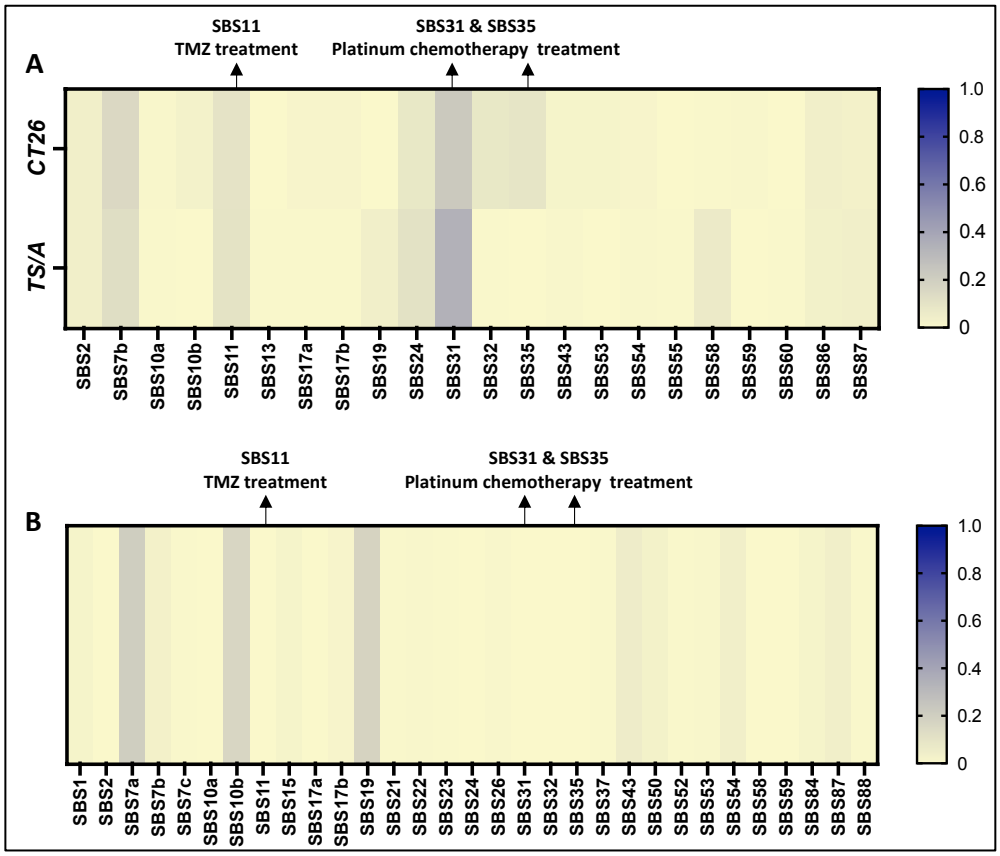

Figure 8: Mutational signatures of the acquired mutations upon chemotherapy. *(A) Heatmap of mutational signatures upon priming with CDDP-TMZ combination in CT26 and TS/A. (B) Heatmap of mutational signatures upon priming with TMZ in CT26. Only COSMIC v 3.3 SBSs with relative value > 0 are represented.*

In line with this result, while MGMT protein levels were stable across all conditions, the expression of the key MMR effectors MSH2 and MSH6 decreased significantly in cells primed with CDDP-TMZ but not with either agent alone or upon *in vitro* priming with 5FU, Oxa, SN38, or their combination (FOLFOXIRI) (**Figure 9A-D**). The abundance of MSH2 and MSH6 were only transiently affected after one single treatment cycle with CDDP-TMZ in CT26 (**Figure 9E**), suggesting that downregulation of MMR proteins occurs over several cycles of treatment. On the other hand, decrease of MSH2 and MSH6 levels persisted twelve weeks after termination of CDDP-TMZ treatment (**Figure 9F**) indicating that, after acquisition, this molecular phenotype is maintained even after the release from drug pressure. Interestingly, protein downregulation of MSH2 and MSH6 was not caused by inactivating mutations of the corresponding genes, since both *Msh2* or *Msh6* coding regions were confirmed to be free from deleterious mutations in all experimental conditions (data not shown).

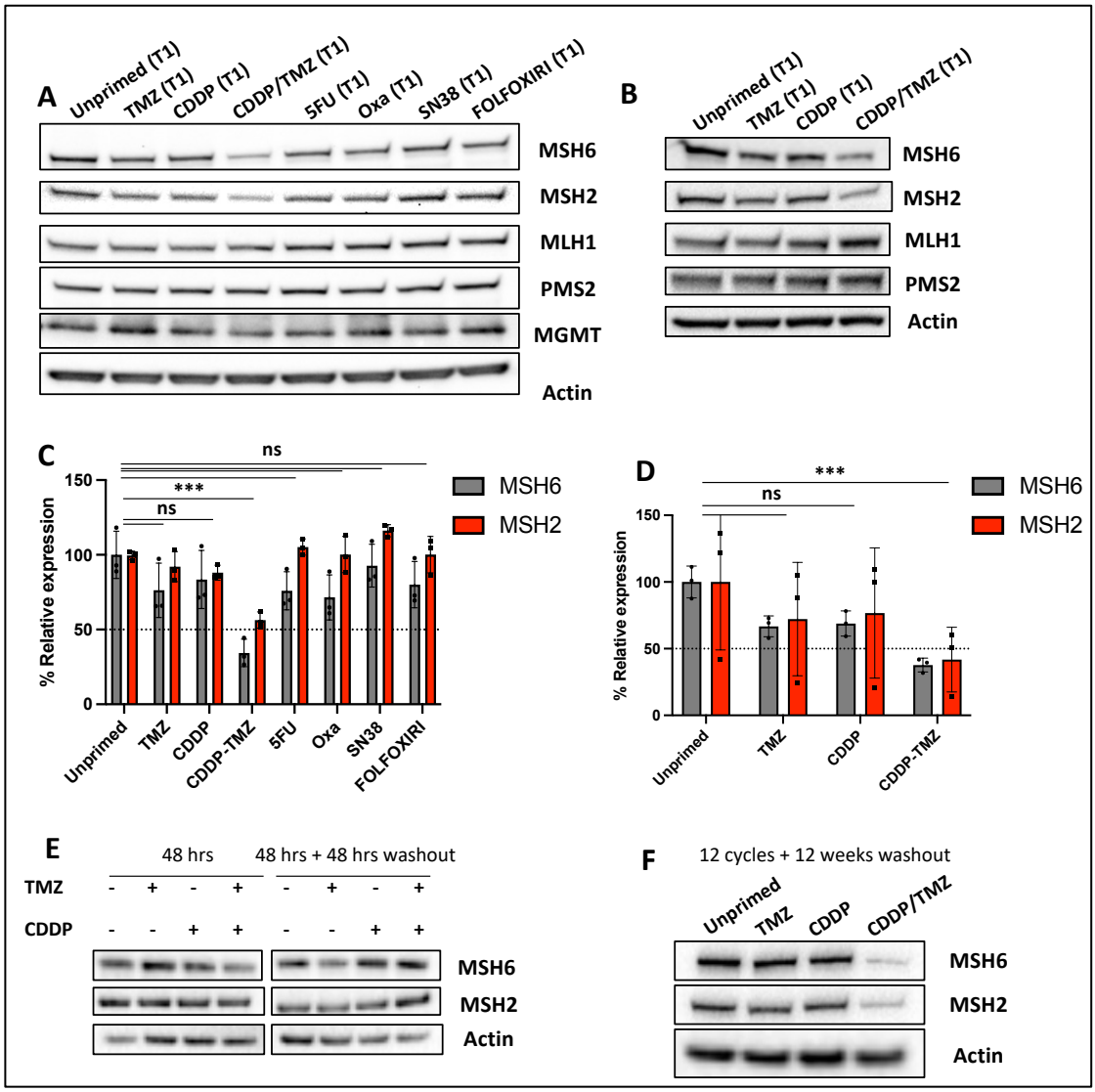

Figure 9: Adaptive downregulation of MSH6 and MSH2 upon priming with CDDP-TMZ combination in CT26 and TS/A. *(A) MGMT and MMR protein expression after 12 cycles of in vitro priming with TMZ, CDDP, CDDP-TMZ, 5FU, Oxa, SN38, and FOLFOXIRI followed by a subsequent washout (T1) in CT26. (B) Quantification of MSH2 and MSH6 expression after priming treatment in CT26. Results represent band intensity average ± SD, actin was used as a loading control for normalization. Statistical significance was evaluated by multiple t-test with FDR approach. ns: not significant; ***p<0.001. (C) MMR protein expression after 12 cycles of in vitro priming with TMZ, CDDP, CDDP-TMZ, followed by a subsequent washout (T1) in TS/A. (D) Quantification of MSH2 and MSH6 expression after priming treatment in TS/A. Results represent band intensity average ± SD, actin was used as a loading control for normalization. Statistical significance was evaluated by multiple t-test with FDR approach. ns: not significant; ***p<0.001. (E) Expression of MSH6 and MSH2 upon short-term treatment with CDDP ± TMZ. Naïve CT26 cells were treated in vitro with the same concentrations of TMZ (25 µM) and CDDP (1.5 µM) for 48 hrs and then kept in drug-free complete medium for additional 48 hrs. (F) CT26 cells primed for 12 cycles with TMZ ± CDDP were kept in culture without additional exposure to treatment for a total of 12 wks.*

Collectively, these results suggest that combined treatment with CDDP and TMZ, but not with standard of care cytotoxic agents used in CRC, leads to adaptive downregulation of MSH2/MSH6 levels and agent-specific clonal and subclonal mutations that are predicted to generate novel neoantigens. The same adaptive

downregulation upon CDDP+TMZ treatment is also observed in a model of breast cancer.

Immune surveillance of cancer cells primed with chemotherapy

To assess whether and to what extent priming with CDDP-TMZ affected immune surveillance, CRC CT26 cells were injected subcutaneously into the flank of immunodeficient (NODSCID) and immunocompetent syngeneic (BALB/c) mice after *in vitro* chemo-priming, together with cells treated for an equivalent amount of time (12 weeks) with vehicle alone that served as negative control (unprimed cells) (Figure 5). Cells treated with FOLFOXIRI were also included in the experiment. Priming with both combinatorial chemotherapy regimens induced a modest tumor growth delay in immunodeficient mice (**Figure 10A**). When injected in syngeneic immunocompetent mice, CRC cells primed with CDDP-TMZ were completely rejected by 31 out of 40 mice**,** while CRC cells treated with FOLFOXIRI grew slower as compared to unprimed cells but we did not observe any rejection (**Figure 10B**). Moreover, while the growth delay resulted in a measurable but minimal survival benefit in both immunodeficient and immunocompetent mice injected with FOLFOXIRI primed cells (**Figure 10C-D**), the survival outcome was striking among immunocompetent mice injected with CDDP-TMZ primed cells. Interestingly, the rejecting group remained tumor-free and alive for more than 100 days, until the end of the experiment (**Figure 10D**). Intrigued by these results, we repeated the injection of CDDP-TMZ-primed cells in a larger number of immunocompetent syngeneic mice, and confirmed the pattern of rejection and the overall high rejection rate (>75%) observed in the first experiment (**Figure 10E-F**).

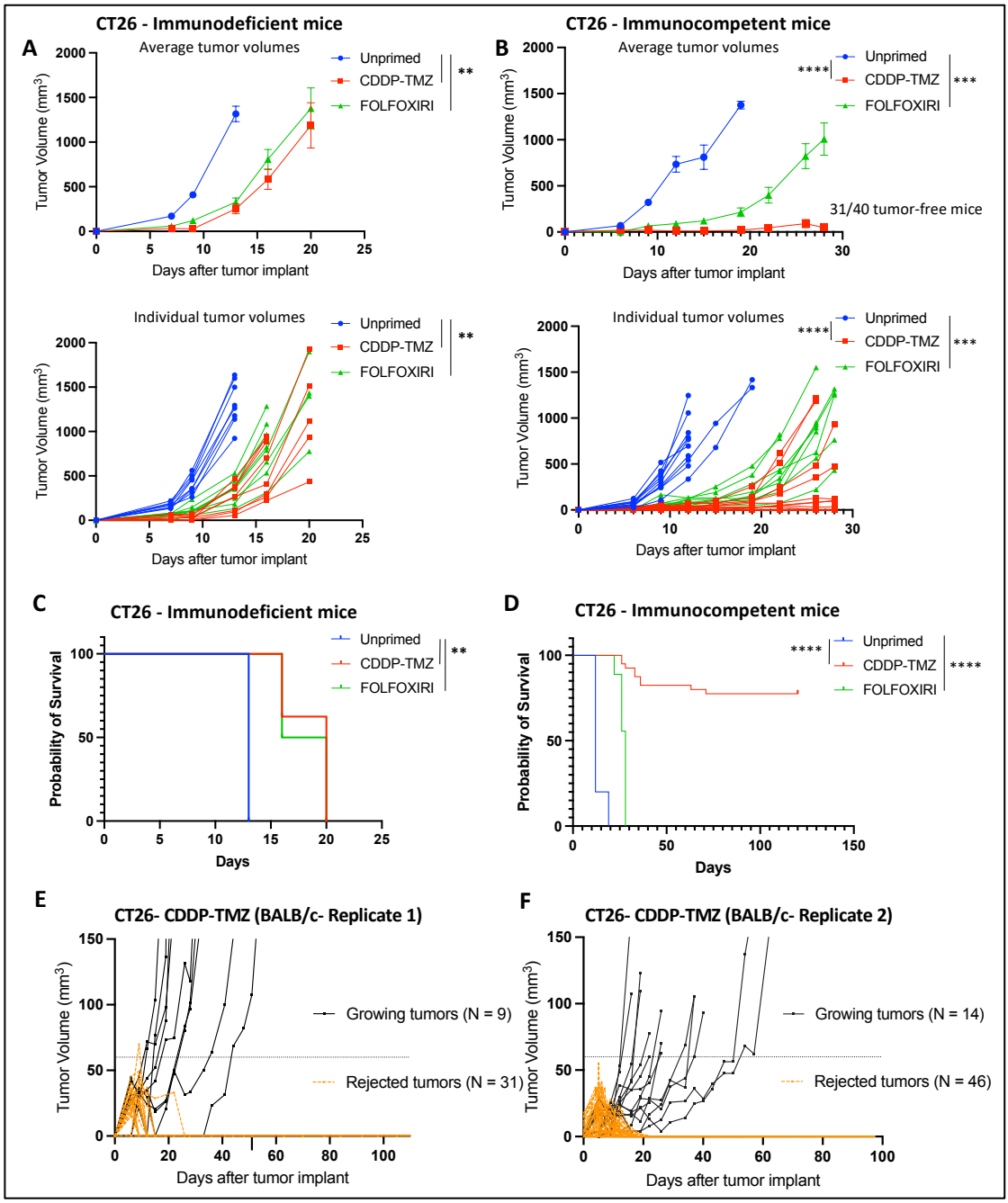

Figure 10: Cancer cells primed with CDDP-TMZ are immunogenic in syngeneic mice models of colorectal cancer. *(A) Average (up) and individual (down) volumes of tumors derived from unprimed, CDDP-TMZ-primed and FOLFOXIRI-primed CT26 cells grown in immunodeficient (NODSCID) mice. (B) Average of tumor volumes from unprimed, CDDP-TMZ-primed and FOLFOXIRI-primed CT26 injected in immunocompetent (BALB/c) mice. (C) Survival curves for unprimed and primed tumors in immunodeficient and (D) immunocompetent mice. (E) Detailed view of CDDP-TMZ-primed tumor volumes from single mice in immunocompetent BALB/c model from panel B. (F) Biological replicate of subcutaneous injection of 5 x 10^5 CDDP-TMZ-primed CT26 cells/mouse in a new batch of 60 BALB/c mice. A total of 5 x 10^5 cells were injected in the flank of each mouse. Tumor growth was monitored three times per week and reported in the graph as average of mice tumor volumes (mm^3) ± SEM. Each experimental group included at least 8 animals. Statistical significance evaluated by Mann-Whitney test and log-rank test: ns: non-significant; **p<0.01; ***p<0.001; ****p<0.0001.*

Of note, neither TMZ or CDDP used as single priming agents led to growth control or rejection in immunocompetent and immunodeficient mice (**Figure 11**), thus confirming

that the immunogenic features are specifically induced by the combined CDDP-TMZ treatment.

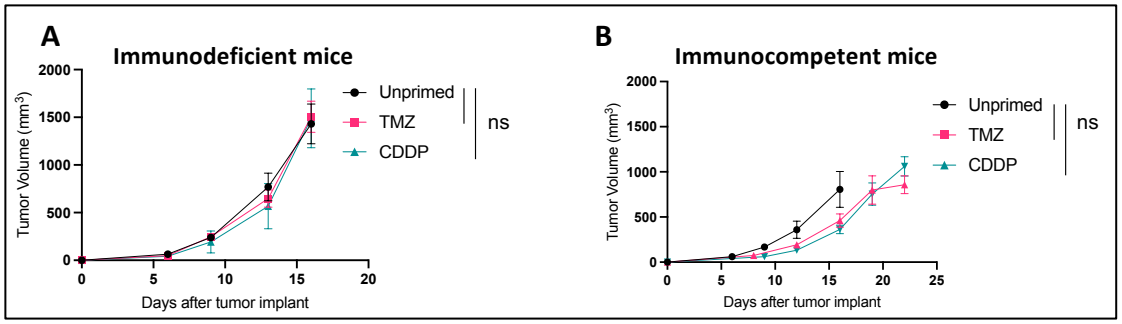

Figure 11: In vivo growth of CT26 cells primed with TMZ or CDDP used as single agents. *(A) Average tumor volumes for subcutaneous tumors derived from unprimed, TMZ-primed and CDDP-primed CT26 grown in immunodeficient (NODSCID); (B) Average tumor volumes for subcutaneous tumors derived from unprimed, TMZ-primed and CDDP-primed CT26 grown in immunocompetent (BALB/c) mice. Statistical significance evaluated by Mann-Whitney test: ns: non-significant.*

In order to expand the significance of the findings, we also performed the *in vivo* experiments with the breast cancer model (TS/A). Both primed and unprimed TS/A were tumorigenic when injected orthotopically in the mammary fat pad of immunodeficient and syngeneic immunocompetent mice, with no spontaneous rejections evidenced, likely reflecting a lower acquisition of immunogenic mutations compared to CT26 (**Figure 12A-B**). However, treatment with anti-PD1 induced a significant immune surveillance only towards CDDP-TMZ-primed tumors, which translated to a 25% complete tumor regression rate (**Figure 12C-F**). As already shown for CT26, also in TS/A the priming with TMZ or CDDP used as single agents was not immunogenic and did not sensitize tumors to anti-PD1 treatment.

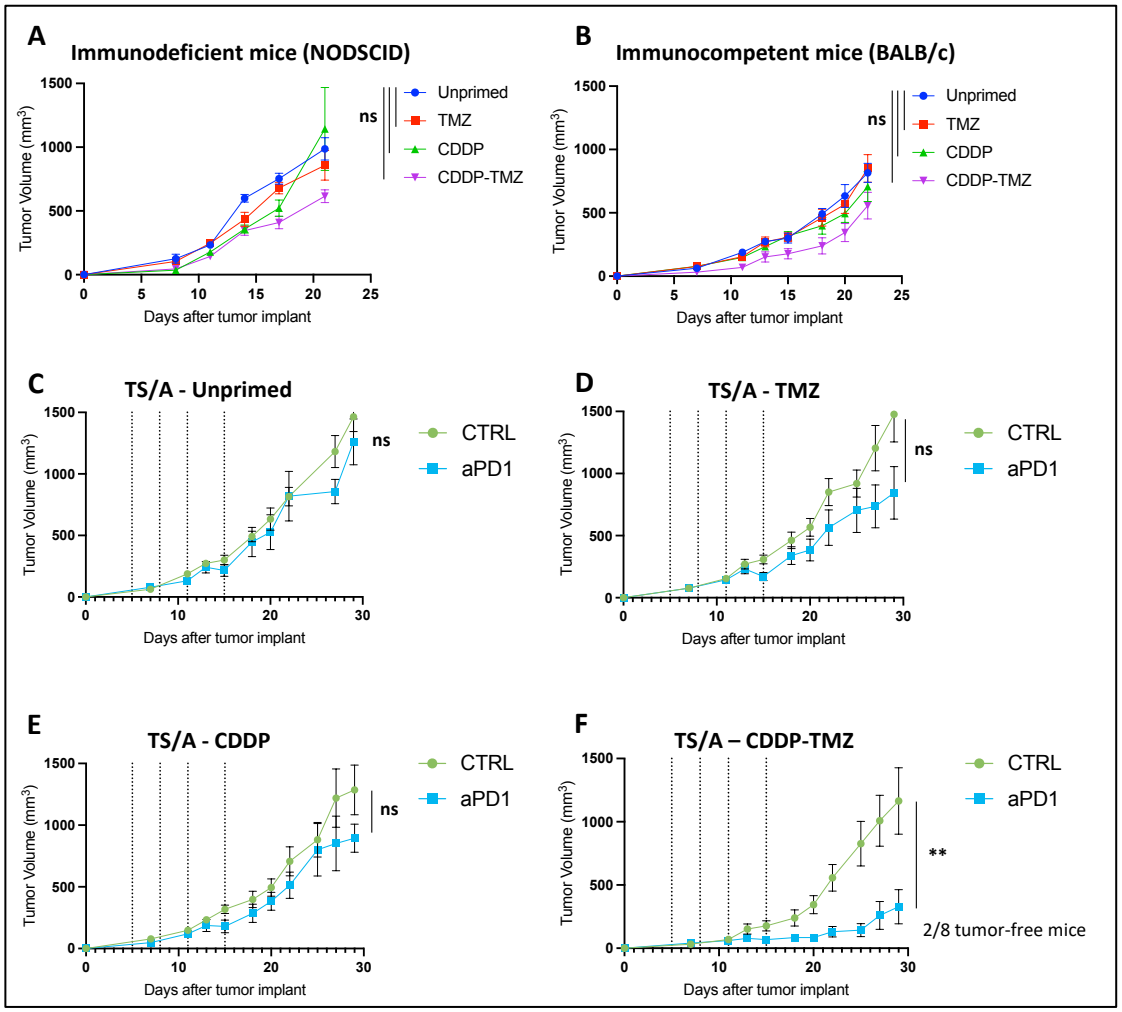

Figure 12: Breast cancer cells primed with CDDP, TMZ, or their combination are tumorigenic in mice and only CDDP-TMZ primed cells respond to anti PD-1. *1 x 10^5 unprimed or primed TS/A cells were injected 1:1 in PBS:Matrigel in the mammary fat pad of the lower right mammary gland of immunodeficient (A) or immunocompetent (B) mice. (C-F): Response of unprimed and primed TS/A to ICB treatment using anti-PD1. 1 x 10^5 unprimed or primed TS/A cells were injected 1:1 in PBS:Matrigel in the mammary fat pad of the lower right mammary gland of immunocompetent mice. At day 5, when all tumors were palpable, mice were randomized to receive either anti-PD1 or control. ICB treatment was effective only in tumors primed with CDDP-TMZ combination, in which 25% (2/8) mice exhibited complete regression. Tumor growth was monitored three times per week and reported in the graph as average of tumor volumes (mm^3) ± SEM. Each experimental group included at least 7 animals. Statistical significance evaluated by Mann-Whitney test at the last available day for the control arm. ns: non-significant; **p<0.01.*

As with regards to the survival of mice injected orthotopically with TS/A breast cancer after priming, the only group experiencing a significant benefit was the CDDP-TMZ-priming condition, in which we observed long-term survival for mice with responding tumors (**Figure 13**). Altogether, these findings confirm the immunogenic potential of combined CDDP-TMZ priming in both CRC and breast cancer models.

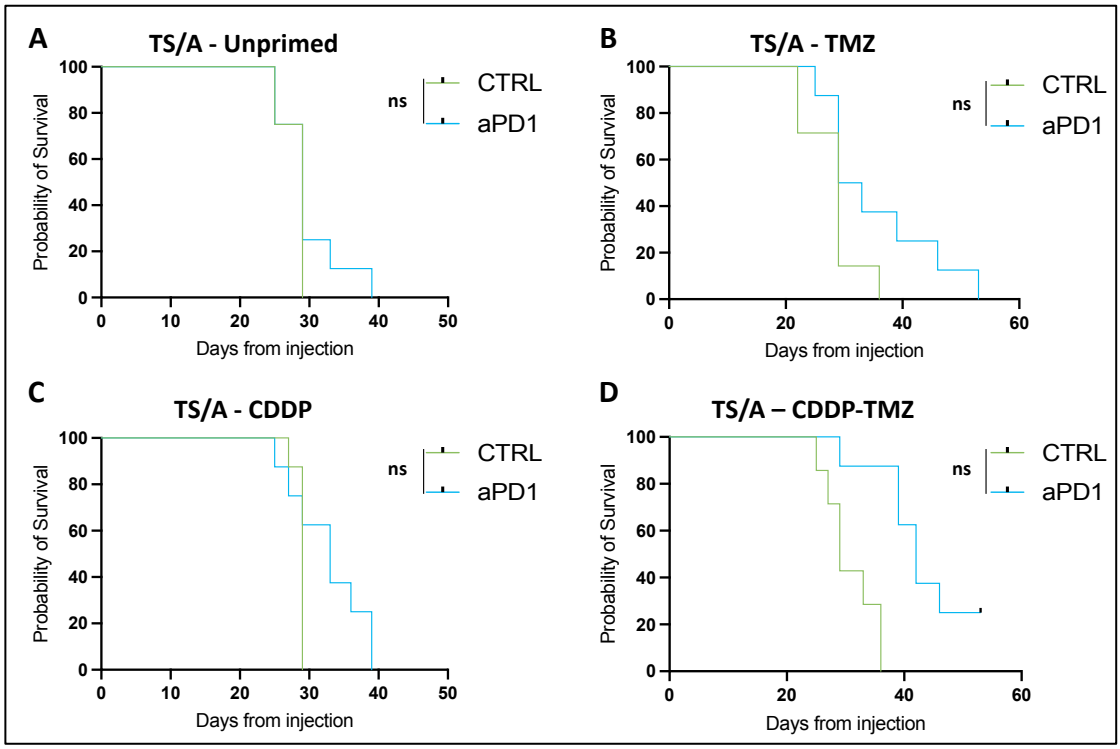

Figure 13: Survival analysis of the mice bearing orthotopic tumors derived from unprimed or primed TS/A. *(A-C) Treatment with anti-PD1 (aPD1) has no effect on survival for mice bearing unprimed or single agent primed TS/A; (D) Treatment with aPD1 significantly extends survival of CDDP-TMZ-primed tumors, with the 2 mice bearing tumors in complete response still alive at the end of the experiment. Statistical significance evaluated by log-rank test: ns: non-significant; ***p<0.001.*

Rejection of CDDP-TMZ-primed tumors is mediated by CD8+ T cells and confers protective anti-tumor memory

After having ascertained the efficacy of CDDP-TMZ priming in inducing hypermutation and immunogenic features in both colorectal and breast cancer models, we decided to investigate the mechanisms underlying this phenotype. In order to identify the main immunological mediators triggered by CDDP-TMZ priming, we performed subcutaneous injection of CDDP-TMZ-primed CT26 cells in mice in which CD8+ and/or CD4+ T cells were selectively depleted with blocking antibodies (**Figure 14A**). Briefly, mice were randomized into 4 arms: vehicle (CTRL), anti-CD8 blocking antibody (aCD8), anti-CD4 blocking antibody (aCD4), and a combination of the two (aCD8 + aCD4). Overall, at the end of the experiment, the proportion of tumor-free mice in the different arms was 10 out of 14 in the CTRL arm, 8 out of 8 in the aCD4 arm, and 0 out of 8 both in the aCD8 and aCD8+aCD4 arms (**Figure 14B-C**). Specifically, the depletion of CD8+ T cells promptly induced rapid tumor outgrowth by day 23 in both single aCD8 and combined aCD8+aCD4 treatment arms. In the control arm only 4/14 (29%) mice displayed tumor growth scattered over time, while the

remaining 10/14 (71%) mice remained tumor free until the end of the experiment (**Figure 14C**), consistently with the rejection rate previously shown (Figure 10E-F). No tumor growth occurred in the presence of anti-CD4 antibodies, likely reflecting an enhancement of CD8+ T cell-mediated immune response induced by the depletion of CD4+ T regulatory cells, as previously described[159,161].

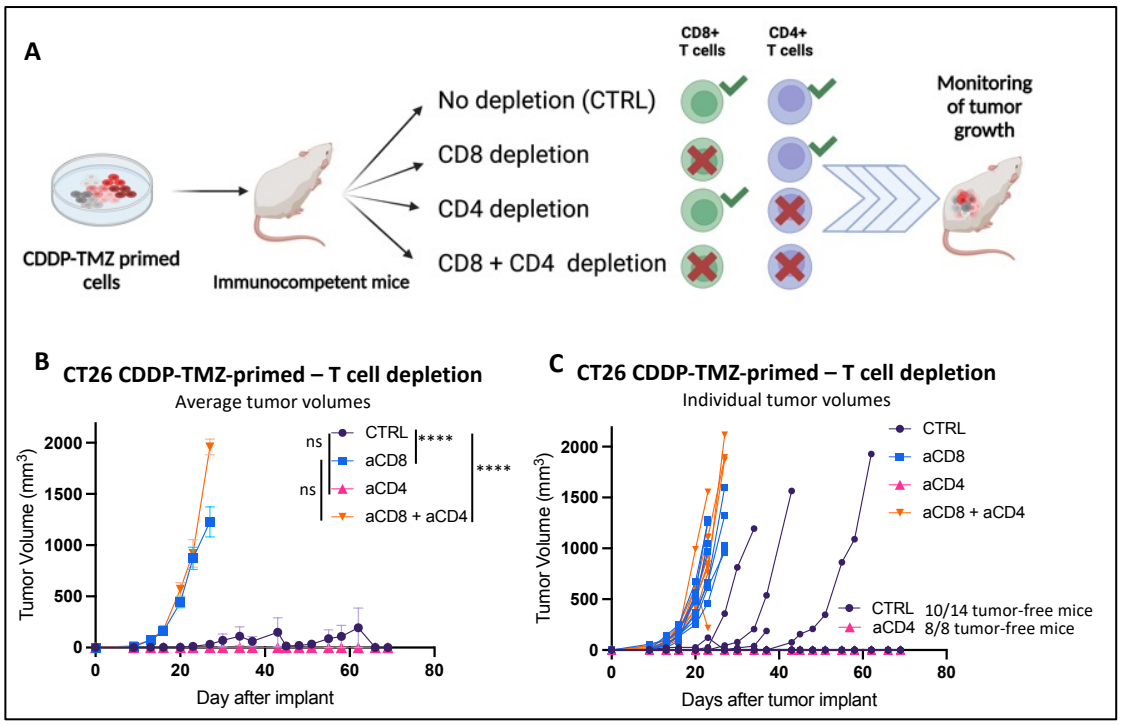

Figure 14: Rejection of CDDP-TMZ-primed tumors is mediated by CD8+ T cells. *(A) Graphical summary for CD8+ and/or CD4+ T cells depletion experiment. A total of 5 x 10^5 CDDP-TMZ-primed CT26 cells were injected in the flank of each immunocompetent (BALB/c) mouse. Mice were randomized into 4 treatment groups: control (CTRL) receiving only the vehicle; CD8 depletion (aCD8) receiving murine anti-CD8a antibody; CD4 depletion (aCD4) receiving murine anti-CD4 antibody; CD8 and CD4 depletion receiving both murine aCD8 and aCD4 antibodies. (B-C) Tumor growth of CDDP-TMZ-primed CT26 tumors upon T cell depletion. (B) Average of mice tumor volumes (mm^3) ± SEM ; (C) tumor volumes from individual mice. Each experimental group included at least 8 animals.*

Furthermore, we evaluated the immunological memory elicited by the rejection of chemotherapy primed cells. To achieve this, we rechallenged mice which had previously rejected CDDP-TMZ-primed tumors with cells primed with either TMZ or CDDP as single agents, as well as unprimed cells. We found that a previous rejection of CDDP-TMZ-primed cells induced significant protection against tumor formation across all experimental conditions (**Figure 15A**). This result implies an activation of the immune system also against pre-existing shared (i.e., non-chemotherapy-induced) cancer neoantigens, leading to immune recognition and elimination of unprimed cells. To further investigate whether a pre-existing immunological memory against primed

cells is necessary to achieve immune surveillance towards unprimed cells, we designed an additional experiment in immunocompetent tumor-naïve mice in which the injection of CDDP-TMZ-primed cells was paralleled by a concomitant contralateral injection of unprimed cells. With this purpose, we tested three sets of conditions: (i) bilateral injection of unprimed cells, (ii) bilateral injection of CDDP-TMZ-primed cells, and (iii) injection of CDDP-TMZ-primed and unprimed cells on opposite flanks of the same mice (**Figure 15B**). Interestingly, the growth of unprimed CRC cells was unaffected by the contralateral presence of CDDP-TMZ-primed or unprimed cells (**Figure 15C**).

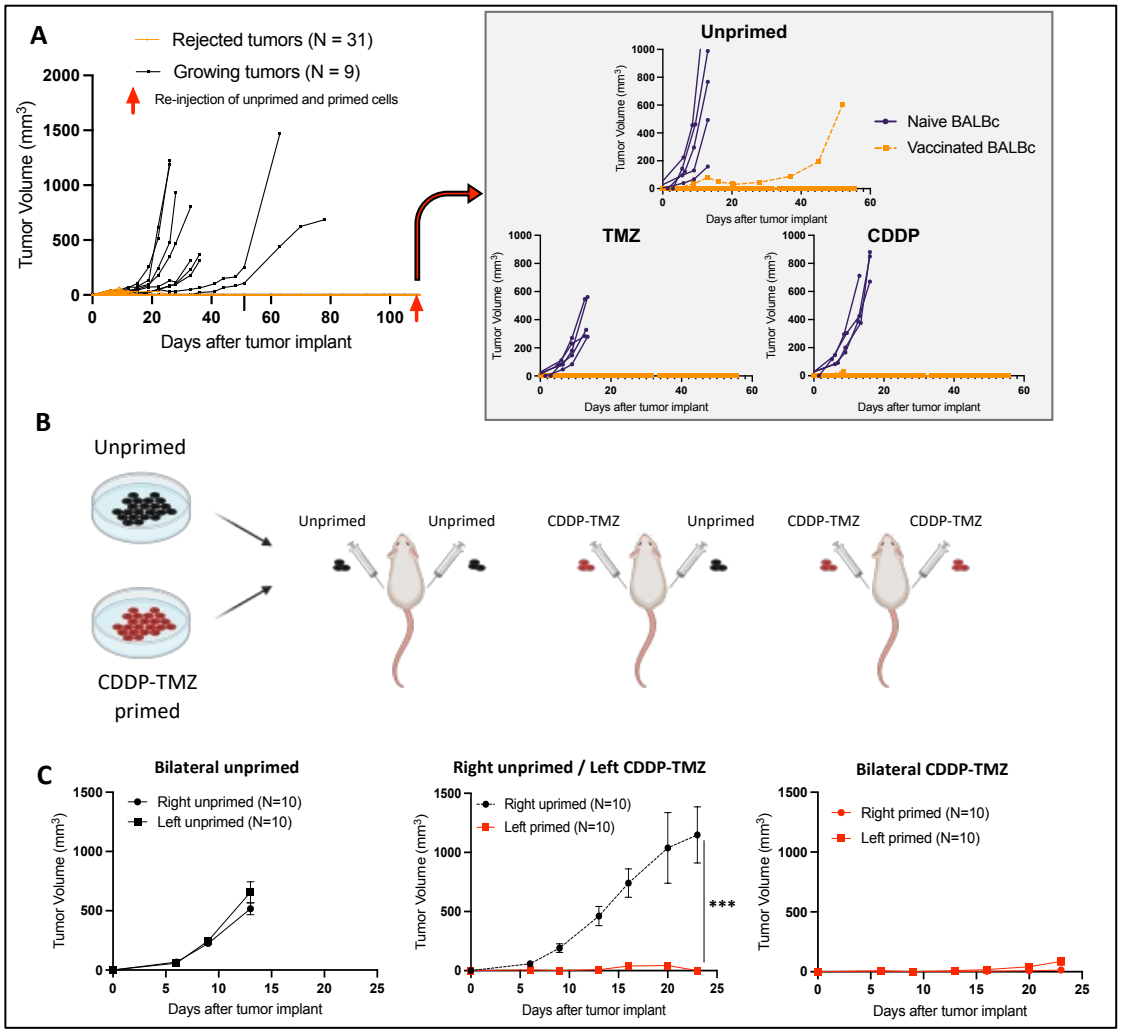

Figure 15: Immunological memory elicited by rejection of chemotherapy-primed tumors. *(A) Effect of rechallenge in immunocompetent mice that previously rejected CDDP-TMZ-primed tumors. Subsequent inoculation of CT26 unprimed or primed with single agent TMZ or CDDP (red arrow) in previously challenged (vaccinated) BALB/c mice, compared with naïve BALB/c mice. N = 10 in vaccinated BALB/c group, N = 5 in naïve BALB/c group. (B-C) Simultaneous injection of unprimed and CDDP-TMZ-primed cells does not lead to immune surveillance towards unprimed cells (B) Graphical summary: simultaneous injection of unprimed and CDDP-TMZ-primed CT26 in the two flanks of the same animal, in three different sets of conditions: bilateral unprimed cells, bilateral primed cells, contralateral unprimed and primed cells. A total of 2.5 x 10^5 cells were injected in each flank to parallel the total number of cells used in the other experiments; (C) Growth of CDDP-TMZ-primed and unprimed cells after bilateral injection. Tumor growth was monitored two times per week and reported in the graph as single mice or average of*

*mice tumor volumes (mm^3) ± SEM. Each experimental group was composed of 10 animals. Statistical significance evaluated by Mann-Whitney test: ns: non-significant; ***p<0.001.*

These results indicate that the establishment of a specific immune response against antigens induced by CDDP-TMZ is driving tumor control by CD8+ effector T cells. Furthermore, immune rejection elicited by CDDP-TMZ leads to immunological memory against both unprimed and chemotherapy-primed cancer cells. This protective effect was abolished in case of a simultaneous injection of primed and unprimed cells in the same mice.

Chemotherapy-induced mutations are actively immunoedited and shape the immune fitness of CDDP-TMZ primed tumors

Next, to study how genomic alterations induced by CDDP-TMZ priming affected tumor immune surveillance, we monitored the fate of individual mutations induced by chemotherapy in cells transplanted in parallel in immunodeficient and immunocompetent mice (Figure 5). Our rationale was that chemotherapy-driven mutations retained in tumors that grew in both immunodeficient and immunocompetent mice could be considered immunologically neutral (immune neutral mutations). Conversely, mutations that underwent negative selection exclusively in immunocompetent mice were likely immunologically eliminated (immunoedited mutations, **Figure 16A**).

Interestingly, we found that only CDDP-TMZ-induced mutations were significantly and recurrently immunoedited in immunocompetent mice whereas the proportion of negatively selected mutations in the single agent TMZ or CDDP, as well as in the FOLFOXIRI combination arms was negligible (**Figure 16B**).

To study the mutational processes that are more likely to be associated to the onset of mutations undergoing active immune selection, we compared the distribution of mutational signatures in the subgroups of immune edited or neutral mutations. Among those undergoing immunological editing we found an enrichment of mutations located in defined genomic contexts (**Figure 16C-D**). In particular, we noticed that SBS31 (associated to platinum treatment) showed a noticeable enrichment in the group of immune edited mutations, accounting for about 26% of all the mutations in this subgroup, while being virtually absent in the subgroup of immunologically neutral mutations (**Figure 16C**). Conversely, SBS11, which is etiologically linked to TMZ

exposure and is strongly induced by CDDP-TMZ combination, was equally represented in immunologically neutral and edited mutations (**Figure 16D**).

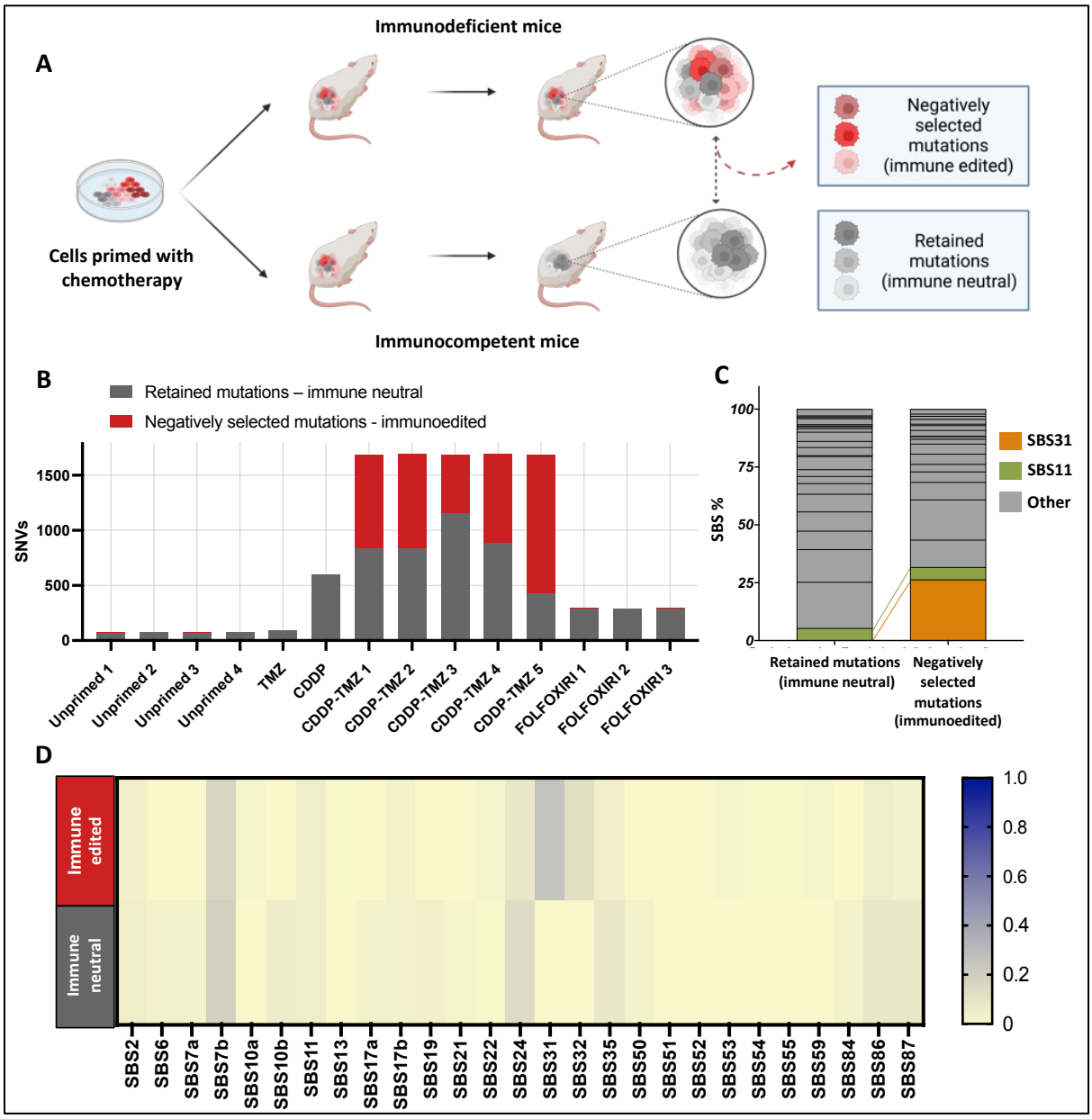

Figure 16: Immunoediting of chemotherapy-induced mutations preferentially involves CDDP-TMZ primed tumors. *(A) Graphical summary: mutations emerging after in vitro priming phase were monitored in tumors grown in immunodeficient and immunocompetent syngeneic mice. Mutations retained in both in vivo models are listed as immune neutral, whereas mutations maintained in tumors grown in immunodeficient mice and negatively selected in immunocompetent mice are indicated as immunoedited. See methods for details. (B) Distribution of immunoedited and immune neutral chemotherapy-induced mutations from single tumors grown in immunocompetent mice across the tested priming treatments (unprimed, TMZ single agent, CDDP single agent, CDDP-TMZ combination, FOLFOXIRI combination). (C) Relative distribution of SBS31 and SBS11 in immune neutral and immunoedited groups of mutations. (D) Heatmap of the relative abundance of SBS mutational signatures (COSMIC v3.3) in the subgroup of immune neutral and immunoedited mutations. Only SBSs with relative value >0 in one of the conditions are represented.*

Additionally, with the aim of dissecting the role of neoantigens in immune surveillance, we focused on the neoantigens deriving from chemotherapy-induced mutations whose transcripts are consistently expressed in cancer cells after the priming treatment, by selecting a threshold of > 10 Fragments Per Kilobase Million (FPKM) (**Figure 17A**). By deploying the same workflow used to define immunoediting of mutations, we discovered that more than 60% of the expressed predicted neoantigens arising upon chemotherapy-induced mutations (CDDP-TMZ priming) were recurrently and selectively lost in tumors grown in immunocompetent animals (**Figure 17B**). Intrigued by these results, we next assessed the allelic distribution of the mutations from which the predicted neoantigens are derived, and found a statistically significant enrichment for a higher allelic frequence in the group of immunoedited compared to the immune neutral neoantigens (**Figure 17C**), underlining the impact of the clonality of neoantigens in their immunogenicity. The same holds true when the distribution of the allelic frequency of mutations that were recurrently immunoedited was considered (median VAF: 11.49% vs 4.76% for immunoedited and immune neutral mutations, respectively) (**Figure 17D**). Immunoescaped CDDP-TMZ-primed tumors did not display genetic alterations known to be implicated in evasion from immune surveillance such as loss of HLA, alterations in the antigen presenting machinery, and/or in interferon gamma signaling pathway (see Methods for the list of genes). All these findings suggest a perturbation of cancer evolution and immune modulation of the clonal architecture of primed cells, as previously shown[162].

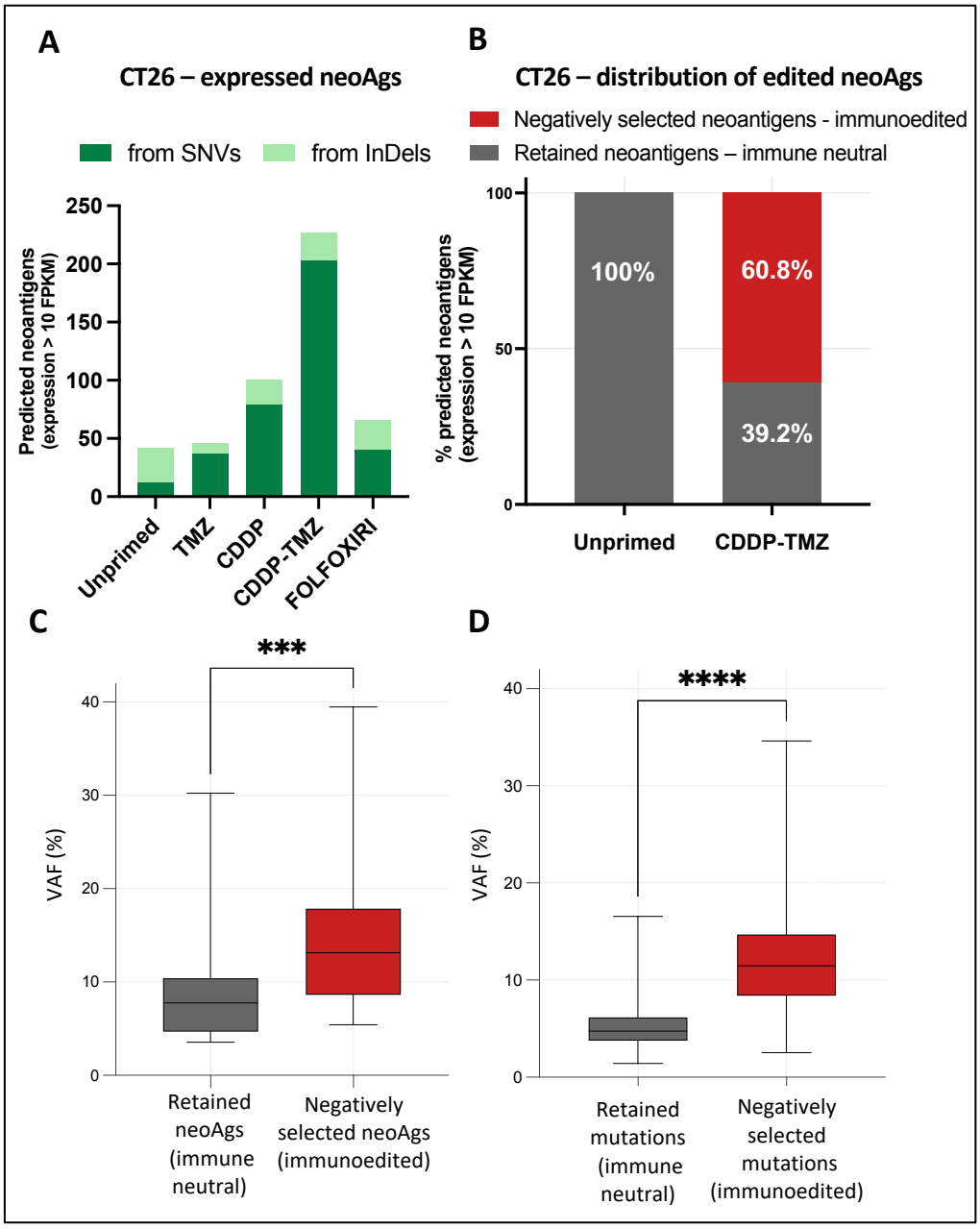

Figure 17: Impact of clonality on the immunoediting of chemotherapy-induced mutations and neoantigens. *(A) Prediction of acquired neoantigens originating from SNVs and InDels in CT26 after the priming treatment (T1), filtered for expression levels > 10 FPKM. (B) Relative distribution of expressed acquired neoantigens undergoing immune selection, filtered for expression levels > 10 FPKM. Results represent the median values of mutations/neoantigens derived from at least 3 different tumors grown in immunocompetent and immunodeficient mice for each condition. (C) Distribution of the allelic frequency of the mutations associated to expressed (FPKM>10) predicted neoantigens. D) Distribution of the allelic frequency for all the immune neutral and the immunoedited chemotherapy-induced mutations. Statistical significance evaluated by Mann-Whitney test: ***p<0.001, ****p<0.0001. FPKM: Fragments Per Kilobase Million.*

Finally, with the aim to intercept antigen-independent mechanisms of immune sensitization associated with chemotherapy, we monitored the transcriptional phenotype of CT26 cells after the priming phase at the moment of *in vivo* injection (T1) (**Figure 18**). Although several immune-related gene sets were transcriptionally

enriched in chemotherapy-primed cells -including tumor necrosis factor (TNF) alpha and interferon (IFN) gamma and alpha response pathways- the analyses did not identify transcriptional changes specific for CDDP-TMZ-primed cells, the only ones undergoing immune-mediated rejection. The fact that these pathways were equally represented in cells primed with different single agents and combinations, while immune surveillance is only evident for CDDP-TMZ-primed cells, suggests that transcriptional rewiring is unlikely the sole responsible for the immunological phenotype. While this finding does not rule out the impact of antigen-independent mechanisms in the immune surveillance of CDDP-TMZ-primed cells, it indicates that these are not sufficient to drive the phenotype. Altogether, these results support the immunological relevance of chemotherapy-induced mutations in driving the immune response.

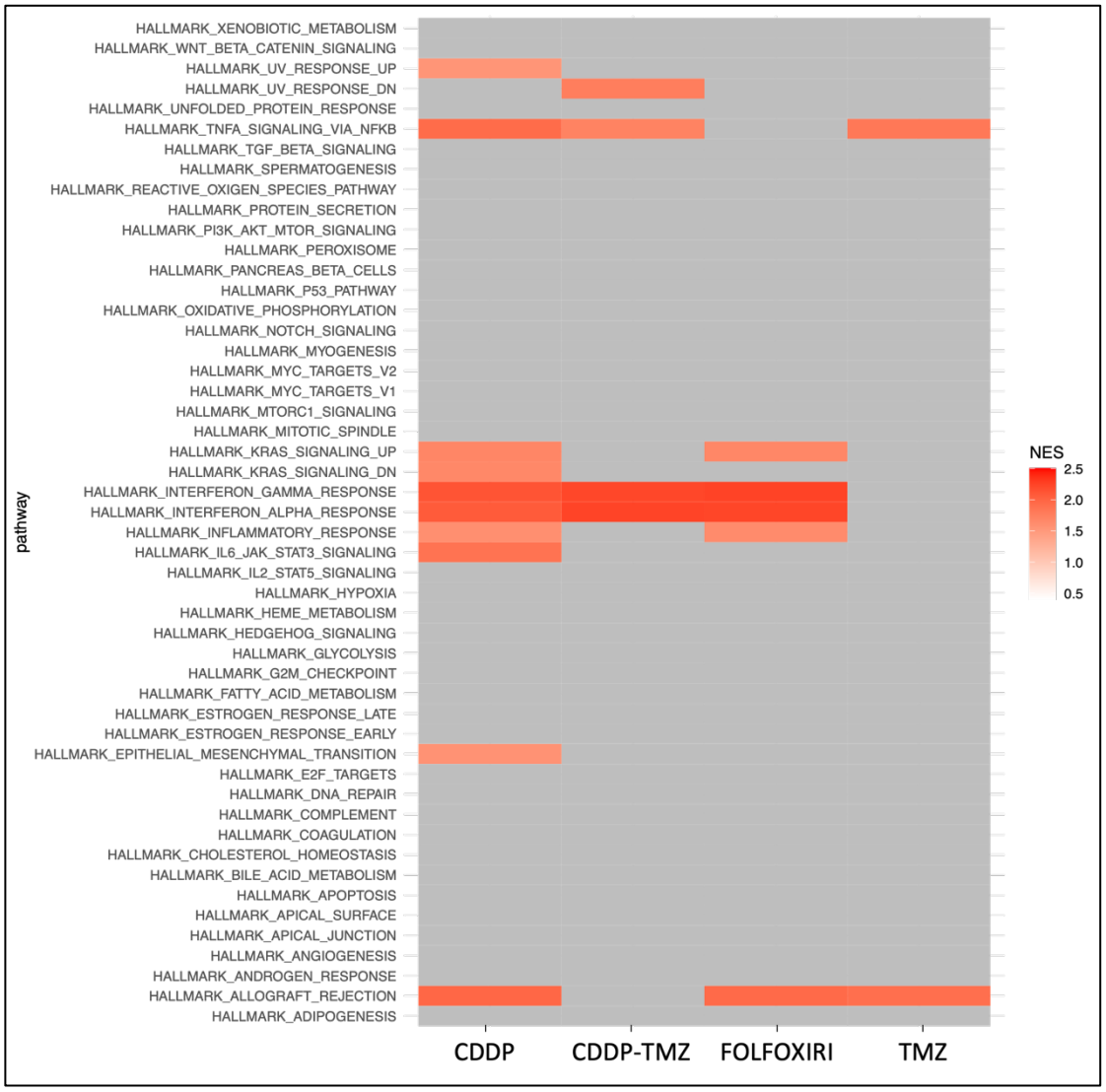

Figure 18: Enrichment of immune-related gene sets is a common feature for cytotoxic priming treatments. *Gene set enrichment analysis (GSEA) with MSigDB hallmarks gene sets of CT26 cells was performed after the priming period and prior to inoculation into mice. Only significant differences in normalized enriched score (NES) computed versus the unprimed condition were evidenced (scales of red), while non-significant differences are shown in grey. Three different replicates for conditions were sequenced and used for the analyses.*

CDDP-TMZ combination treatment is immunogenic *in vivo* and synergizes with ICB

We next studied the impact of the CDDP-TMZ combination therapy on immune surveillance *in vivo* by performing treatments of chemo-naïve syngeneic CRC tumors in immunocompetent mice. Mice with established tumors were randomized into 4 treatment groups: vehicle control, aPD1 treatment alone, CDDP + TMZ combination, aPD1 + CDDP + TMZ combination (**Figure 19A**). Anti-PD1 treatment alone had no effect on tumor growth compared to the control, whereas CDDP-TMZ treatment was associated to a statistically significant growth delay under treatment, despite no clear volumetric decrease compared to baseline (**Figure 19B**). Of note, all tumors treated

with CDDP+TMZ+ ICB underwent volumetric shrinkage and half of them were completely rejected, with mice remaining tumor-free until the end of the experiment (**Figure 19C**).

To investigate the effects of chemotherapy on T cell infiltration, we performed an immunohistochemistry (IHC) analysis for T cell markers on tumor samples collected at the end of chemotherapy treatment with CDDP-TMZ, while samples obtained from the control arm served as controls. The same analyses were conducted on immunoescaped tumors excised at the time of relapse after the end of the chemo-immunotherapy (**Figure 19D**). The number of T regulatory cells (T-regs, Foxp3+) was significantly decreased by the CDDP-TMZ combination, whereas a significant enrichment of T-regs was present at the time of relapse after the end of chemo-immunotherapy (**Figure 19E**). We observed CD8+ T cytotoxic cell infiltration increase upon chemotherapy treatment which was however not statistically significant with respect to control, while a significant decrease was observed for tumors that relapsed after concomitant chemo-immunotherapy, confirming their effective immune escape (**Figure 19F**). Levels of CD4+ T helper cells were not affected across the different conditions (**Figure 19G**).

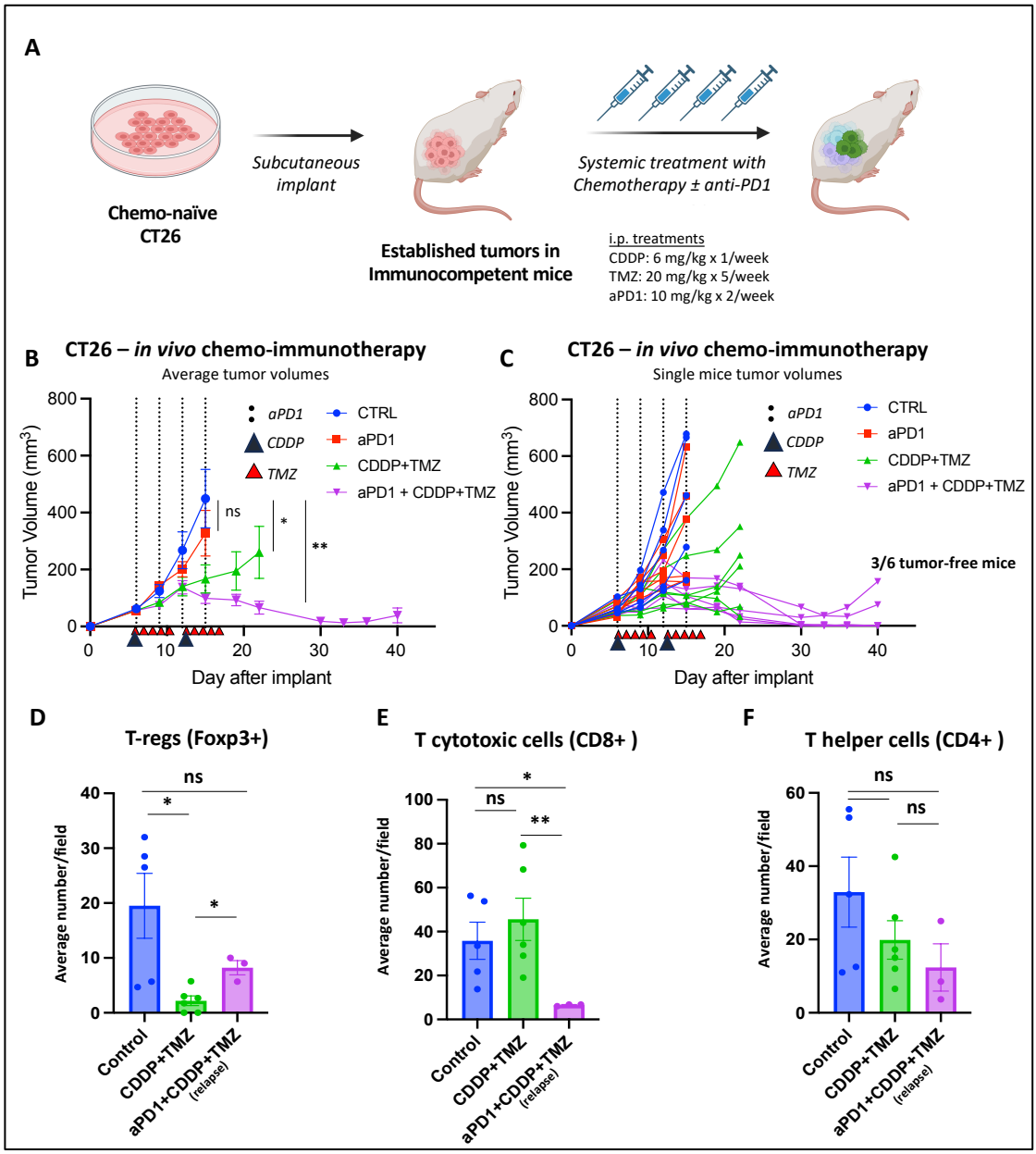

Figure 19: In vivo concomitant treatment with CDDP and TMZ is immunogenic and induces complete regressions in combination with anti-PD1. *(A) Graphical summary: a total of 5 x 105 chemotherapy-naïve CT26 cells were injected in the flank of immunocompetent mice until measurable tumors were established (average of tumor volumes > 50 mm3). After that, mice were randomized in 4 groups: vehicle control, anti-PD1 (aPD1), CDDP+TMZ and CDDP+TMZ+aPD1. (B) Tumor growth of naïve CT26-derived tumors treated in vivo with aPD1, CDDP+TMZ, or their combination (aPD1+CDDP+TMZ). The combined chemo-immunotherapy (aPD1+CDDP+TMZ) induces deep shrinkage in all tumors. CDDP was administered ip at 6 mg/kg once a week (black arrowhead), TMZ was administered ip for 5 consecutive days a week at 20 mg/kg, for a total of 2 weeks (red arrowhead). Anti-PD1 was administered ip every 2 other days at 250 µg/mouse for a total of 4 doses (dashed line). Results represent average tumor volumes (mm3) ± SEM. Statistical significance evaluated by Mann-Whitney test at the last available day for the control arm. ns: non-significant; *p<0.05; **p<0.01. (C) Single mice tumor volumes of naïve CT26-derived tumors treated in vivo with aPD1, chemotherapy (CDDP+TMZ), or their combination (aPD1+CDDP+TMZ). The combined chemo-immunotherapy induces complete tumor regressions in half of the mice. (D-F) Quantification of T cell subpopulations (Foxp3+/T-regs, CD8+, CD4+) in tumors obtained at end of the treatment (Control and CDDP+TMZ arm) or at the moment of tumor relapse after initial tumor control (aPD1+CDDP+TMZ arm). Each dot represents the average number of positive cells/ 40X field in at least 4 different fields for each slide. Results represent average number ± SEM. Statistical significance evaluated with Welch's t test. *p<0.05; **p<0.01.*

Collectively, these results indicate that *in vivo* treatment with CDDP-TMZ for two weeks has immunogenic potential, and that combining such chemotherapy with PD1 blockade achieves long-lasting complete tumor rejections.

5 DISCUSSION

Immunotherapy has revolutionized the treatment and survival expectations of cancer patients. However, only 5% of metastatic CRC patients are currently eligible to treatment with immune checkpoint inhibitors[136]. The identification of strategies capable of converting *cold* non-immunogenic into *hot* immunogenic tumors sensitive to immunotherapy is an area of active investigation. This work was conceived to assess the potential of a rationally designed combination of commonly used chemotherapeutic agents to enhance immunogenicity of CRC cells, leading to immune-mediated tumor growth control. We employed an intermittent *in vitro* treatment with clinically relevant drug concentrations to mimic the pulsatile exposure of cancer cells to cytotoxic agents which is performed during clinical treatment.

While combinations of immune checkpoint inhibitors with current standard-of-care chemotherapy regimens have shown limited clinical benefit in CRC[140,163,164], we found that concomitant treatment with CDDP and TMZ induces a remarkable increase in TMB in a murine CRC model, coupled with an increase in the predicted neoantigen load. Of note, the combination leads to immune recognition of primed cells and to a high rate of complete rejections (75% in the CT26 model). Mechanistically, the mutational increase may be favored by the adaptive downregulation of the MSH6/MSH2 heterodimer (MutS-alpha complex), thus confirming our initial hypothesis regarding the potential induction of MMR downregulation as a convergent DNA repair adaptation upon combination with CDDP and TMZ [43,145]. Interestingly, we found that inactivation of MMR did not involve genetic alterations in the coding sequence of *Msh2* and/or *Msh6* genes at least in the models employed in our study. This is suggestive of an inheritable epigenetic mechanism leading to protein downregulation of MSH2/MSH6. Notably, in this system MMR downregulation does not lead to the emergence of mutational signatures associated with MMR deficiency. However, it has been shown that a partial impairment of the MMR system is needed for the establishment of the alkylating mutational signature (SBS11)[40,63]. Furthermore, the prevalent increase of SNVs over InDels differs from what would have been expected if complete MMR deficiency had occurred [63]. Importantly, since we set a relatively high threshold of allele frequency for mutational calling (see Methods), it remains possible that we failed to detect the dMMR mutational signatures due to their sublconal level or the prevalence of other mutational events. It should also be noted that, as we and others previously reported, a long

timeframe is needed for the accumulation of MSI prototypic mutational signatures even when the MMR system is genetically inactivated [88,165].

Among the different chemotherapeutic agents we tested, effective immune surveillance was observed only upon CDDP-TMZ priming, and this was also replicated in the poorly immunogenic breast cancer model. Interestingly, in both colorectal and breast cancer models the induction of clonal mutations following the CDDP-TMZ priming was similar (about 15-18 mutations/Mb) and both models showed the same mutational scars. This result compares favorably with other attempts to increase immune responsiveness using alkylating agents, in which rejection was much less consistent across models[166]. Of note, while we only investigated the combination of cisplatin with TMZ, given the overlapping role of MMR in mediating both cisplatin and carboplatin cytotoxicity and treatment resistance[156,170], the elicited phenotype may be similar using carboplatin as the combination partner.

Importantly, CDDP-TMZ mediated immune surveillance is dependent upon CD8+ T cell, suggesting a central role for MHC class I - associated neoantigens in driving the anticancer response. Additionally, successful rejection of CDDP-TMZ-primed cells is protective towards subsequent injection of both primed and unprimed tumor cells, pointing at cross-activation against pre-existing non-chemotherapy-induced cancer neoantigens. Interestingly, while mice that have previously rejected CDDP-TMZ-primed tumors are able to reject unprimed tumors, a simultaneous injection of primed and unprimed cells on the two flanks of the same immunocompetent mice leads to the unrestricted growth of the unprimed tumors. Although not experimentally investigated, we could speculate that the difference in the immune surveillance in these two contexts depends on the intercurrent time between the immunological priming and the challenge with the unprimed CT26. In particular, it has been already shown that vaccination with mutagenized cancer cells expressing novel neoantigens provides protection towards the growth of parental cancer cells devoid of the acquired neoantigens[172]. This effect is, however, only reported when mice are vaccinated 10 days before the injection of the parental non-immunogenic cells[172]. A potential mechanism leading to such cross reactivity is the so-called *antigen spreading*[174]. Another potential clue derives from a recent work from the Spranger's group[176]. This paper shows how strongly immunogenic neoantigens (in our case the ones induced by chemotherapy treatment) may stimulate the cross-priming of weaker pre-existing clonal neoantigens, thus increasing their immunogenicity and potentiating immune surveillance. However, since primary

antigen-specific T cell responses typically peak at 9-11 days[178], as also shown in our data, it is likely that a concurrent bilateral injection of unprimed and primed CT26 cells does not provide enough time for the cross-presentation to take place, resulting in immune control of the more immunogenic (primed) tumor and the immune escape of the less immunogenic (unprimed) countepart.

The absence of rejections upon FOLFOXIRI (the most intense regimen used in the clinic for mCRC [136]), may provide a biological explanation to the limited clinical benefit observed by the combinations of immune checkpoint inhibitors with 5FU-based chemotherapy regimens in mCRC [140,163,164]. In this regard, however, the relevance of other immunoregulatory activities elicited by the treatment should not be excluded.

To establish a functional link between chemotherapy-induced mutations and immune surveillance, we investigated the immune fitness of the cancer subclones by monitoring them in the presence or absence of a functional immune system. Our findings revealed that the CDDP-TMZ combination triggers a mutational spectrum that is subjected to immune depletion, while CDDP and TMZ monotherapy or the FOLFOXIRI regimen do not. The robust immunoediting of CDDP-TMZ-induced mutations in tumors that evade immune surveillance, together with the absence of other known genetic events responsible for immune escape, suggests the selection of less immunogenic cancer cell subclones as a mechanism of immune evasion in accordance with previous studies [162]. Moreover, our data points to a direct relationship between the clonality of CDDP-TMZ-induced variants and their immunogenicity. This is in accordance with previous observations linking neoantigen clonality to antitumor immune response[107,108,167].

An accepted model of clonal evolution under the selective pressure of cytotoxic agents (including platinum agents) involves an initial clonal restriction due to the elimination of chemotherapy-sensitive subclones, followed by clonal expansion of resistant or tolerant subclones[44,168]. Accordingly, we postulate that the most immunogenic mutations induced by the CDDP-TMZ arose early in drug tolerant/resistant subclones, which would account for their higher clonal level at the end of the priming phase. We also found that the immunoedited mutations are associated to the SBS 31 mutational signature. In particular, SBS 31 alone encompasses more than one quarter of all the immunoedited mutations, while this signature is virtually absent in the group of immunologically neutral mutations. This observation is relevant in light of the etiology of SBS 31, which has been experimentally correlated to platinum treatment [63,169]. Importantly, the immunogenic potential of mutations associated with SBS 31 and its

enrichment in immunoedited mutations could be linked to an early mutational event, explaining the observed clonal abundance and, consequently, its immunogenic relevance.

The *in vivo* combination of anti-PD1 with CDDP-TMZ on chemotherapy-naïve tumors led to a significant shrinkage in all mice, and complete cure in half of them, a remarkable finding with potential clinical relevance.

We acknowledge that the present study has some limitations. The *in vitro* models that we used artificially separate the priming from the editing phase. While this limits how the approach parallels potential treatments schedules, it also provides a critical advantage. Specifically, the *in vitro* priming experiment was designed to effectively explore the impact of the quantity and the quality of chemotherapy-induced mutations on the immunogenicity of CRC cells in terms of *antigenicity*. The fact that combinatorial treatment with CDDP-TMZ induces active immunosurveillance also when priming is performed *in vivo* confirms the potential clinical relevance of our findings. As matter of fact, while chemotherapy-induced hypermutation likely plays a relevant role in rejection of *in vitro* primed tumors, additional antigen-independent immunoregulatory mechanisms, such as the reduction of immune suppressive T-regs, may be in place when treatment is administered *in vivo*, potentially enhancing the anticancer activity of the chemo-immunotherapy regimen.

Another important consideration is that the negative impact of chemotherapeutic treatment on the functionality of the immune system is not negligible in cancer patients. However, we and others recently provided evidence that at least TMZ treatment alone does not hamper the efficacy of subsequent immunotherapy cycles [40,41]. Relatedly, before the advent of immunotherapy, several phase II trials have shown the feasibility and tolerability of CDDP and TMZ combinations in metastatic melanoma and glioblastoma multiforme [171,173,175,177]. Accordingly, an ongoing phase II trial is investigating the triplet combination of CDDP, TMZ, and nivolumab (anti-PD1) in previously treated pMMR mCRC (NCT04457284) with the aim to explore the relationship between induced tumor hypermutation and tumor response.

The broad concept of enhancing the immunogenicity of cancer cells through treatment with alkylating agents is not novel and precedes the development of immune checkpoint inhibitors[179–181]. However, its clinical application has been hindered by the view that the resulting hypermutation is largely subclonal and therefore not immunologically relevant, and possibly even counterproductive for initiating a functional immune

response[37,107]. Nevertheless, chemo-immunotherapy combinations, particularly those containing platinum compounds, are currently standard-of-care in the treatment of NSCLC, esophagogastric and biliary tract cancers[182–184]. Here we provide preclinical evidence showing how the administration of CDDP-TMZ in a translationally-relevant schedule can lead to drug-induced immune surveillance. Our evidences indicate that active immunoediting of chemotherapy-induced mutations is ultimately associated with tumor control, resulting in immune-mediated rejection, along with the establishment of immunological memory.

Overall, these findings provide the rationale for the clinical testing of new combinations of commonly used cytotoxic drugs in immunologically cold pMMR CRCs, which currently lack effective immunotherapy approaches, with the aim to boost immune surveillance through the induction of hypermutation.

6 MATERIALS AND METHODS

Mouse cell lines

CT26 is a murine undifferentiated colon carcinoma cell line obtained from a BALB/c background. CT26 was purchased from ATCC and was cultured in RPMI 1640 10% FBS, 2 mM glutamine and penicillin/ streptomycin (100 units/mL penicillin, 0.1 mg/mL streptomycin). The TS/A breast cancer cell line was established from a moderately differentiated mammary adenocarcinoma that arose spontaneously in a BALB/c mouse[185] and provided by F. Cavallo (Molecular Biotechnology Center, University of Torino). TS/A was cultured in DMEM 10% FBS supplemented with 2 mM glutamine and penicillin/ streptomycin (100 units/mL penicillin, 0.1 mg/mL streptomycin). Before performing the experiments reported in this manuscript, the CT26 and TS/A parental cell lines were injected in the syngeneic background and the resulting tumor was exploited to re-establish *in vitro* a new cell culture. This procedure ensures that the model used is tumorigenic and will not initiate immune surveillance when injected in syngeneic animals. Cells were routinely tested for mycoplasma contamination.

Drug screen of syngeneic cell lines for cytotoxic agents

The sensitivity of CT26 to cytotoxic agents was assayed in short-term (96 hours) proliferation assays. Cells were seeded at $0{,}5x10^3$ cells/well in 200µl of complete medium in 96-multiwell plates at day 0. 12 hours after seeding, serial dilutions of the indicated drugs were added to the cells (ratio 1:2) in technical triplicates, while DMSO-only treated cells were included as controls. Cell viability was assessed after 96 hours by measuring ATP content through Cell Titer-Glo® Luminescent Cell Viability assay (Promega) according to the manufacturer's protocol. Luminescence was measured by the Tecan SPARK M10 plate reader. Cell viability measured for each treatment condition was normalized to viability of DMSO-treated controls. Data represent average ± SD of at least three independent biological replicates.

Long-term *in vitro* treatments

All cytotoxic agents for *in vitro* studies were purchased from Selleckchem: 5-fluorouracil (5FU, Cat. # S1209), oxaliplatin (Oxa, Cat. # S1224), SN38 (Cat. # S4908), temozolomide (TMZ, Cat. # S1237), cisplatin (CDDP, Cat. # S1166).

In vitro priming treatments using TMZ, CDDP, 5FU, Oxa, and SN38 were performed within clinically relevant concentrations [157]. The selected concentrations were in the

range between IC_{25} and IC_{50} in short-term proliferation assays (Figure 4), with the exception of TMZ to which both CT26 and TS/A are largely resistant at clinically relevant concentrations [165]. All the treatments were administered in a pulsatile schedule using treatment 'cycles' (2 days on treatment, followed by a 3 to 5-day treatment washout until reaching about 80% confluence) at each culturing passage, for a total of 12 cycles spanning about 12 weeks. Each passage was performed at 1:10 ratio. The intermittent drug exposure was used to allow for the gradual elimination of sensitive cells with the selection of more tolerant cells at each passage, while avoiding a too stringent selective pressure towards pre-existing cancer subclones completely resistant to cytotoxic drugs. After the last treatment cycle, cells were cultured for at least 2 passages in drug-free complete medium before *in vivo* experiments and genomic or protein analyses.

Western Blot analyses

For western blot assays, cells were cultured in media containing 10% FBS. Proteins were extracted by lysing cell pellets in SDS buffer (50 mM Tris-HCl [pH 7.5], 150 mM NaCl, and 1% SDS). Samples were boiled at 95°C for 10 minutes and sonicated for 15-30 seconds depending on the dimension of the pellet. Eventual residual debris were pelleted by centrifugation and 5 µl of supernatant was used to quantify the protein content. Quantification phase was performed using BCA Protein Assay Reagent Kit (Thermo Scientific). Detection phase was conducted with the enhanced chemiluminescence system (GE Healthcare) and peroxidase-conjugated secondary antibodies (Amersham). Acquisition of the chemiluminescent signal was performed with ChemiDoc Imaging System (Bio-Rad). The primary antibodies used for this assay were: anti-MLH1 (epr3894 from Abcam), anti-PMS2 (163C1251 from Thermo Fisher), anti MSH6 (EPR3945 from Abcam), anti-MSH2 (ab70270 from Abcam), anti-MGMT (MT3.1 from Thermo Fisher), anti-beta Actin (I-19 from Santa Cruz Biotechnology). Band quantification was performed using Image Lab software (Bio-Rad) version 6.1 from images acquired in triplicate.

Animal studies

All animal procedures were approved by the Ethical Commission of the AIRC Institute of Molecular Oncology (IFOM) and by the Italian Ministry of Health. All *in vivo* experiments were executed according to institutional guidelines and international law

and policies and following methods previously described [165]. We used five- to eight-weeks old female BALB/c and NODSCID mice purchased from Charles River (Calco, Como, Italy). Each experiment was performed using at least six mice per group. For subcutaneous injection (CT26), mice were shaved, and 500000 cells resuspended in 100 µl of PBS were injected on the right flank.

For orthotopic injection (TS/A), 100000 cells were injected in 50 µl PBS:Matrigel solution in mammary fat pad of the lower right mammary gland for each mouse. Before injection, cells previously treated *in vitro* were grown for at least 2 passages in absence of treatment to allow for full replicative recovery and elimination of apoptotic cells.

Randomization was used for the experiments in which therapeutic effects had to be evaluated. Tumor size was measured twice a week and volume was calculated using the formula: $V = (d^2 \times D)/2$ (d = minor tumor axis; D = major tumor axis) and reported as tumor volume (mm^3, mean ± SEM of individual tumor volume). Depletion of CD4 and CD8 T cells was performed as previously described [165]. Mouse CD4 depleting antibody (anti-CD4, BioXcell) and mouse CD8a depleting antibody (anti-CD8, BioXcell) were injected intraperitoneally on the same day of tumor inoculation at the dose of 200 µg/mouse, followed by a dose every other 2 days at 100 µg/mouse until the end of the experiment. *In vivo* chemotherapy treatment was started after randomization at an average tumor volume of 50 mm^3 and was administered as follows: cisplatin 6 mg/kg intraperitoneal (i.p.) injection once a week, temozolomide 20 mg/kg i.p. 5 days a week, for a total of two weeks of treatment. ICB was performed as follows: anti-mouse PD1 (aPD1, BioXcell) 12.5 mg/kg i.p. every other 2 days for a total of 4 doses. Mice were maintained in individually ventilated cages containing refinement instruments. Animal welfare was checked by veterinary personnel during all the experiments. Mice were daily monitored for social behaviors, compromised motility and sign of distress. As soon as mice fitness was impaired or displayed sign of pain, animals were sacrificed in accordance with humane endpoint. For the experiments reported in this work, sample size was not predetermined using statistical methods. The investigators were not blinded.

Bilateral injection of primed and unprimed cells in mice

We used five- to eight-weeks old female BALB/c mice purchased from Charles River (Calco, Como, Italy). Each group consisted of 10 BALB/c mice. Mice were shaved bilaterally, and 250000 cells resuspended in 100 µl of PBS were injected in both flanks.

Mice were maintained in individually ventilated cages containing refinement instruments. Animal welfare was checked by veterinary personnel during all the experiments. Mice were daily monitored for social behaviors, compromised motility and sign of distress. As soon as mice fitness was impaired or displayed sign of pain, animals were sacrificed in accordance with humane endpoint. The investigators were not blinded.

Genomic DNA extraction

Genomic DNA was extracted from snap frozen preserved cell pellets and snap frozen tumor fragments using Relia Prep gDNA tissue miniprep system (Promega). In case of snap frozen tumor fragments, we extracted gDNA from fragments deriving from the 4 quadrants of the mass, dividing each tumor in several small pieces and then pooling together the extracted material.

Analysis of drug-induced genomic alterations

Library preparation, exome capture and sequencing were performed by IntegraGen SA (Evry, France). Genomic DNA was captured using Twist Mouse Exome Panel, Twist Bioscience. For detailed explanations of the process, see Gnirke et al [186]. Sequence capture, enrichment and elution were performed according to manufacturer's instruction and protocols (Twist Bioscience) without modification except for library preparation performed with NEBNext® Ultra II kit (New England Biolabs®). For library preparation 150 ng of each genomic DNA were fragmented by sonication and purified to yield fragments of 150-200 bp. Paired-end adaptor oligonucleotides from the NEB kit were ligated on repaired, a-tailed fragments then purified and enriched by 7 PCR cycles. 500 ng of these purified Libraries were then hybridized to the Twist oligo probe capture library for 16 hours in a singleplex reaction. After hybridization, washing, and elution, the eluted fraction was PCR-amplified with 8 cycles, purified and quantified by QPCR to obtain sufficient DNA template for downstream applications. Each eluted-enriched DNA sample was sequenced on an Illumina NovaSeq as Paired End 100 reads. The quality control of data was evaluated through different parameters: total number of raw reads, number of reads correctly mapping to the reference genome, coverage, target enrichment, percentage of reads classified as PCR duplicates, and the median depth. All samples overcame quality control step. Fastq files were aligned to the mouse mm10 reference genome using BWA-mem algorithm with standard

parameters. PCR duplicates were annotated using Picard tool and alignment files were filtered to delete known sequencing artifacts altering analysis results: reads containing more than three mismatches and nucleotides with Phred Score < 30 were filtered out as previous reported [187] . All mutations that were supported by reads having a strand bias or by mismatch in first or last nucleotide of the read were discarded. Alignments of different timepoints were compared to identify mutations and indels acquired post treatment, while common mutations and indels were classified as germline [188]. Since cell lines grown in mice could acquire many alterations not related to the treatment, we decided to perform a supervised analysis for the rest of the study considering only molecular alterations which were previously identified in the T1 timepoint (Figure 5). Indel calling was performed using Pindel, stratifying genomic alteration in acquired and germinal as previous reported [188].

For the calculation of clonal (fractional abundance > 10%) and subclonal analysis, we considered only mutations with a fractional abundance of over 3.4% and 3.7% for CT26 and TS/A, respectively, based on the sequencing parameters of their overall cohorts as previously described[40]. These cut-offs are based on the variant analysis tool that can call mutations with a minimum of 4 mutant reads and on the minimum depth (116X for CT26 and 108X for TS/A) reached in all NGS data. The choice of 10% as the clonal threshold was made for two distinct reasons. Firstly, previous studies have classified CRC and other tumor types into hypermutated and not-hypermutated categories using a 10% threshold[121]. Secondly, we confirmed this threshold experimentally in a previous study. In brief, to assess the effect of different clonal/sublclonal cutoffs, we evaluated the impact of population heterogeneity on TMB increase and TMZ-signature detection in a TMZ-sensitive cell model and its resistant derivatives. Based on these findings, we anticipated that a fraction of 25-30% cells would display the TMZ scar when a clonal effect was detected using 10% as fractional abundance cutoff [40].

RNA extraction and sequencing

Total RNA was extracted from snap frozen preserved cell pellets or tumor fragments using Maxwell RSC simplyRNA tissue system (Promega). In case of snap frozen tumor fragments, we extracted RNA from fragments deriving from the 4 quadrants of the mass, dividing each tumor in several small pieces and then pooling together the extracted material. The quantification of RNA was performed by Thermo Scientific Nanodrop 1000 (Agilent). Control of RNA integrity, library preparation, and

sequencing were performed by Macrogen Europe BV (Amsterdam, Netherlands). RNA integrity was evaluated with the Agilent 2100 Bioanalyzer using the Agilent RNA 6000 Nano Kit. Total RNA was used as input to the Illumina TruSeq RNA Sample Prep Kit, according to the manufacturer's protocol. After library preparation, sequencing was performed on NovaSeqX to get paired-end 2x100 bp reads. Three biologically independent RNA samples were extracted and sequenced for each condition.

Neoantigen prediction analysis

Predicted neoantigens were computed starting from the file of coding variations. First, for each variation we translated the corresponding cDNA into the amino acid sequence modifying it according to the type of alteration. In the case of SNVs, we replaced the normal amino acid with the mutated one in the selected position of the candidate peptide; for frameshifts we take into account every possible peptide generated by the altered frame. Next, mutated peptide sequences were trimmed and then NetMHC 4.0 software [189] was deployed to predict binding affinity to Major histocompatibility (MHC) class I molecules using kmers from 8 to 11 length. MHC Class I haplotype antigens were set to H2-Kd, H2-Dd and H2-Ld for BALB/c background and H2-Kd and H2-Db for NODSCID background. For further analysis only predicted neoantigens with a strong binding affinity (Rank <0.5) were considered.

Mutational Signature Analysis

Mutational matrices of somatic mutations were created using the tool 'SigProfilerMatrixGenerator' (version 1.2.8) [190]. Then, 'fit_to_signatures' function from MutationalPatterns (version 3.4.0) [191] R package was used to perform mutational signature fitting analysis. Mutational signatures reference v3.3 from COSMIC was used as reference in the analysis [192]. Cosine similarity between the sample mutational profile and the fitted mutational signatures was assessed using 'cos_sim_matrix' function. Samples showing cosine similarity < 0.9 were excluded from the analysis as previously reported [40,193,194].

Identification of immunoedited mutations and genetic events responsible for immune evasion

To elucidate which mutations were immunoedited by the immune system, we first identified common mutations between cells at the end of the priming phase (T1) and tumors grown in immunodeficient mice: **(T1-T0) ∩ (T2NODSCID-T0)**. These mutations

correspond to the ones introduced by the treatment and not subject to fitness selection *in vivo*. This set of mutations was used to identify mutations that were still present in the immunocompetent mice (neutral, not immunoedited), and mutations lost in the immunocompetent mice (immunoedited), that are defined hereby:

Neutral mutations: **[(T1-T0) ∩ (T2NODSCID-T0)] ∩ (T2BALBc-T0)**

Immunoedited mutations: **[(T1-T0) ∩ (T2NODSCID-T0)] - (T2BALBc-T0)**

Samples from immunoescaped tumors (i.e., outgrown in immunocompetent mice) were sequenced and we performed an in-depth analysis of the most prevalent genetic mechanisms of cancer immune evasion, as recently summarized by Martinez-Jimenez and colleagues [195]. These included the loss of MHC molecules, loss of antigen presentation or MHC scaffolding (inactivation of *b2m, calr, tap1, tap, tapbp*), loss of MHC transcription activation (mutations in *nlrc5, ciita, rfx5*), inactivation of IFN-gamma pathway (mutations in *jak1, jak, irf2, ifngr1, ifngr2, aplnr, stat1*), loss of *cd58* immune receptor, amplification of *pd-l1*, loss of *setd1*.

Differential gene expression and gene set enrichment analysis (GSEA)

RNA-seq reads were aligned against mm10 using STAR aligner [196] and subsequently RSEM [197] was used for transcript and gene quantification and GENCODE v M23 as gene annotation. Starting from RSEM gene results, differential gene expression analysis was performed between CT26 cells treated with CDDP, CDDP-TMZ, FOLFOXIRI, and TMZ, and untreated CT26 cells using the DESeq2 R bioconductor package[198]. Independent filtering was performed as implemented by the results function and adjusted p-values were calculated using the Benjamini–Hochberg (BH) method. Additionally, log2 fold changes were shrunk using the lfcShrink function. Genes with an adjusted p-value of less than 0.05 were considered differentially expressed. GSEA was performed with the fgsea function from the fGSEA R package [199]. The enrichment analysis was performed considering the Hallmark gene sets derived from Molecular Signatures Database (MSigDB) [200].

Histological examination and immunohistochemistry

For histopathological analyses mouse tumors were fixed in 4% paraformaldehyde (PFA) and processed by a Diapath automatic processor as follows. Tissues were dehydrated through 70% (60 minutes), 2 change of 95% (90 minutes each), and 3

change of 99% (60 minutes each) ethanol, cleared through 3 changes of xylene (90 minutes each), and finally immersed in 3 changes of paraffin, 1 hour each. Samples were embedded in a paraffin block and stored at room temperature (RT) until ready to section. According to standard protocol, Hematoxylin/Eosin (Diapath) was performed on serial sections to assess histological features.

For immunohistochemistry analyses, paraffin was removed with xylene and the sections were rehydrated in graded alcohol. Antigen retrieval was carried out using preheated target retrieval solution for 30 minutes and endogenous peroxidase activity was quenched with 3% hydrogen peroxide in distilled water for 10 minutes at RT. Tissue sections were blocked with 5% FBS in PBS for 60 minutes and incubated 3 hours with primary antibodies for MSH6 (Biocare, CM265AK) MSH2 (Biocare, CM219AK), CD8 (Abcam, AB217394), CD4 (Abcam, AB183685), Foxp3 (Cell Signalling Technologies, CST85061). The antibody binding was detected using a polymer detection kit (GAM-HRP, Microtech) followed by a diaminobenzidine chromogen reaction (Peroxidase substrate kit, DAB, SK-4100; Vector Lab). Quantification of immune markers was performed by manual counting of at least 4 different 40X fields for each slide, and using at least 3 different tumor samples for each condition treatment condition. Operators were blinded with respect to the treatment arm of the samples. Results for each condition were plotted as average number of marked cells/field ± SD. All sections were counterstained with Mayer's hematoxylin and visualized using a bright-field microscope.

Quantification and statistical analysis

Statistical details for each experiment are specified in the corresponding figure legends. Statistical significance was determined by Mann-Whitney test, Welch's t test, and log-rank test (GraphPad Prism) as specified for each experiment and $p < 0.05$ was considered statistically significant.

REFERENCES

1. Burnet, F.M. (1970). The concept of immunological surveillance. Prog Exp Tumor Res *13*, 1–27. https://doi.org/10.1159/000386035.

2. Kroemer, G., Chan, T.A., Eggermont, A.M.M., and Galluzzi, L. (2024). Immunosurveillance in clinical cancer management. CA Cancer J Clin *74*, 187–202. https://doi.org/10.3322/caac.21818.

3. Calì, B., Molon, B., and Viola, A. (2017). Tuning cancer fate: the unremitting role of host immunity. Open Biol *7*, 170006. https://doi.org/10.1098/rsob.170006.

4. Hanahan, D. (2022). Hallmarks of Cancer: New Dimensions. Cancer Discov *12*, 31–46. https://doi.org/10.1158/2159-8290.CD-21-1059.

5. Hanahan, D., and Weinberg, R.A. (2011). Hallmarks of cancer: the next generation. Cell *144*, 646–674. https://doi.org/10.1016/j.cell.2011.02.013.

6. Freeman, G.J., Long, A.J., Iwai, Y., Bourque, K., Chernova, T., Nishimura, H., Fitz, L.J., Malenkovich, N., Okazaki, T., Byrne, M.C., et al. (2000). Engagement of the Pd-1 Immunoinhibitory Receptor by a Novel B7 Family Member Leads to Negative Regulation of Lymphocyte Activation. Journal of Experimental Medicine *192*, 1027–1034. https://doi.org/10.1084/jem.192.7.1027.

7. Krummel, M.F., and Allison, J.P. (1995). CD28 and CTLA-4 have opposing effects on the response of T cells to stimulation. Journal of Experimental Medicine *182*, 459–465. https://doi.org/10.1084/jem.182.2.459.

8. van Elsas, A., Hurwitz, A.A., and Allison, J.P. (1999). Combination Immunotherapy of B16 Melanoma Using Anti–Cytotoxic T Lymphocyte–Associated Antigen 4 (Ctla-4) and Granulocyte/Macrophage Colony-Stimulating Factor (Gm-Csf)-Producing Vaccines Induces Rejection of Subcutaneous and Metastatic Tumors Accompanied by Autoimmune Depigmentation. Journal of Experimental Medicine *190*, 355–366. https://doi.org/10.1084/jem.190.3.355.

9. Pardoll, D.M. (2012). The blockade of immune checkpoints in cancer immunotherapy. Nat Rev Cancer *12*, 252–264. https://doi.org/10.1038/nrc3239.

10. Robert, C. (2020). A decade of immune-checkpoint inhibitors in cancer therapy. Nat Commun *11*, 3801. https://doi.org/10.1038/s41467-020-17670-y.

11. Zhang, Y., and Zhang, Z. (2020). The history and advances in cancer immunotherapy: understanding the characteristics of tumor-infiltrating immune cells and their therapeutic implications. Cell Mol Immunol *17*, 807–821. https://doi.org/10.1038/s41423-020-0488-6.

12. Pilard, C., Ancion, M., Delvenne, P., Jerusalem, G., Hubert, P., and Herfs, M. (2021). Cancer immunotherapy: it's time to better predict patients' response. Br J Cancer *125*, 927–938. https://doi.org/10.1038/s41416-021-01413-x.

13. Matzinger, P. (2002). The danger model: a renewed sense of self. Science *296*, 301–305. https://doi.org/10.1126/science.1071059.

14. Janeway, C.A., Goodnow, C.C., and Medzhitov, R. (1996). Danger - pathogen on the premises! Immunological tolerance. Curr Biol *6*, 519–522. https://doi.org/10.1016/s0960-9822(02)00531-6.

15. Galluzzi, L., Humeau, J., Buqué, A., Zitvogel, L., and Kroemer, G. (2020). Immunostimulation with chemotherapy in the era of immune checkpoint inhibitors. Nat Rev Clin Oncol *17*, 725–741. https://doi.org/10.1038/s41571-020-0413-z.

16. Smith, C.C., Selitsky, S.R., Chai, S., Armistead, P.M., Vincent, B.G., and Serody, J.S. (2019). Alternative tumour-specific antigens. Nat Rev Cancer *19*, 465–478. https://doi.org/10.1038/s41568-019-0162-4.

17. Yarchoan, M., Johnson, B.A., Lutz, E.R., Laheru, D.A., and Jaffee, E.M. (2017). Targeting neoantigens to augment antitumour immunity. Nat Rev Cancer *17*, 209–222. https://doi.org/10.1038/nrc.2016.154.

18. Jones, P.A., Ohtani, H., Chakravarthy, A., and De Carvalho, D.D. (2019). Epigenetic therapy in immune-oncology. Nat Rev Cancer *19*, 151–161. https://doi.org/10.1038/s41568-019-0109-9.

19. Bagchi, A. (2020). Unusual nature of long non-coding RNAs coding for “unusual peptides.” Gene *729*, 144298. https://doi.org/10.1016/j.gene.2019.144298.

20. Garg, A.D., and Agostinis, P. (2017). Cell death and immunity in cancer: From danger signals to mimicry of pathogen defense responses. Immunol Rev *280*, 126–148. https://doi.org/10.1111/imr.12574.

21. Galluzzi, L., Buqué, A., Kepp, O., Zitvogel, L., and Kroemer, G. (2017). Immunogenic cell death in cancer and infectious disease. Nat Rev Immunol *17*, 97–111. https://doi.org/10.1038/nri.2016.107.

22. Gong, T., Liu, L., Jiang, W., and Zhou, R. (2020). DAMP-sensing receptors in sterile inflammation and inflammatory diseases. Nat Rev Immunol *20*, 95–112. https://doi.org/10.1038/s41577-019-0215-7.

23. Ozga, A.J., Chow, M.T., and Luster, A.D. (2021). Chemokines and the immune response to cancer. Immunity *54*, 859–874. https://doi.org/10.1016/j.immuni.2021.01.012.

24. Salmon, H., Remark, R., Gnjatic, S., and Merad, M. (2019). Host tissue determinants of tumour immunity. Nat Rev Cancer *19*, 215–227. https://doi.org/10.1038/s41568-019-0125-9.

25. Galluzzi, L., Yamazaki, T., and Kroemer, G. (2018). Linking cellular stress responses to systemic homeostasis. Nat Rev Mol Cell Biol *19*, 731–745. https://doi.org/10.1038/s41580-018-0068-0.

26. Pakos-Zebrucka, K., Koryga, I., Mnich, K., Ljujic, M., Samali, A., and Gorman, A.M. (2016). The integrated stress response. EMBO Rep *17*, 1374–1395. https://doi.org/10.15252/embr.201642195.

27. Wang, Z., Chen, J., Hu, J., Zhang, H., Xu, F., He, W., Wang, X., Li, M., Lu, W., Zeng, G., et al. (2019). cGAS/STING axis mediates a topoisomerase II inhibitor-induced tumor immunogenicity. J Clin Invest *129*, 4850–4862. https://doi.org/10.1172/JCI127471.

28. Sistigu, A., Yamazaki, T., Vacchelli, E., Chaba, K., Enot, D.P., Adam, J., Vitale, I., Goubar, A., Baracco, E.E., Remédios, C., et al. (2014). Cancer cell-autonomous contribution of type I interferon signaling to the efficacy of chemotherapy. Nat Med *20*, 1301–1309. https://doi.org/10.1038/nm.3708.

29. Kasikova, L., Hensler, M., Truxova, I., Skapa, P., Laco, J., Belicova, L., Praznovec, I., Vosahlikova, S., Halaska, M.J., Brtnicky, T., et al. (2019). Calreticulin exposure correlates with robust adaptive antitumor immunity and favorable prognosis in ovarian carcinoma patients. J Immunother Cancer *7*, 312. https://doi.org/10.1186/s40425-019-0781-z.

30. Galluzzi, L., Vitale, I., Warren, S., Adjemian, S., Agostinis, P., Martinez, A.B., Chan, T.A., Coukos, G., Demaria, S., Deutsch, E., et al. (2020). Consensus guidelines for the definition, detection and interpretation of immunogenic cell death. J Immunother Cancer *8*, e000337. https://doi.org/10.1136/jitc-2019-000337.

31. Ma, Y., Adjemian, S., Mattarollo, S.R., Yamazaki, T., Aymeric, L., Yang, H., Portela Catani, J.P., Hannani, D., Duret, H., Steegh, K., et al. (2013). Anticancer chemotherapy-induced intratumoral recruitment and differentiation of antigen-presenting cells. Immunity *38*, 729–741. https://doi.org/10.1016/j.immuni.2013.03.003.

32. Fucikova, J., Moserova, I., Urbanova, L., Bezu, L., Kepp, O., Cremer, I., Salek, C., Strnad, P., Kroemer, G., Galluzzi, L., et al. (2015). Prognostic and Predictive Value of DAMPs and DAMP-Associated Processes in Cancer. Front Immunol *6*, 402. https://doi.org/10.3389/fimmu.2015.00402.

33. Melief, C.J.M., and Kessler, J.H. (2017). Novel insights into the HLA class I immunopeptidome and T-cell immunosurveillance. Genome Med *9*, 44. https://doi.org/10.1186/s13073-017-0439-8.

34. Kucab, J.E., Zou, X., Morganella, S., Joel, M., Nanda, A.S., Nagy, E., Gomez, C., Degasperi, A., Harris, R., Jackson, S.P., et al. (2019). A Compendium of Mutational Signatures of Environmental Agents. Cell *177*, 821-836.e16. https://doi.org/10.1016/j.cell.2019.03.001.

35. Pich, O., Muiños, F., Lolkema, M.P., Steeghs, N., Gonzalez-Perez, A., and Lopez-Bigas, N. (2019). The mutational footprints of cancer therapies. Nat Genet *51*, 1732–1740. https://doi.org/10.1038/s41588-019-0525-5.

36. O'Donnell, T., Christie, E.L., Ahuja, A., Buros, J., Aksoy, B.A., Bowtell, D.D.L., Snyder, A., and Hammerbacher, J. (2018). Chemotherapy weakly contributes to predicted neoantigen expression in ovarian cancer. BMC Cancer *18*, 87. https://doi.org/10.1186/s12885-017-3825-0.

37. Helleday, T. (2019). Making immunotherapy ‘cold’ tumours ‘hot’ by chemotherapy-induced mutations—a misconception. Annals of Oncology *30*, 360–361. https://doi.org/10.1093/annonc/mdz013.

38. Cahill, D.P., Levine, K.K., Betensky, R.A., Codd, P.J., Romany, C.A., Reavie, L.B., Batchelor, T.T., Futreal, P.A., Stratton, M.R., Curry, W.T., et al. (2007). Loss of the mismatch repair protein MSH6 in human glioblastomas is associated with tumor progression during temozolomide treatment. Clin Cancer Res *13*, 2038–2045. https://doi.org/10.1158/1078-0432.CCR-06-2149.

39. Germano, G., Lamba, S., Rospo, G., Barault, L., Magrì, A., Maione, F., Russo, M., Crisafulli, G., Bartolini, A., Lerda, G., et al. (2017). Inactivation of DNA repair triggers neoantigen generation and impairs tumour growth. Nature *552*, 116–120. https://doi.org/10.1038/nature24673.

40. Crisafulli, G., Sartore-Bianchi, A., Lazzari, L., Pietrantonio, F., Amatu, A., Macagno, M., Barault, L., Cassingena, A., Bartolini, A., Luraghi, P., et al. (2022). Temozolomide Treatment Alters Mismatch Repair and Boosts Mutational Burden in Tumor and Blood of Colorectal Cancer Patients. Cancer Discov *12*, 1656–1675. https://doi.org/10.1158/2159-8290.CD-21-1434.

41. Morano, F., Raimondi, A., Pagani, F., Lonardi, S., Salvatore, L., Cremolini, C., Murgioni, S., Randon, G., Palermo, F., Antonuzzo, L., et al. (2022). Temozolomide Followed by Combination With Low-Dose Ipilimumab and Nivolumab in Patients With Microsatellite-Stable, O6-Methylguanine-DNA Methyltransferase-Silenced Metastatic Colorectal Cancer: The MAYA Trial. J Clin Oncol *40*, 1562–1573. https://doi.org/10.1200/JCO.21.02583.

42. Fink, D., Zheng, H., Nebel, S., Norris, P.S., Aebi, S., Lin, T.P., Nehmé, A., Christen, R.D., Haas, M., MacLeod, C.L., et al. (1997). In vitro and in vivo resistance to cisplatin in cells that have lost DNA mismatch repair. Cancer Res *57*, 1841–1845.

43. Sawant, A., Kothandapani, A., Zhitkovich, A., Sobol, R.W., and Patrick, S.M. (2015). Role of mismatch repair proteins in the processing of cisplatin interstrand cross-links. DNA Repair *35*, 126–136. https://doi.org/10.1016/j.dnarep.2015.10.003.

44. Rottenberg, S., Disler, C., and Perego, P. (2021). The rediscovery of platinum-based cancer therapy. Nat Rev Cancer *21*, 37–50. https://doi.org/10.1038/s41568-020-00308-y.

45. Vanderlugt, C.L., Begolka, W.S., Neville, K.L., Katz-Levy, Y., Howard, L.M., Eagar, T.N., Bluestone, J.A., and Miller, S.D. (1998). The functional significance of epitope spreading and its regulation by co-stimulatory molecules. Immunol Rev *164*, 63–72. https://doi.org/10.1111/j.1600-065x.1998.tb01208.x.

46. Barreto, J.N., McCullough, K.B., Ice, L.L., and Smith, J.A. (2014). Antineoplastic agents and the associated myelosuppressive effects: a review. J Pharm Pract *27*, 440–446. https://doi.org/10.1177/0897190014546108.

47. Nakashima, K., Aoshima, M., Ohfuji, S., Suzuki, K., Katsurada, M., Katsurada, N., Misawa, M., Otsuka, Y., Kondo, K., and Hirota, Y. (2017). Immunogenicity of trivalent influenza vaccine in patients with lung cancer undergoing anticancer chemotherapy. Hum Vaccin Immunother *13*, 543–550. https://doi.org/10.1080/21645515.2016.1246094.

48. Dimeloe, S., Frick, C., Fischer, M., Gubser, P.M., Razik, L., Bantug, G.R., Ravon, M., Langenkamp, A., and Hess, C. (2014). Human regulatory T cells lack the cyclophosphamide-extruding transporter ABCB1 and are more susceptible to cyclophosphamide-induced apoptosis. Eur J Immunol *44*, 3614–3620. https://doi.org/10.1002/eji.201444879.

49. Otsubo, D., Yamashita, K., Fujita, M., Nishi, M., Kimura, Y., Hasegawa, H., Suzuki, S., and Kakeji, Y. (2015). Early-phase Treatment by Low-dose 5-Fluorouracil or Primary Tumor Resection Inhibits MDSC-mediated Lung Metastasis Formation. Anticancer Res *35*, 4425–4431.

50. Ma, Y., Mattarollo, S.R., Adjemian, S., Yang, H., Aymeric, L., Hannani, D., Portela Catani, J.P., Duret, H., Teng, M.W.L., Kepp, O., et al. (2014). CCL2/CCR2-dependent recruitment of functional antigen-presenting cells into tumors upon chemotherapy. Cancer Res *74*, 436–445. https://doi.org/10.1158/0008-5472.CAN-13-1265.

51. Vincent, J., Mignot, G., Chalmin, F., Ladoire, S., Bruchard, M., Chevriaux, A., Martin, F., Apetoh, L., Rébé, C., and Ghiringhelli, F. (2010). 5-Fluorouracil selectively kills tumor-associated myeloid-derived suppressor cells resulting in enhanced T cell-dependent antitumor immunity. Cancer Res *70*, 3052–3061. https://doi.org/10.1158/0008-5472.CAN-09-3690.

52. Kodumudi, K.N., Woan, K., Gilvary, D.L., Sahakian, E., Wei, S., and Djeu, J.Y. (2010). A novel chemoimmunomodulating property of docetaxel: suppression of myeloid-derived suppressor cells in tumor bearers. Clin Cancer Res *16*, 4583–4594. https://doi.org/10.1158/1078-0432.CCR-10-0733.

53. Beyranvand Nejad, E., van der Sluis, T.C., van Duikeren, S., Yagita, H., Janssen, G.M., van Veelen, P.A., Melief, C.J.M., van der Burg, S.H., and Arens, R. (2016). Tumor Eradication by Cisplatin Is Sustained by CD80/86-Mediated Costimulation of CD8+ T Cells. Cancer Res *76*, 6017–6029. https://doi.org/10.1158/0008-5472.CAN-16-0881.

54. Sung, H., Ferlay, J., Siegel, R.L., Laversanne, M., Soerjomataram, I., Jemal, A., and Bray, F. (2021). Global Cancer Statistics 2020: GLOBOCAN Estimates of Incidence and Mortality Worldwide for 36 Cancers in 185 Countries. CA Cancer J Clin *71*, 209–249. https://doi.org/10.3322/caac.21660.

55. Di Nicolantonio, F., Vitiello, P.P., Marsoni, S., Siena, S., Tabernero, J., Trusolino, L., Bernards, R., and Bardelli, A. (2021). Precision oncology in metastatic colorectal cancer - from biology to medicine. Nat Rev Clin Oncol *18*, 506–525. https://doi.org/10.1038/s41571-021-00495-z.

56. Diaz, L.A., Shiu, K.-K., Kim, T.-W., Jensen, B.V., Jensen, L.H., Punt, C., Smith, D., Garcia-Carbonero, R., Benavides, M., Gibbs, P., et al. (2022). Pembrolizumab versus chemotherapy for microsatellite instability-high or mismatch repair-deficient metastatic colorectal cancer (KEYNOTE-177): final analysis of a randomised, open-label, phase 3 study. Lancet Oncol *23*, 659–670. https://doi.org/10.1016/S1470-2045(22)00197-8.

57. André, T., Lonardi, S., Wong, K.Y.M., Lenz, H.-J., Gelsomino, F., Aglietta, M., Morse, M.A., Van Cutsem, E., McDermott, R., Hill, A., et al. (2022). Nivolumab plus low-dose ipilimumab in previously treated patients with microsatellite instability-high/mismatch repair-deficient metastatic colorectal cancer: 4-year follow-up from CheckMate 142. Ann Oncol, S0923-7534(22)01737-9. https://doi.org/10.1016/j.annonc.2022.06.008.

58. Lenz, H.-J., Van Cutsem, E., Luisa Limon, M., Wong, K.Y.M., Hendlisz, A., Aglietta, M., García-Alfonso, P., Neyns, B., Luppi, G., Cardin, D.B., et al. (2022). First-Line Nivolumab Plus Low-Dose Ipilimumab for Microsatellite Instability-High/Mismatch Repair-Deficient Metastatic Colorectal Cancer: The Phase II CheckMate 142 Study. J Clin Oncol *40*, 161–170. https://doi.org/10.1200/JCO.21.01015.

59. Rousseau, B., Bieche, I., Pasmant, E., Hamzaoui, N., Leulliot, N., Michon, L., de Reynies, A., Attignon, V., Foote, M.B., Masliah-Planchon, J., et al. (2022). PD-1 Blockade in Solid Tumors with Defects in Polymerase Epsilon. Cancer Discov *12*, 1435–1448. https://doi.org/10.1158/2159-8290.CD-21-0521.

60. Ganesh, K., Stadler, Z.K., Cercek, A., Mendelsohn, R.B., Shia, J., Segal, N.H., and Diaz, L.A. (2019). Immunotherapy in colorectal cancer: rationale, challenges and potential. Nat Rev Gastroenterol Hepatol *16*, 361–375. https://doi.org/10.1038/s41575-019-0126-x.

61. Germano, G., Amirouchene-Angelozzi, N., Rospo, G., and Bardelli, A. (2018). The Clinical Impact of the Genomic Landscape of Mismatch Repair-Deficient Cancers. Cancer Discov *8*, 1518–1528. https://doi.org/10.1158/2159-8290.CD-18-0150.

62. Lahouel, K., Younes, L., Danilova, L., Giardiello, F.M., Hruban, R.H., Groopman, J., Kinzler, K.W., Vogelstein, B., Geman, D., and Tomasetti, C. (2020). Revisiting the tumorigenesis timeline with a data-driven generative model. Proc Natl Acad Sci U S A *117*, 857–864. https://doi.org/10.1073/pnas.1914589117.

63. Alexandrov, L.B., Kim, J., Haradhvala, N.J., Huang, M.N., Tian Ng, A.W., Wu, Y., Boot, A., Covington, K.R., Gordenin, D.A., Bergstrom, E.N., et al. (2020). The repertoire of mutational signatures in human cancer. Nature *578*, 94–101. https://doi.org/10.1038/s41586-020-1943-3.

64. Koopman, M., Kortman, G. a. M., Mekenkamp, L., Ligtenberg, M.J.L., Hoogerbrugge, N., Antonini, N.F., Punt, C.J.A., and van Krieken, J.H.J.M. (2009). Deficient mismatch repair system in patients with sporadic advanced colorectal cancer. Br J Cancer *100*, 266–273. https://doi.org/10.1038/sj.bjc.6604867.

65. Popat, S., Hubner, R., and Houlston, R.S. (2005). Systematic review of microsatellite instability and colorectal cancer prognosis. J Clin Oncol *23*, 609–618. https://doi.org/10.1200/JCO.2005.01.086.

66. Sinicrope, F.A., Foster, N.R., Thibodeau, S.N., Marsoni, S., Monges, G., Labianca, R., Kim, G.P., Yothers, G., Allegra, C., Moore, M.J., et al. (2011). DNA mismatch repair status and colon cancer recurrence and survival in clinical trials of 5-fluorouracil-based adjuvant therapy. J Natl Cancer Inst *103*, 863–875. https://doi.org/10.1093/jnci/djr153.

67. Argilés, G., Tabernero, J., Labianca, R., Hochhauser, D., Salazar, R., Iveson, T., Laurent-Puig, P., Quirke, P., Yoshino, T., Taieb, J., et al. (2020). Localised colon cancer: ESMO Clinical Practice Guidelines for diagnosis, treatment and follow-up. Ann Oncol *31*, 1291–1305. https://doi.org/10.1016/j.annonc.2020.06.022.

68. Sinicrope, F.A., and Sargent, D.J. (2012). Molecular pathways: microsatellite instability in colorectal cancer: prognostic, predictive, and therapeutic implications. Clin Cancer Res *18*, 1506–1512. https://doi.org/10.1158/1078-0432.CCR-11-1469.

69. Boland, C.R., and Goel, A. (2010). Microsatellite instability in colorectal cancer. Gastroenterology *138*, 2073-2087.e3. https://doi.org/10.1053/j.gastro.2009.12.064.

70. Hampel, H., Frankel, W.L., Martin, E., Arnold, M., Khanduja, K., Kuebler, P., Clendenning, M., Sotamaa, K., Prior, T., Westman, J.A., et al. (2008). Feasibility of screening for Lynch syndrome among patients with colorectal cancer. J Clin Oncol *26*, 5783–5788. https://doi.org/10.1200/JCO.2008.17.5950.

71. Amodio, V., Mauri, G., Reilly, N.M., Sartore-Bianchi, A., Siena, S., Bardelli, A., and Germano, G. (2021). Mechanisms of Immune Escape and Resistance to Checkpoint Inhibitor Therapies in Mismatch Repair Deficient Metastatic Colorectal Cancers. Cancers (Basel) *13*, 2638. https://doi.org/10.3390/cancers13112638.

72. Haradhvala, N.J., Kim, J., Maruvka, Y.E., Polak, P., Rosebrock, D., Livitz, D., Hess, J.M., Leshchiner, I., Kamburov, A., Mouw, K.W., et al. (2018). Distinct mutational signatures characterize concurrent loss of polymerase proofreading and mismatch repair. Nat Commun *9*, 1746. https://doi.org/10.1038/s41467-018-04002-4.

73. Chung, J., Maruvka, Y.E., Sudhaman, S., Kelly, J., Haradhvala, N.J., Bianchi, V., Edwards, M., Forster, V.J., Nunes, N.M., Galati, M.A., et al. (2021). DNA Polymerase and Mismatch Repair Exert Distinct Microsatellite Instability Signatures in Normal and Malignant Human Cells. Cancer Discov *11*, 1176–1191. https://doi.org/10.1158/2159-8290.CD-20-0790.

74. Venderbosch, S., Nagtegaal, I.D., Maughan, T.S., Smith, C.G., Cheadle, J.P., Fisher, D., Kaplan, R., Quirke, P., Seymour, M.T., Richman, S.D., et al. (2014). Mismatch repair status and BRAF mutation status in metastatic colorectal cancer patients: a pooled analysis of the CAIRO, CAIRO2, COIN, and FOCUS studies.

Clin Cancer Res *20*, 5322–5330. https://doi.org/10.1158/1078-0432.CCR-14-0332.

75. De Smedt, L., Lemahieu, J., Palmans, S., Govaere, O., Tousseyn, T., Van Cutsem, E., Prenen, H., Tejpar, S., Spaepen, M., Matthijs, G., et al. (2015). Microsatellite instable vs stable colon carcinomas: analysis of tumour heterogeneity, inflammation and angiogenesis. Br J Cancer *113*, 500–509. https://doi.org/10.1038/bjc.2015.213.

76. Galon, J., Costes, A., Sanchez-Cabo, F., Kirilovsky, A., Mlecnik, B., Lagorce-Pagès, C., Tosolini, M., Camus, M., Berger, A., Wind, P., et al. (2006). Type, density, and location of immune cells within human colorectal tumors predict clinical outcome. Science *313*, 1960–1964. https://doi.org/10.1126/science.1129139.

77. Galon, J., Mlecnik, B., Bindea, G., Angell, H.K., Berger, A., Lagorce, C., Lugli, A., Zlobec, I., Hartmann, A., Bifulco, C., et al. (2014). Towards the introduction of the "Immunoscore" in the classification of malignant tumours. J Pathol *232*, 199–209. https://doi.org/10.1002/path.4287.

78. Pagès, F., Mlecnik, B., Marliot, F., Bindea, G., Ou, F.-S., Bifulco, C., Lugli, A., Zlobec, I., Rau, T.T., Berger, M.D., et al. (2018). International validation of the consensus Immunoscore for the classification of colon cancer: a prognostic and accuracy study. Lancet *391*, 2128–2139. https://doi.org/10.1016/S0140-6736(18)30789-X.

79. Huyghe, N., Baldin, P., and Van den Eynde, M. (2020). Immunotherapy with immune checkpoint inhibitors in colorectal cancer: what is the future beyond deficient mismatch-repair tumours? Gastroenterol Rep (Oxf) *8*, 11–24. https://doi.org/10.1093/gastro/goz061.

80. Maby, P., Tougeron, D., Hamieh, M., Mlecnik, B., Kora, H., Bindea, G., Angell, H.K., Fredriksen, T., Elie, N., Fauquembergue, E., et al. (2015). Correlation between Density of CD8+ T-cell Infiltrate in Microsatellite Unstable Colorectal Cancers and Frameshift Mutations: A Rationale for Personalized Immunotherapy. Cancer Res *75*, 3446–3455. https://doi.org/10.1158/0008-5472.CAN-14-3051.

81. Kim, H., Jen, J., Vogelstein, B., and Hamilton, S.R. (1994). Clinical and pathological characteristics of sporadic colorectal carcinomas with DNA replication errors in microsatellite sequences. Am J Pathol *145*, 148–156.

82. Guidoboni, M., Gafà, R., Viel, A., Doglioni, C., Russo, A., Santini, A., Del Tin, L., Macrì, E., Lanza, G., Boiocchi, M., et al. (2001). Microsatellite instability and high content of activated cytotoxic lymphocytes identify colon cancer patients with a favorable prognosis. Am J Pathol *159*, 297–304. https://doi.org/10.1016/S0002-9440(10)61695-1.

83. Llosa, N.J., Cruise, M., Tam, A., Wicks, E.C., Hechenbleikner, E.M., Taube, J.M., Blosser, R.L., Fan, H., Wang, H., Luber, B.S., et al. (2015). The vigorous immune microenvironment of microsatellite instable colon cancer is balanced by multiple

counter-inhibitory checkpoints. Cancer Discov *5*, 43–51. https://doi.org/10.1158/2159-8290.CD-14-0863.

84. Lin, A., Zhang, J., and Luo, P. (2020). Crosstalk Between the MSI Status and Tumor Microenvironment in Colorectal Cancer. Front Immunol *11*, 2039. https://doi.org/10.3389/fimmu.2020.02039.

85. Becht, E., de Reyniès, A., Giraldo, N.A., Pilati, C., Buttard, B., Lacroix, L., Selves, J., Sautès-Fridman, C., Laurent-Puig, P., and Fridman, W.H. (2016). Immune and Stromal Classification of Colorectal Cancer Is Associated with Molecular Subtypes and Relevant for Precision Immunotherapy. Clin Cancer Res *22*, 4057–4066. https://doi.org/10.1158/1078-0432.CCR-15-2879.

86. Ciardiello, D., Vitiello, P.P., Cardone, C., Martini, G., Troiani, T., Martinelli, E., and Ciardiello, F. (2019). Immunotherapy of colorectal cancer: Challenges for therapeutic efficacy. Cancer Treat Rev *76*, 22–32. https://doi.org/10.1016/j.ctrv.2019.04.003.

87. Picard, E., Verschoor, C.P., Ma, G.W., and Pawelec, G. (2020). Relationships Between Immune Landscapes, Genetic Subtypes and Responses to Immunotherapy in Colorectal Cancer. Front Immunol *11*, 369. https://doi.org/10.3389/fimmu.2020.00369.

88. Rospo, G., Lorenzato, A., Amirouchene-Angelozzi, N., Magrì, A., Cancelliere, C., Corti, G., Negrino, C., Amodio, V., Montone, M., Bartolini, A., et al. (2019). Evolving neoantigen profiles in colorectal cancers with DNA repair defects. Genome Med *11*, 42. https://doi.org/10.1186/s13073-019-0654-6.

89. Kosugi, S., Momozawa, Y., Liu, X., Terao, C., Kubo, M., and Kamatani, Y. (2019). Comprehensive evaluation of structural variation detection algorithms for whole genome sequencing. Genome Biol *20*, 117. https://doi.org/10.1186/s13059-019-1720-5.

90. Mardis, E.R. (2019). Neoantigens and genome instability: impact on immunogenomic phenotypes and immunotherapy response. Genome Med *11*, 71. https://doi.org/10.1186/s13073-019-0684-0.

91. Nakayama, M. (2014). Antigen Presentation by MHC-Dressed Cells. Front Immunol *5*, 672. https://doi.org/10.3389/fimmu.2014.00672.

92. Bjerregaard, A.-M., Nielsen, M., Hadrup, S.R., Szallasi, Z., and Eklund, A.C. (2017). MuPeXI: prediction of neo-epitopes from tumor sequencing data. Cancer Immunol Immunother *66*, 1123–1130. https://doi.org/10.1007/s00262-017-2001-3.

93. Richters, M.M., Xia, H., Campbell, K.M., Gillanders, W.E., Griffith, O.L., and Griffith, M. (2019). Best practices for bioinformatic characterization of neoantigens for clinical utility. Genome Med *11*, 56. https://doi.org/10.1186/s13073-019-0666-2.

94. Hundal, J., Carreno, B.M., Petti, A.A., Linette, G.P., Griffith, O.L., Mardis, E.R., and Griffith, M. (2016). pVAC-Seq: A genome-guided in silico approach to

identifying tumor neoantigens. Genome Med *8*, 11. https://doi.org/10.1186/s13073-016-0264-5.

95. Le, D.T., Durham, J.N., Smith, K.N., Wang, H., Bartlett, B.R., Aulakh, L.K., Lu, S., Kemberling, H., Wilt, C., Luber, B.S., et al. (2017). Mismatch repair deficiency predicts response of solid tumors to PD-1 blockade. Science *357*, 409–413. https://doi.org/10.1126/science.aan6733.

96. Mandal, R., Samstein, R.M., Lee, K.-W., Havel, J.J., Wang, H., Krishna, C., Sabio, E.Y., Makarov, V., Kuo, F., Blecua, P., et al. (2019). Genetic diversity of tumors with mismatch repair deficiency influences anti-PD-1 immunotherapy response. Science *364*, 485–491. https://doi.org/10.1126/science.aau0447.

97. Segal, N.H., Parsons, D.W., Peggs, K.S., Velculescu, V., Kinzler, K.W., Vogelstein, B., and Allison, J.P. (2008). Epitope landscape in breast and colorectal cancer. Cancer Res *68*, 889–892. https://doi.org/10.1158/0008-5472.CAN-07-3095.

98. Gubin, M.M., Zhang, X., Schuster, H., Caron, E., Ward, J.P., Noguchi, T., Ivanova, Y., Hundal, J., Arthur, C.D., Krebber, W.-J., et al. (2014). Checkpoint blockade cancer immunotherapy targets tumour-specific mutant antigens. Nature *515*, 577–581. https://doi.org/10.1038/nature13988.

99. Giannakis, M., Mu, X.J., Shukla, S.A., Qian, Z.R., Cohen, O., Nishihara, R., Bahl, S., Cao, Y., Amin-Mansour, A., Yamauchi, M., et al. (2016). Genomic Correlates of Immune-Cell Infiltrates in Colorectal Carcinoma. Cell Rep *15*, 857–865. https://doi.org/10.1016/j.celrep.2016.03.075.

100. Gubin, M.M., and Schreiber, R.D. (2015). CANCER. The odds of immunotherapy success. Science *350*, 158–159. https://doi.org/10.1126/science.aad4140.

101. Van Allen, E.M., Miao, D., Schilling, B., Shukla, S.A., Blank, C., Zimmer, L., Sucker, A., Hillen, U., Foppen, M.H.G., Goldinger, S.M., et al. (2015). Genomic correlates of response to CTLA-4 blockade in metastatic melanoma. Science *350*, 207–211. https://doi.org/10.1126/science.aad0095.

102. Passaro, A., Stenzinger, A., and Peters, S. (2020). Tumor Mutational Burden as a Pan-cancer Biomarker for Immunotherapy: The Limits and Potential for Convergence. Cancer Cell *38*, 624–625. https://doi.org/10.1016/j.ccell.2020.10.019.

103. Rousseau, B., Foote, M.B., Maron, S.B., Diplas, B.H., Lu, S., Argilés, G., Cercek, A., and Diaz, L.A. (2021). The Spectrum of Benefit from Checkpoint Blockade in Hypermutated Tumors. N Engl J Med *384*, 1168–1170. https://doi.org/10.1056/NEJMc2031965.

104. Schumacher, T.N., Scheper, W., and Kvistborg, P. (2019). Cancer Neoantigens. Annu Rev Immunol *37*, 173–200. https://doi.org/10.1146/annurev-immunol-042617-053402.

105. Turajlic, S., Litchfield, K., Xu, H., Rosenthal, R., McGranahan, N., Reading, J.L., Wong, Y.N.S., Rowan, A., Kanu, N., Al Bakir, M., et al. (2017). Insertion-and-deletion-derived tumour-specific neoantigens and the immunogenic phenotype: a pan-cancer analysis. Lancet Oncol *18*, 1009–1021. https://doi.org/10.1016/S1470-2045(17)30516-8.

106. Schumacher, T.N., and Schreiber, R.D. (2015). Neoantigens in cancer immunotherapy. Science *348*, 69–74. https://doi.org/10.1126/science.aaa4971.

107. McGranahan, N., Furness, A.J.S., Rosenthal, R., Ramskov, S., Lyngaa, R., Saini, S.K., Jamal-Hanjani, M., Wilson, G.A., Birkbak, N.J., Hiley, C.T., et al. (2016). Clonal neoantigens elicit T cell immunoreactivity and sensitivity to immune checkpoint blockade. Science *351*, 1463–1469. https://doi.org/10.1126/science.aaf1490.

108. Bortolomeazzi, M., Keddar, M.R., Montorsi, L., Acha-Sagredo, A., Benedetti, L., Temelkovski, D., Choi, S., Petrov, N., Todd, K., Wai, P., et al. (2021). Immunogenomics of Colorectal Cancer Response to Checkpoint Blockade: Analysis of the KEYNOTE 177 Trial and Validation Cohorts. Gastroenterology *161*, 1179–1193. https://doi.org/10.1053/j.gastro.2021.06.064.

109. Gerlinger, M. (2021). Immunotherapy Sensitivity of Mismatch Repair-Deficient Cancer: Mutation Load Is Not Enough. Cancer Cell *39*, 16–18. https://doi.org/10.1016/j.ccell.2020.12.016.

110. Lu, C., Guan, J., Lu, S., Jin, Q., Rousseau, B., Lu, T., Stephens, D., Zhang, H., Zhu, J., Yang, M., et al. (2021). DNA Sensing in Mismatch Repair-Deficient Tumor Cells Is Essential for Anti-tumor Immunity. Cancer Cell *39*, 96-108.e6. https://doi.org/10.1016/j.ccell.2020.11.006.

111. Decout, A., Katz, J.D., Venkatraman, S., and Ablasser, A. (2021). The cGAS-STING pathway as a therapeutic target in inflammatory diseases. Nat Rev Immunol *21*, 548–569. https://doi.org/10.1038/s41577-021-00524-z.

112. Schadt, L., Sparano, C., Schweiger, N.A., Silina, K., Cecconi, V., Lucchiari, G., Yagita, H., Guggisberg, E., Saba, S., Nascakova, Z., et al. (2019). Cancer-Cell-Intrinsic cGAS Expression Mediates Tumor Immunogenicity. Cell Rep *29*, 1236-1248.e7. https://doi.org/10.1016/j.celrep.2019.09.065.

113. Marcus, A., Mao, A.J., Lensink-Vasan, M., Wang, L., Vance, R.E., and Raulet, D.H. (2018). Tumor-Derived cGAMP Triggers a STING-Mediated Interferon Response in Non-tumor Cells to Activate the NK Cell Response. Immunity *49*, 754-763.e4. https://doi.org/10.1016/j.immuni.2018.09.016.

114. Woo, S.-R., Fuertes, M.B., Corrales, L., Spranger, S., Furdyna, M.J., Leung, M.Y.K., Duggan, R., Wang, Y., Barber, G.N., Fitzgerald, K.A., et al. (2014). STING-dependent cytosolic DNA sensing mediates innate immune recognition of immunogenic tumors. Immunity *41*, 830–842. https://doi.org/10.1016/j.immuni.2014.10.017.

115. Westcott, P.M.K., Sacks, N.J., Schenkel, J.M., Ely, Z.A., Smith, O., Hauck, H., Jaeger, A.M., Zhang, D., Backlund, C.M., Beytagh, M.C., et al. (2021). Low neoantigen expression and poor T-cell priming underlie early immune escape in colorectal cancer. Nat Cancer *2*, 1071–1085. https://doi.org/10.1038/s43018-021-00247-z.

116. Amodio, V., Lamba, S., Chilà, R., Cattaneo, C.M., Mussolin, B., Corti, G., Rospo, G., Berrino, E., Tripodo, C., Pisati, F., et al. (2023). Genetic and pharmacological modulation of DNA mismatch repair heterogeneous tumors promotes immune surveillance. Cancer Cell *41*, 196-209.e5. https://doi.org/10.1016/j.ccell.2022.12.003.

117. Dolcetti, R., Viel, A., Doglioni, C., Russo, A., Guidoboni, M., Capozzi, E., Vecchiato, N., Macrì, E., Fornasarig, M., and Boiocchi, M. (1999). High prevalence of activated intraepithelial cytotoxic T lymphocytes and increased neoplastic cell apoptosis in colorectal carcinomas with microsatellite instability. Am J Pathol *154*, 1805–1813. https://doi.org/10.1016/S0002-9440(10)65436-3.

118. Smyrk, T.C., Watson, P., Kaul, K., and Lynch, H.T. (2001). Tumor-infiltrating lymphocytes are a marker for microsatellite instability in colorectal carcinoma. Cancer *91*, 2417–2422.

119. Hewish, M., Lord, C.J., Martin, S.A., Cunningham, D., and Ashworth, A. (2010). Mismatch repair deficient colorectal cancer in the era of personalized treatment. Nat Rev Clin Oncol *7*, 197–208. https://doi.org/10.1038/nrclinonc.2010.18.

120. Viale, G., Trapani, D., and Curigliano, G. (2017). Mismatch Repair Deficiency as a Predictive Biomarker for Immunotherapy Efficacy. Biomed Res Int *2017*, 4719194. https://doi.org/10.1155/2017/4719194.

121. Cancer Genome Atlas Network (2012). Comprehensive molecular characterization of human colon and rectal cancer. Nature *487*, 330–337. https://doi.org/10.1038/nature11252.

122. Brahmer, J.R., Drake, C.G., Wollner, I., Powderly, J.D., Picus, J., Sharfman, W.H., Stankevich, E., Pons, A., Salay, T.M., McMiller, T.L., et al. (2023). Phase I Study of Single-Agent Anti-Programmed Death-1 (MDX-1106) in Refractory Solid Tumors: Safety, Clinical Activity, Pharmacodynamics, and Immunologic Correlates. J Clin Oncol *41*, 715–723. https://doi.org/10.1200/JCO.22.02270.

123. Le, D.T., Uram, J.N., Wang, H., Bartlett, B.R., Kemberling, H., Eyring, A.D., Skora, A.D., Luber, B.S., Azad, N.S., Laheru, D., et al. (2015). PD-1 Blockade in Tumors with Mismatch-Repair Deficiency. N Engl J Med *372*, 2509–2520. https://doi.org/10.1056/NEJMoa1500596.

124. Research, C. for D.E. and (2019). FDA grants accelerated approval to pembrolizumab for first tissue/site agnostic indication. FDA.

125. Lenz, H.-J., Lonardi, S., Elez, E., Van Cutsem, E., Jensen, L.H., Bennouna, J., Mendez, G., Schenker, M., De La Fouchardiere, C., Limon, M.L., et al. (2024).

Nivolumab (NIVO) plus ipilimumab (IPI) vs chemotherapy (chemo) as first-line (1L) treatment for microsatellite instability-high/mismatch repair-deficient (MSI-H/dMMR) metastatic colorectal cancer (mCRC): Expanded efficacy analysis from CheckMate 8HW. JCO *42*, 3503–3503. https://doi.org/10.1200/JCO.2024.42.16_suppl.3503.

126. Chalabi Myriam, Verschoor Yara L., Tan Pedro Batista, Balduzzi Sara, Van Lent Anja U., Grootscholten Cecile, Dokter Simone, Büller Nikè V., Grotenhuis Brechtje A., Kuhlmann Koert, et al. (2024). Neoadjuvant Immunotherapy in Locally Advanced Mismatch Repair–Deficient Colon Cancer. New England Journal of Medicine *390*, 1949–1958. https://doi.org/10.1056/NEJMoa2400634.

127. Cercek, A., Lumish, M., Sinopoli, J., Weiss, J., Shia, J., Lamendola-Essel, M., El Dika, I.H., Segal, N., Shcherba, M., Sugarman, R., et al. (2022). PD-1 Blockade in Mismatch Repair-Deficient, Locally Advanced Rectal Cancer. N Engl J Med *386*, 2363–2376. https://doi.org/10.1056/NEJMoa2201445.

128. Mestrallet, G., Brown, M., Bozkus, C.C., and Bhardwaj, N. (2023). Immune escape and resistance to immunotherapy in mismatch repair deficient tumors. Front Immunol *14*, 1210164. https://doi.org/10.3389/fimmu.2023.1210164.

129. Alouani, E., Rousseau, B., Andre, T., and Marabelle, A. (2022). Immunotherapy advances in cancers with mismatch repair or proofreading deficiencies. Nat Cancer *3*, 1414–1417. https://doi.org/10.1038/s43018-022-00497-5.

130. Overman, M.J., Kopetz, S., McDermott, R.S., Leach, J., Lonardi, S., Lenz, H.-J., Morse, M.A., Desai, J., Hill, A., Axelson, M.D., et al. (2016). Nivolumab ± ipilimumab in treatment (tx) of patients (pts) with metastatic colorectal cancer (mCRC) with and without high microsatellite instability (MSI-H): CheckMate-142 interim results. JCO *34*, 3501–3501. https://doi.org/10.1200/JCO.2016.34.15_suppl.3501.

131. Wu, Q., Wang, Z., Luo, Y., and Xie, X. (2023). Efficacy and safety of immune checkpoint inhibitors in Proficient Mismatch Repair (pMMR)/ Non-Microsatellite Instability-High (non-MSI-H) metastatic colorectal cancer: a study based on 39 cohorts incorporating 1723 patients. BMC Immunol *24*, 27. https://doi.org/10.1186/s12865-023-00564-1.

132. Lakatos, E., Williams, M.J., Schenck, R.O., Cross, W.C.H., Househam, J., Zapata, L., Werner, B., Gatenbee, C., Robertson-Tessi, M., Barnes, C.P., et al. (2020). Evolutionary dynamics of neoantigens in growing tumors. Nat Genet *52*, 1057–1066. https://doi.org/10.1038/s41588-020-0687-1.

133. Chalabi, M., Fanchi, L.F., Dijkstra, K.K., Van den Berg, J.G., Aalbers, A.G., Sikorska, K., Lopez-Yurda, M., Grootscholten, C., Beets, G.L., Snaebjornsson, P., et al. (2020). Neoadjuvant immunotherapy leads to pathological responses in MMR-proficient and MMR-deficient early-stage colon cancers. Nat Med *26*, 566–576. https://doi.org/10.1038/s41591-020-0805-8.

134. Bullock, A.J., Schlechter, B.L., Fakih, M.G., Tsimberidou, A.M., Grossman, J.E., Gordon, M.S., Wilky, B.A., Pimentel, A., Mahadevan, D., Balmanoukian, A.S., et al. (2024). Botensilimab plus balstilimab in relapsed/refractory microsatellite stable metastatic colorectal cancer: a phase 1 trial. Nat Med. https://doi.org/10.1038/s41591-024-03083-7.

135. Di Nicolantonio, F., Vitiello, P.P., Marsoni, S., Siena, S., Tabernero, J., Trusolino, L., Bernards, R., and Bardelli, A. (2021). Precision oncology in metastatic colorectal cancer - from biology to medicine. Nat Rev Clin Oncol *18*, 506–525. https://doi.org/10.1038/s41571-021-00495-z.

136. Cervantes, A., Adam, R., Roselló, S., Arnold, D., Normanno, N., Taïeb, J., Seligmann, J., De Baere, T., Osterlund, P., Yoshino, T., et al. (2023). Metastatic colorectal cancer: ESMO Clinical Practice Guideline for diagnosis, treatment and follow-up. Ann Oncol *34*, 10–32. https://doi.org/10.1016/j.annonc.2022.10.003.

137. Chen, T., Tongpeng, S., Lu, Z., Topatana, W., Juengpanich, S., Li, S., Hu, J., Cao, J., Lee, C., Tian, Y., et al. (2022). DNA damage response inhibition-based combination therapies in cancer treatment: Recent advances and future directions. Aging and Cancer *3*, 44–67. https://doi.org/10.1002/aac2.12047.

138. Chabanon, R.M., Rouanne, M., Lord, C.J., Soria, J.-C., Pasero, P., and Postel-Vinay, S. (2021). Targeting the DNA damage response in immuno-oncology: developments and opportunities. Nat Rev Cancer *21*, 701–717. https://doi.org/10.1038/s41568-021-00386-6.

139. Larroquette, M., Domblides, C., Lefort, F., Lasserre, M., Quivy, A., Sionneau, B., Bertolaso, P., Gross-Goupil, M., Ravaud, A., and Daste, A. (2021). Combining immune checkpoint inhibitors with chemotherapy in advanced solid tumours: A review. European Journal of Cancer *158*, 47–62. https://doi.org/10.1016/j.ejca.2021.09.013.

140. Antoniotti, C., Rossini, D., Pietrantonio, F., Catteau, A., Salvatore, L., Lonardi, S., Boquet, I., Tamberi, S., Marmorino, F., Moretto, R., et al. (2022). Upfront FOLFOXIRI plus bevacizumab with or without atezolizumab in the treatment of patients with metastatic colorectal cancer (AtezoTRIBE): a multicentre, open-label, randomised, controlled, phase 2 trial. Lancet Oncol *23*, 876–887. https://doi.org/10.1016/S1470-2045(22)00274-1.

141. Antoniotti, C., Rossini, D., Pietrantonio, F., Salvatore, L., Marmorino, F., Ambrosini, M., Lonardi, S., Bensi, M., Moretto, R., Tamberi, S., et al. (2023). FOLFOXIRI plus bevacizumab and atezolizumab as upfront treatment of unresectable metastatic colorectal cancer (mCRC): Updated and overall survival results of the phase II randomized AtezoTRIBE study. JCO *41*, 3500–3500. https://doi.org/10.1200/JCO.2023.41.16_suppl.3500.

142. Antoniotti, C., Boccaccino, A., Seitz, R., Giordano, M., Catteau, A., Rossini, D., Pietrantonio, F., Salvatore, L., McGregor, K., Bergamo, F., et al. (2023). An Immune-Related Gene Expression Signature Predicts Benefit from Adding Atezolizumab to FOLFOXIRI plus Bevacizumab in Metastatic Colorectal Cancer.

Clin Cancer Res *29*, 2291–2298. https://doi.org/10.1158/1078-0432.CCR-22-3878.

143. Lenz, H.-J., Parikh, A., Spigel, D.R., Cohn, A.L., Yoshino, T., Kochenderfer, M., Elez, E., Shao, S.H., Deming, D., Holdridge, R., et al. (2024). Modified FOLFOX6 plus bevacizumab with and without nivolumab for first-line treatment of metastatic colorectal cancer: phase 2 results from the CheckMate 9X8 randomized clinical trial. J Immunother Cancer *12*, e008409. https://doi.org/10.1136/jitc-2023-008409.

144. Damato, A., Bergamo, F., Antonuzzo, L., Nasti, G., Iachetta, F., Romagnani, A., Gervasi, E., Larocca, M., and Pinto, C. (2021). FOLFOXIRI/Bevacizumab Plus Nivolumab as First-Line Treatment in Metastatic Colorectal Cancer RAS/BRAF Mutated: Safety Run-In of Phase II NIVACOR Trial. Front Oncol *11*, 766500. https://doi.org/10.3389/fonc.2021.766500.

145. Pietrantonio, F., Randon, G., Romagnoli, D., Di Donato, S., Benelli, M., and de Braud, F. (2020). Biomarker-guided implementation of the old drug temozolomide as a novel treatment option for patients with metastatic colorectal cancer. Cancer Treat Rev *82*, 101935. https://doi.org/10.1016/j.ctrv.2019.101935.

146. Sartore-Bianchi, A., Pietrantonio, F., Amatu, A., Milione, M., Cassingena, A., Ghezzi, S., Caporale, M., Berenato, R., Falcomatà, C., Pellegrinelli, A., et al. (2017). Digital PCR assessment of MGMT promoter methylation coupled with reduced protein expression optimises prediction of response to alkylating agents in metastatic colorectal cancer patients. Eur J Cancer *71*, 43–50. https://doi.org/10.1016/j.ejca.2016.10.032.

147. Barault, L., Amatu, A., Bleeker, F.E., Moutinho, C., Falcomatà, C., Fiano, V., Cassingena, A., Siravegna, G., Milione, M., Cassoni, P., et al. (2015). Digital PCR quantification of MGMT methylation refines prediction of clinical benefit from alkylating agents in glioblastoma and metastatic colorectal cancer. Ann Oncol *26*, 1994–1999. https://doi.org/10.1093/annonc/mdv272.

148. Amatu, A., Barault, L., Moutinho, C., Cassingena, A., Bencardino, K., Ghezzi, S., Palmeri, L., Bonazzina, E., Tosi, F., Ricotta, R., et al. (2016). Tumor MGMT promoter hypermethylation changes over time limit temozolomide efficacy in a phase II trial for metastatic colorectal cancer. Ann Oncol *27*, 1062–1067. https://doi.org/10.1093/annonc/mdw071.

149. Roos, W.P., Batista, L.F.Z., Naumann, S.C., Wick, W., Weller, M., Menck, C.F.M., and Kaina, B. (2007). Apoptosis in malignant glioma cells triggered by the temozolomide-induced DNA lesion O6-methylguanine. Oncogene *26*, 186–197. https://doi.org/10.1038/sj.onc.1209785.

150. Ganesh, K., Stadler, Z.K., Cercek, A., Mendelsohn, R.B., Shia, J., Segal, N.H., and Diaz, L.A. (2019). Immunotherapy in colorectal cancer: rationale, challenges and potential. Nat Rev Gastroenterol Hepatol *16*, 361–375. https://doi.org/10.1038/s41575-019-0126-x.

151. Sartore-Bianchi, A., Pietrantonio, F., Amatu, A., Milione, M., Cassingena, A., Ghezzi, S., Caporale, M., Berenato, R., Falcomatà, C., Pellegrinelli, A., et al. (2017). Digital PCR assessment of MGMT promoter methylation coupled with reduced protein expression optimises prediction of response to alkylating agents in metastatic colorectal cancer patients. Eur J Cancer *71*, 43–50. https://doi.org/10.1016/j.ejca.2016.10.032.

152. Kothandapani, A., Sawant, A., Dangeti, V.S.M.N., Sobol, R.W., and Patrick, S.M. (2013). Epistatic role of base excision repair and mismatch repair pathways in mediating cisplatin cytotoxicity. Nucleic Acids Res *41*, 7332–7343. https://doi.org/10.1093/nar/gkt479.

153. Vaisman, A., Varchenko, M., Umar, A., Kunkel, T.A., Risinger, J.I., Barrett, J.C., Hamilton, T.C., and Chaney, S.G. (1998). The role of hMLH1, hMSH3, and hMSH6 defects in cisplatin and oxaliplatin resistance: correlation with replicative bypass of platinum-DNA adducts. Cancer Res *58*, 3579–3585.

154. Mello, J.A., Acharya, S., Fishel, R., and Essigmann, J.M. (1996). The mismatch-repair protein hMSH2 binds selectively to DNA adducts of the anticancer drug cisplatin. Chem Biol *3*, 579–589. https://doi.org/10.1016/s1074-5521(96)90149-0.

155. Fink, D., Nebel, S., Aebi, S., Zheng, H., Cenni, B., Nehmé, A., Christen, R.D., and Howell, S.B. (1996). The role of DNA mismatch repair in platinum drug resistance. Cancer Res *56*, 4881–4886.

156. Tian, H., Yan, L., Xiao-fei, L., Hai-yan, S., Juan, C., and Shan, K. (2019). Hypermethylation of mismatch repair gene hMSH2 associates with platinum-resistant disease in epithelial ovarian cancer. Clinical Epigenetics *11*, 153. https://doi.org/10.1186/s13148-019-0748-4.

157. Liston, D.R., and Davis, M. (2017). Clinically Relevant Concentrations of Anticancer Drugs: A Guide for Nonclinical Studies. Clin Cancer Res *23*, 3489–3498. https://doi.org/10.1158/1078-0432.CCR-16-3083.

158. Goodspeed, A., Jean, A., and Costello, J.C. (2019). A Whole-genome CRISPR Screen Identifies a Role of MSH2 in Cisplatin-mediated Cell Death in Muscle-invasive Bladder Cancer. Eur Urol *75*, 242–250. https://doi.org/10.1016/j.eururo.2018.10.040.

159. Chen, C.-Y., Ueha, S., Ishiwata, Y., Yokochi, S., Yang, D., Oppenheim, J.J., Ogiwara, H., Shichino, S., Deshimaru, S., Shand, F.H.W., et al. (2019). Combined treatment with HMGN1 and anti-CD4 depleting antibody reverses T cell exhaustion and exerts robust anti-tumor effects in mice. Journal for ImmunoTherapy of Cancer *7*, 21. https://doi.org/10.1186/s40425-019-0503-6.

160. Galluzzi, L., Senovilla, L., Vitale, I., Michels, J., Martins, I., Kepp, O., Castedo, M., and Kroemer, G. (2012). Molecular mechanisms of cisplatin resistance. Oncogene *31*, 1869–1883. https://doi.org/10.1038/onc.2011.384.

161. Palmeri, J.R., Lax, B.M., Peters, J.M., Duhamel, L., Stinson, J.A., Santollani, L., Lutz, E.A., Pinney, W., Bryson, B.D., and Dane Wittrup, K. (2024). CD8+ T cell priming that is required for curative intratumorally anchored anti-4-1BB immunotherapy is constrained by Tregs. Nat Commun *15*, 1900. https://doi.org/10.1038/s41467-024-45625-0.

162. Matsushita, H., Vesely, M.D., Koboldt, D.C., Rickert, C.G., Uppaluri, R., Magrini, V.J., Arthur, C.D., White, J.M., Chen, Y.-S., Shea, L.K., et al. (2012). Cancer exome analysis reveals a T-cell-dependent mechanism of cancer immunoediting. Nature *482*, 400–404. https://doi.org/10.1038/nature10755.

163. Fumet, J.-D., Chibaudel, B., Bennouna, J., Borg, C., Martin-Babau, J., Cohen, R., Fonck, M., Taieb, J., Thibaudin, M., Limagne, E., et al. (2021). 433P Durvalumab and tremelimumab in combination with FOLFOX in patients with previously untreated RAS-mutated metastatic colorectal cancer: First results of efficacy at one year for phase II MEDITREME trial. Annals of Oncology *32*, S551. https://doi.org/10.1016/j.annonc.2021.08.954.

164. Lenz, H.-J., Parikh, A., Spigel, D.R., Cohn, A.L., Yoshino, T., Kochenderfer, M., Elez, E., Shao, S.H., Deming, D., Holdridge, R., et al. (2024). Modified FOLFOX6 plus bevacizumab with and without nivolumab for first-line treatment of metastatic colorectal cancer: phase 2 results from the CheckMate 9X8 randomized clinical trial. J Immunother Cancer *12*, e008409. https://doi.org/10.1136/jitc-2023-008409.

165. Germano, G., Lamba, S., Rospo, G., Barault, L., Magrì, A., Maione, F., Russo, M., Crisafulli, G., Bartolini, A., Lerda, G., et al. (2017). Inactivation of DNA repair triggers neoantigen generation and impairs tumour growth. Nature *552*, 116–120. https://doi.org/10.1038/nature24673.

166. Kuczynski, E.A., Krueger, J., Chow, A., Xu, P., Man, S., Sundaravadanam, Y., Miller, J.K., Krzyzanowski, P.M., and Kerbel, R.S. (2018). Impact of Chemical-Induced Mutational Load Increase on Immune Checkpoint Therapy in Poorly Responsive Murine Tumors. Mol Cancer Ther *17*, 869–882. https://doi.org/10.1158/1535-7163.MCT-17-1091.

167. Gejman, R.S., Chang, A.Y., Jones, H.F., DiKun, K., Hakimi, A.A., Schietinger, A., and Scheinberg, D.A. (2018). Rejection of immunogenic tumor clones is limited by clonal fraction. Elife *7*, e41090. https://doi.org/10.7554/eLife.41090.

168. Greaves, M., and Maley, C.C. (2012). Clonal evolution in cancer. Nature *481*, 306–313. https://doi.org/10.1038/nature10762.

169. Boot, A., Huang, M.N., Ng, A.W.T., Ho, S.-C., Lim, J.Q., Kawakami, Y., Chayama, K., Teh, B.T., Nakagawa, H., and Rozen, S.G. (2018). In-depth characterization of the cisplatin mutational signature in human cell lines and in esophageal and liver tumors. Genome Res. *28*, 654–665. https://doi.org/10.1101/gr.230219.117.

170. Wang, J.Y.J., and Edelmann, W. (2006). Mismatch repair proteins as sensors of alkylation DNA damage. Cancer Cell *9*, 417–418. https://doi.org/10.1016/j.ccr.2006.05.013.

171. Cortot, A., Gerinière, L., Robinet, G., Breton, J., Corre, R., Falchero, L., Berard, H., Gimenez, C., Chavaillon, J., Perol, M., et al. (2006). Phase II trial of temozolomide and cisplatin followed by whole brain radiotherapy in non-small-cell lung cancer patients with brain metastases: a GLOT-GFPC study. Annals of oncology : official journal of the European Society for Medical Oncology *17*. https://doi.org/10.1093/annonc/mdl146.

172. Lussier, D.M., Alspach, E., Ward, J.P., Miceli, A.P., Runci, D., White, J.M., Mpoy, C., Arthur, C.D., Kohlmiller, H.N., Jacks, T., et al. (2021). Radiation-induced neoantigens broaden the immunotherapeutic window of cancers with low mutational loads. Proceedings of the National Academy of Sciences *118*, e2102611118. https://doi.org/10.1073/pnas.2102611118.

173. Seiter, K., Katragadda, S., Ponce, D., Rasul, M., and Ahmed, N. (2009). Temozolomide and cisplatin in relapsed/refractory acute leukemia. Journal of hematology & oncology *2*. https://doi.org/10.1186/1756-8722-2-21.

174. Brossart, P. (2020). The Role of Antigen Spreading in the Efficacy of Immunotherapies. Clin Cancer Res *26*, 4442–4447. https://doi.org/10.1158/1078-0432.CCR-20-0305.

175. Silvani, A., Eoli, M., Salmaggi, A., Lamperti, E., Maccagnano, E., Broggi, G., and Boiardi, A. (2004). Phase II trial of cisplatin plus temozolomide, in recurrent and progressive malignant glioma patients. J Neurooncol *66*, 203–208. https://doi.org/10.1023/b:neon.0000013479.64348.69.

176. Nguyen, K.B., Roerden, M., Copeland, C.J., Backlund, C.M., Klop-Packel, N.G., Remba, T., Kim, B., Singh, N.K., Birnbaum, M.E., Irvine, D.J., et al. (2023). Decoupled neoantigen cross-presentation by dendritic cells limits anti-tumor immunity against tumors with heterogeneous neoantigen expression. eLife *12*, e85263. https://doi.org/10.7554/eLife.85263.

177. Zustovich, F., Lombardi, G., Della Puppa, A., Rotilio, A., Scienza, R., and Pastorelli, D. (2009). A phase II study of cisplatin and temozolomide in heavily pre-treated patients with temozolomide-refractory high-grade malignant glioma. Anticancer Res *29*, 4275–4279.

178. Bousso, P., Levraud, J.-P., Kourilsky, P., and Abastado, J.-P. (1999). The Composition of a Primary T Cell Response Is Largely Determined by the Timing of Recruitment of Individual T Cell Clones. J Exp Med *189*, 1591–1600.

179. Bonmassar, E., Bonmassar, A., Vadlamudi, S., and Goldin, A. (1970). Immunological alteration of leukemic cells in vivo after treatment with an antitumor drug. Proc Natl Acad Sci U S A *66*, 1089–1095. https://doi.org/10.1073/pnas.66.4.1089.

180. Bonmassar, E., Bonmassar, A., Vadlamudi, S., and Goldin, A. (1972). Antigenic changes of L1210 leukemia in mice treated with 5-(3,3-dimethyl-1-triazeno)imidazole-4-carboxamide. Cancer Res *32*, 1446–1450.

181. Puccetti, P., Romani, L., and Fioretti, M.C. (1987). Chemical xenogenization of experimental tumors. Cancer Metast Rev *6*, 93–111. https://doi.org/10.1007/BF00052845.

182. Garassino, M.C., Gadgeel, S., Speranza, G., Felip, E., Esteban, E., Dómine, M., Hochmair, M.J., Powell, S.F., Bischoff, H.G., Peled, N., et al. (2023). Pembrolizumab Plus Pemetrexed and Platinum in Nonsquamous Non–Small-Cell Lung Cancer: 5-Year Outcomes From the Phase 3 KEYNOTE-189 Study. JCO *41*, 1992–1998. https://doi.org/10.1200/JCO.22.01989.

183. Patruni, S., Fayyaz, F., Bien, J., Phillip, T., and King, D.A. (2023). Immunotherapy in the Management of Esophagogastric Cancer: A Practical Review. JCO Oncology Practice *19*, 107–115. https://doi.org/10.1200/OP.22.00226.

184. Kelley, R.K., Ueno, M., Yoo, C., Finn, R.S., Furuse, J., Ren, Z., Yau, T., Klümpen, H.-J., Chan, S.L., Ozaka, M., et al. (2023). Pembrolizumab in combination with gemcitabine and cisplatin compared with gemcitabine and cisplatin alone for patients with advanced biliary tract cancer (KEYNOTE-966): a randomised, double-blind, placebo-controlled, phase 3 trial. The Lancet *401*, 1853–1865. https://doi.org/10.1016/S0140-6736(23)00727-4.

185. Nanni, P., de Giovanni, C., Lollini, P.L., Nicoletti, G., and Prodi, G. (1983). TS/A: a new metastasizing cell line from a BALB/c spontaneous mammary adenocarcinoma. Clin Exp Metastasis *1*, 373–380. https://doi.org/10.1007/BF00121199.

186. Gnirke, A., Melnikov, A., Maguire, J., Rogov, P., LeProust, E.M., Brockman, W., Fennell, T., Giannoukos, G., Fisher, S., Russ, C., et al. (2009). Solution hybrid selection with ultra-long oligonucleotides for massively parallel targeted sequencing. Nat Biotechnol *27*, 182–189. https://doi.org/10.1038/nbt.1523.

187. Crisafulli, G., Mussolin, B., Cassingena, A., Montone, M., Bartolini, A., Barault, L., Martinetti, A., Morano, F., Pietrantonio, F., Sartore-Bianchi, A., et al. (2019). Whole exome sequencing analysis of urine trans-renal tumour DNA in metastatic colorectal cancer patients. ESMO Open *4*, e000572. https://doi.org/10.1136/esmoopen-2019-000572.

188. Corti, G., Bartolini, A., Crisafulli, G., Novara, L., Rospo, G., Montone, M., Negrino, C., Mussolin, B., Buscarino, M., Isella, C., et al. (2019). A Genomic Analysis Workflow for Colorectal Cancer Precision Oncology. Clin Colorectal Cancer *18*, 91-101.e3. https://doi.org/10.1016/j.clcc.2019.02.008.

189. Andreatta, M., and Nielsen, M. (2016). Gapped sequence alignment using artificial neural networks: application to the MHC class I system. Bioinformatics *32*, 511–517. https://doi.org/10.1093/bioinformatics/btv639.

190. Bergstrom, E.N., Huang, M.N., Mahto, U., Barnes, M., Stratton, M.R., Rozen, S.G., and Alexandrov, L.B. (2019). SigProfilerMatrixGenerator: a tool for visualizing and exploring patterns of small mutational events. BMC Genomics *20*, 685. https://doi.org/10.1186/s12864-019-6041-2.

191. Blokzijl, F., Janssen, R., van Boxtel, R., and Cuppen, E. (2018). MutationalPatterns: comprehensive genome-wide analysis of mutational processes. Genome Med *10*, 33. https://doi.org/10.1186/s13073-018-0539-0.

192. Tate, J.G., Bamford, S., Jubb, H.C., Sondka, Z., Beare, D.M., Bindal, N., Boutselakis, H., Cole, C.G., Creatore, C., Dawson, E., et al. (2019). COSMIC: the Catalogue Of Somatic Mutations In Cancer. Nucleic Acids Res *47*, D941–D947. https://doi.org/10.1093/nar/gky1015.

193. Islam, S.M.A., and Alexandrov, L.B. (2021). Bioinformatic Methods to Identify Mutational Signatures in Cancer. Methods Mol Biol *2185*, 447–473. https://doi.org/10.1007/978-1-0716-0810-4_28.

194. Battuello, P., Corti, G., Bartolini, A., Lorenzato, A., Sogari, A., Russo, M., Di Nicolantonio, F., Bardelli, A., and Crisafulli, G. (2024). Mutational signatures of colorectal cancers according to distinct computational workflows. Brief Bioinform *25*, bbae249. https://doi.org/10.1093/bib/bbae249.

195. Martínez-Jiménez, F., Priestley, P., Shale, C., Baber, J., Rozemuller, E., and Cuppen, E. (2023). Genetic immune escape landscape in primary and metastatic cancer. Nat Genet *55*, 820–831. https://doi.org/10.1038/s41588-023-01367-1.

196. Dobin, A., Davis, C.A., Schlesinger, F., Drenkow, J., Zaleski, C., Jha, S., Batut, P., Chaisson, M., and Gingeras, T.R. (2013). STAR: ultrafast universal RNA-seq aligner. Bioinformatics *29*, 15–21. https://doi.org/10.1093/bioinformatics/bts635.

197. Li, B., and Dewey, C.N. (2011). RSEM: accurate transcript quantification from RNA-Seq data with or without a reference genome. BMC Bioinformatics *12*, 323. https://doi.org/10.1186/1471-2105-12-323.

198. Love, M.I., Huber, W., and Anders, S. (2014). Moderated estimation of fold change and dispersion for RNA-seq data with DESeq2. Genome Biology *15*, 550. https://doi.org/10.1186/s13059-014-0550-8.

199. Korotkevich, G., Sukhov, V., Budin, N., Shpak, B., Artyomov, M.N., and Sergushichev, A. (2016). Fast gene set enrichment analysis. https://doi.org/10.1101/060012.

200. Subramanian, A., Tamayo, P., Mootha, V.K., Mukherjee, S., Ebert, B.L., Gillette, M.A., Paulovich, A., Pomeroy, S.L., Golub, T.R., Lander, E.S., et al. (2005). Gene set enrichment analysis: a knowledge-based approach for interpreting genome-wide expression profiles. Proc Natl Acad Sci U S A *102*, 15545–15550. https://doi.org/10.1073/pnas.0506580102.

ACKNOWLEDGEMENTS

Research endeavors are no easy tasks and can't be pursued alone.
This work could have not been possible without the help and support from many people: Sara, Paolo, Vito, Vittorio, Gaia, Monik, Giovanni C., Mary and Giovanni G. I have been lucky to work with you! To the MD-PhD gang (Giorgio, Gianluca, Silvia): thanks for keeping up the mood and the spirit through good and bad times!

I also wish to thank the internal and external reviewers of this doctoral thesis for the excellent feedbacks and suggestions that have helped shaping this thesis and the corresponding manuscript: Prof Silvia Giordano, Prof Jan Paul Medema, Prof Stefano Indraccolo.

My heartfelt gratitude goes to the people that made the difference over these years, both friends (Nico, Mari, Vito, Paolo, Maria, Ele, Matteo…) and family (Nello, Lina, Marilou, Federico). Special thanks to my Tessy, who carries the weight of having a weird boyfriend with an insane passion for unprofitable research activities that a medical doctor should stay away from…

Last but not least, I need to thank Alberto, who believed (or pretended very well to believe) in a medical oncologist who pipettes on working hours. Many songs by the Queen have a totally different meaning now, and in the concert of life "*Under pressure*" is long played before each "*Another one bites the dust*", while "*Lazing on a Sunday afternoon*" is often left out of the lineup…

It's been a fantastic journey!